Inês do Carmo Viegas Baptista

Characterization of TRIB2 following PI3K inhibition

Mestrado em Oncobiologia:
Mecanismos Moleculares do Cancro

Trabalho efetuado sob a orientação de:
Professor Doutor Wolfgang Link
Professor Doutor Richard Hill

UNIVERSIDADE DO ALGARVE

Departamento de Ciências Biomédicas e Medicina

2015

Characterization of TRIB2 following PI3K inhibition

Declaração de autoria de trabalho

Declaro ser a autora deste trabalho, que é original e inédito. Autores e trabalhos consultados estão devidamente citados no texto e constam da listagem de referências incluída.

ASSINATURA:_____

Acknowledgements

First of all, I must give my gratitude to my supervisors. I would like to thank Dr Wolfgang Link for the opportunity, the guidance and the support throughout the research and writing of my thesis. To Dr Richard Hill, I thank you for your patience, motivation and the knowledge you bestowed on me, I will be eternally in your debt.

I would like to thank all my laboratory colleagues Marta, Neuton, Eduarda and Gisela, for their support and companionship during the last year. You are all crazy but lab work wouldn't be the same without you there.

I will also thank my friends for their encouragement, nagging and patience for my "social reclusion" during my writing of the thesis.

Finally, my thanks to my family for always believing in me. To my sister Vera, for always pushing me to my limits. To my mother Ana, for always supporting me in my endeavours. Last but not least, to my father Augusto, who is gone but I am sure would be proud.

Abstract

Cancer can be defined as an unbalance between cell proliferation and apoptosis. The PI3K/AKT signalling pathway is one of the most mutated pathways in cancer and is involved in cell growth and survival. The transcription factor FOXO3a is a critical effector of this pathway and its inactivation by AKT prevents the expression of genes involved in cell cycle arrest and apoptosis. The TRIB2 protein was found to be a repressor of FOXO3a, and over expressed in many types of cancer. Importantly, TRIB2confers resistance to PI3K inhibitors which are being tested in clinical trials.

This work shows that following PI3K inhibitor treatment, there is an increase of the TRIB2 protein levels by reducing proteasomal degradation. Furthermore, the TRIB2 COP1 binding domain is critical for AKT activation and subsequent FOXO repression.

Altogether, our results provide insight into the mechanism underlying TRIB2 mediated tumorigenesis and drug resistance implicating the binding and activation of AKT and suggests a role of TRIB2 in acquired resistance against PI3K inhibitors.

Keywords – Cancer, Melanoma, TRIB2, FOXO3a, PI3K signalling, MDM2

Resumo

O Cancro é caracterizado por uma proliferação celular descontrolada oriunda de danos e/ou mutações no ADN. Estas alterações surgem na grande maioria de erros durante o processo de replicação, falhas nos mecanismos de reparação, exposição a fatores ambientais ou a agentes cancerígenas. Existem seis alterações essências que uma célula normal submete-se na transformação em célula tumoral: evasão a supressores externos de crescimento celular, sinalização constitutiva de proliferação, evasão à apoptose (morte celular programada), capacidade própria de induzir angiogênese (produção de novos vasos sanguíneos), potencial replicativo ilimitado que torna a célula "imortal" e capacidade metastática de invadir outro tecidos. Recentemente, mais quatro características foram adicionadas, sendo elas: evasão ao sistema imunitário, instabilidade genómica, desregulação do balanço energético celular e capacidade de inflamação indutora de tumores.

O Cancro é uma das maiores ameaças á saúde humana a nível mundial. Dentro dos tipos de cancro mais preocupantes está o cancro de pele, mais especificamente o Melanoma. Esta forma agressiva de cancro de pele desenvolve-se a partir de melanócitos, células especializadas na produção de melanina. Embora este tipo de cancro de pele seja uma minoria (menos de 5% dos casos totais), é um dos mais letais, sendo responsável por aproximadamente 80% de todas as mortes devido a cancro de pele. Com a sua incidência dentro da faixa etária dos 30 aos 60 anos, em particular em pessoas de pele mais clara. O facto de cada vez mais surgirem casos de jovens entre os 25-29 anos é alarmante. O aumento anual da sua incidência têm-se refletido numa subida na taxa de mortalidade associada a este tipo de cancro.

Esta doença oncológica é extremamente agressiva e heterogénea, com vários subtipos histológicos e perfis mutacionais. Adere-se o problema que os tratamentos convencionais são pouco eficazes e as drogas mais recentes que conseguem ter resultados tornam-se ineficazes devido aos tumores adquirirem resistência num espaço de meses. A totalidade destes factos confere aos pacientes um prognóstico pessimista.

Devido a estes factos, a investigação científica têm-se empenhado em perceber os mecanismos moleculares afetados por esta patologia e em como esse conhecimento pode auxiliar na produção de tratamentos mais eficazes. É o caso da via de sinalização de PI3K,

que se verificou ser desregulada em Melanoma, que levou ao desenvolvimento de inibidores capazes de reverter esta alteração, como BEZ235.

A via de sinalização de PI3K/AKT é importante na regulação de diversos processos biológicos, tais como proliferação celular, metabolismo, crescimento celular e apoptose. Esta via é ativada pela ligação de fatores de crescimento ao recetor de tirosina quinase na membrana celular. Este recetor, através de fosforilação, ativa PI3K que converte fosfatidil inositol 4,5-difosfato (PIP2) em fosfatidil inositol 3,4,5-trifosfato (PIP3). Este processo é regulado negativamente por PTEN, uma fosfatase que tem como substrato PIP3. O aumento de PIP3 recruta AKT para a membrana, fazendo com que seja ativado por outras quinases através de fosforilação dos seus resíduos Treonina 308 e Serina 473. Após esta ativação, AKT fosforila várias moléculas alvo no citoplasma e no núcleo, como por exemplo p27, BAD, GSK3, MDM2 e FOXO.

Os fatores FOXO são uma família de fatores de transcrição que funcionam como ativadores ou repressores, dependendo dos seus cofatores a quando da sua ligação ao ADN. Esta família é fundamental em processos como apoptose, metabolismo, diferenciação celular, inflamação, proliferação e resposta ao *stress* oxidativo.

O fator de transcrição p53 é responsável pela regulação de vários genes envolvidos em apoptose, paragem do ciclo celular, senescência, metabolismo e autofagia. Devido a estas funções, é considerado o "guardião do genoma" e o seu papel contra o desenvolvimento tumoral é bem conhecido. O p53 é regulado por MDM2, uma ubiquitina ligase responsável pela sua ubiquitinação e consequente degradação proteossómica. Na verdade, p53 e MDM2 exercem um *feedback loop*, sendo que o gene de MDM2 é um dos alvos de p53, mantendo assim os níveis de p53 constantes dentro da célula.

O TRIB2 é um gene que tem sido associado ao desenvolvimento de cancro e foi recentemente considerado um biomarcador para o prognóstico e para a progressão de Melanoma. A sua sobre expressão proteica afeta negativamente os tratamentos convencionais a este tipo de cancro. Também está implicado na regulação negativa de FOXO. Dado que este fator de transcrição é uma das vias que as drogas usadas nas terapias utilizam para exercer efeitos citotóxicos e/ou citostáticos sobre as células tumorais, a regulação que TRIB2 exerce sobre FOXO evidencia o seu papel na resistência a quimioterapêuticos (como o clássico DTIC ou o inibidor BEZ235).

Pesquisas antecedentes feitas pelo nosso grupo laboratorial demonstraram que o uso de inibidores de PI3K estabilizam os níveis proteicos de TRIB2 e que existe uma interação entre TRIB2 e AKT. Neste trabalho, procuramos perceber como TRIB2 é regulado dentro da célula e como interage com a via de sinalização PI3K/AKT.

Durante a nossa investigação constatámos que os níveis proteicos de TRIB2 eram estabilizados na presença de inibidores de PI3K devido a um decréscimo da sua degradação proteossómica. Isto implica que a via de sinalização de PI3K está envolvida na modificação translacional de TRIB2 necessária para a sua degradação. Os mecanismos envolvidos nesta degradação e os seus participantes permanecem desconhecidos. No entanto, estes resultados conseguem demonstrar como TRIB2 influencia a resistência a drogas, como verificado nos casos de Melanoma.

Também observámos que a interação entre AKT e TRIB2 é feita através do domínio de ligação a COP1 existente na zona C-terminal de TRIB2. Verificámos que esta interação implica um decréscimo na expressão de genes envolvidos em apoptose e em paragem do ciclo celular como FasLG e p27, respetivamente. Estes resultados evidenciam que a interação entre AKT e TRIB2 está relacionada com a regulação negativa de FOXO. Como confirmação, avaliámos os níveis proteicos de p27 e BIM, genes regulados por os fatores FOXO. Estes resultados implicam que TRIB2 funciona como uma proteína *scaffold* ou adaptadora, que permite a ativação de AKT no resíduo Serina 473.

Em conjunto, estes resultados demonstram como a regulação de TRIB2 e a sua interação com AKT auxiliam as células tumorais a adquirirem resistência a quimioterapêuticos, não só no tratamento de Melanoma mas em outras patologias oncológicas onde a via de sinalização de PI3K/AKT esteja alterada.

Palavras-chave: Cancro, Melanoma, TRIB2, FOXO3a, via de sinalização de PI3K, MDM2

Table of Contents

Figure list

Table list

Appendix list

Abbreviations list

4E-BP	eIF4E-binding protein
AJCC	American Joint Commission on Cancer
AKT	Protein kinase B
AML	Acute myeloid leukaemia
ATF4	Activating transcription factor 4
BAD	Bcl-2-associated death promoter
BAX	Bcl-2-associated X protein
Bcl-2	B-cell lymphoma 2
Bcl-XL	B-cell lymphoma extra large
BIM	Bcl-2 interacting mediator of cell death
CDK	Cyclin-dependent kinase
CDKN2A	Cyclin-dependent kinase inhibitor 2A
C/EBP	CCAAT/enhancer-binding protein
COP1	Constitutive morphogenesis 1
CREB	Cyclic-AMP response element binding protein
CTLA-4	Cytotoxic T-lymphocyte associated antigen 4
DTIC	Dacarbazine
FasLG	Fas ligand
FDA	Food and drug Administration
FOXO	Forkhead box O transcription factor
FYVE	Fab-1, YG-LO23, Vps27 and EEA1
GAP	GTPase-activating protein
GPCR	G-protein coupled receptor
GSK3	Glycogen synthase kinase 3
HER2	Human epidermal growth factor receptor 2
IAP1	Inhibitor of apoptosis protein 1
IkB	I-kappa-B
IKKα	Inhibitor of kappa B kinase α
IL-2	Interleukin 2
ILK	Integrin-linked kinase
LDH	Lactate dehydrogenase
MAPKK	Mitogen-activated protein kinase kinase

Mcl-1	Myeloid cell leukaemia 1
MDM2	Murine double minute 2
MnSOD	Manganese superoxide dismutase
mTOR	Mammalian target of rapamycin
mTORC2	Mammalian target of rapamycin complex 2
NF-kB	Nuclear factor kappa-light-chain-enhancer of activated B cells
NSCLC	Non-small cells lung cancer
P70S6K1	P70 ribosomal protein S6 kinase
PD1	Programmed death receptor 1
PDK1	3'-phosphoinositide-dependent kinase 1
PD-L1	Programmed death ligand 1
PHLPP	Pleckstrin homology domain leucine-rich repeat protein phosphatase
PI3K	Phosphatidylinositol-3 kinase
PIP2	Phosphatidylinositol-4,5-diphosphate
PIP3	Phosphatidylinositol-3,4,5-triphosphate
PP2A	Protein phosphatase 2A
PTEN	Phosphatase and tensin homologue deleted on chromosome 10
PUMA	P53 upregulated modulator of apoptosis
Rb	Retinoblastoma protein
Rheb	RAS homolog enriched in brain
RPTK	Receptor protein tyrosine kinase
Sesn3	Sestrin 3
SGK	Serum- and glucocorticoid-inducible kinase
Smurf1	SMAD ubiquitination regulatory factor 1
TRAIL	Tumor necrosis factor-related apoptosis inducing ligand
TRIB2	Tribbles homolog 2
TSC	Tuberous sclerosis complex
TSC2	Tuberous sclerosis complex protein 2 or Tuberin
WHO	World Health Organization

1. Introduction

1.1- Cancer

Cancer is characterized by unregulated cell proliferation typically arising as a result of DNA damage/mutations. Typically this occurs by environmental factors such as ultraviolet radiation, diet, pollution or viral infection. However, these can also occur through punctual mutations, errors in replication and/or by failings in the cell's DNA repair machinery (1).

The hallmarks of cancer describe the necessary, minimum genetic alterations that a normal cell must undergo to become transformed (1). These include the evasion of growth suppressors, constitutive proliferative signalling, the avoidance of apoptosis (programmed cell death), the capacity to induce angiogenesis (formation of new blood vessels), replicative immortality and activating invasion/metastasis (1). These six were the original principal hallmarks however since these were described, four additional hallmarks have been incorporated. These are avoiding immune destruction, genome instability, deregulating cellular energetics and tumour-promoting inflammation (1).

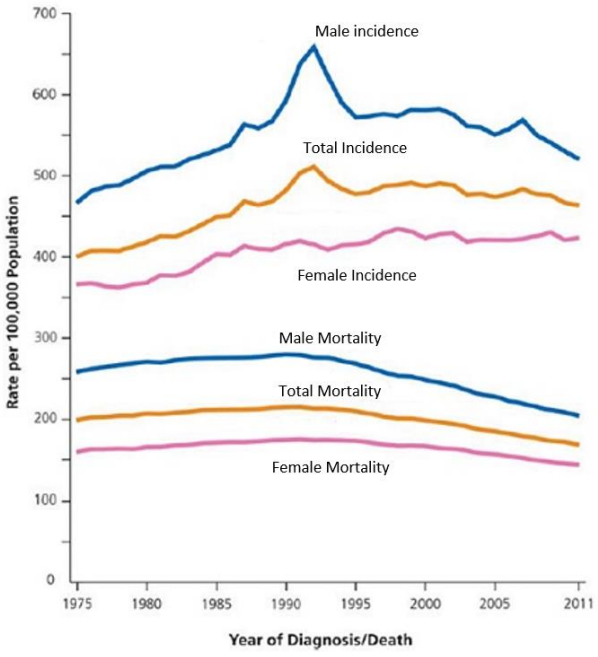

Figure 1.1.1 - Trends in cancer incidence and mortality rates. Trends for both sexes in the United States from 1975 to 2011. Adapted from Siegel et al.; Cancer Statistics, 2015; CA CANCER J CLIN 2015;65:5–29

Cancer in general is a major health issue world-wide. According to the World Health Organization (WHO), 8.2 million people died of cancer world-wide in 2012 and 30 % of cancer cases can be prevented. With the increase of life expectancy, the likelihood of developing any type of tumour also increases (Figure 1.1). Combined with an improvement in detection technics, there was a rise of cancer incidence (2). In compensation, the advances in treatments have allowed to lower the mortality rate.

The tumorigenesis process can be influenced by many factors such as genetic susceptibility and lifestyle, leading to a heterogeneity of tumours amongst patients. Even

the contribution of a person's diet to the development of cancer is not yet fully understood. To add to the problem, there are many examples of tumour resistance to most treatments.

The first step in the standard treatment for a majority of cancers is surgery (if the tumour is located within an operable region). Assuming that the tumour can be removed, the patient will be subjected to adjuvant treatment that includes radiotherapy and/or chemotherapy. Radiotherapy consists of using radiation to damage the DNA and kill any actively dividing cells (including both normal and tumour cells). Chemotherapy uses drugs to achieve the same objective. Chemotherapy must take in consideration many factors such as type of cancer, its extent and localization. Both types of treatment are given in cycles to allow the patients to recover from the inherent toxicities of these therapeutic approaches.

The greatest problems in the treatment of cancer are late diagnosis, poor patient response to treatment and the re-emergence of resistant cancer cells following a variable remission period. Many patients are treated with a combination of chemotherapeutics and still have little to no objective response to therapy. Furthermore, the patients that do have a measurable response typically acquire resistance to treatments in a short period of time. This delay between remission and the emergence of resistant cancer cells is highly variable and is dependent on the type of cancer. Consequently there has been a great focus in developing new therapeutic agents and modalities. One of this new treatments is immunotherapy. This modality is based upon the interplay between the tumours and the microenvironment where they are located. Immunotherapy can be used to increase the patients' immune system to recognise and subsequently eliminate the cancer cells (3). As cancers harbour many genetic mutations, a number of some tumours have proteins that can be recognize as foreign antigens (4). While promising, most tumours are identified as "self" by the host and thus are able to escape immune system detection. The use of targeted molecules capable of inducing an antitumour immune response can help gain a chemotherapeutic effect, by "boosting" the detection capabilities of the immune system (3).

Another approach to cancer treatment is targeted therapy. By investigating the aberrant molecular pathways in cancer, many therapeutic targets have been identified. These potential targets must be as exclusive to the tumour cells as possible to avoid indirectly affecting any normal cells exposed to the therapeutic. Many such chemotherapeutics have already been developed and have proven to be considerably more

effective than the previous non-specific drugs. A prime example is Gleevec© (Imatinib) that targets the mutant fusion protein Bcr-Abl and is used for the treatment of leukaemia. Another example is Vemurafenib that can inhibit the kinase of the mutation *B-RAF*^{V600E} and is used to treat metastatic melanoma (5). The greatest advantage of targeted therapy is that allows to develop a personalized treatment for each patient according to the "characteristics" of their tumour. These (and others) are extensively reviewed in Shtivelman *et al.* (6) .

1.2- Melanoma

Melanoma is a type of skin cancer with its origin in mutated melanocytes. Although a minority amongst the other types of skin cancer (constituting less than 5% of all skin cancer cases), melanoma is responsible for over 80% of all skin cancer deaths (4).

In the last decade, the incidence rate of melanoma has dramatically increased with an average increase of 3-8% per year that continues to rise annually (7). In the United States alone, there will be an estimated 73870 new cases and 9940 deaths for just 2015 alone (2). Men are more prone to develop malignant melanoma (1 in 34) than women (1 in 53). This is thought to be due to sex-specific behaviour and environmental exposure differences (2).

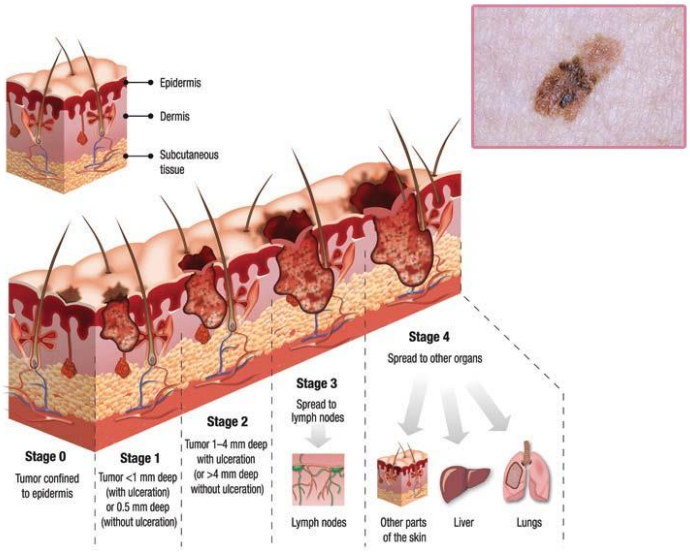

Figure 1.2.1 – Progression of skin cancer. Squematic of histologic progress of melanoma throughout its many stages

Melanoma is a malignant neoplasm of melanocytes, cells specialized in producing melanin (skin pigment) that are localized within the basal layer of the epidermis (8). The transformation of melanocytes can arise from multiple sources such as accumulation of genetic alterations, interaction between environmental factors and impaired DNA repair. Melanoma spreads along the epidermis initially and as the tumour develops it invades in depth through the skin layers (Figure 1.2).

The primary method to recognize a suspicious cutaneous lesion as early melanoma is the ABCDE acronym (asymmetry, border irregularity, colour variegation, diameter and evolving lesions) (8). This method is useful in early detection but it is limited since it cannot evaluate melanomas with vertical growth. This approach is complemented by dermoscopy, a non-invasive procedure that aids in the visualization of sub-surface structures (8).

The staging of melanoma involves many parameters. Initially melanoma is classified based on the thickness (T), the number of lymph nodes affected (N) and the number of metastases (M) (9). Disease stage also takes in consideration ulceration, the rate of mitosis (expressed in number of mitosis per square millimetre of primary tumour) (8) and the levels of lactate dehydrogenase (LDH). The TNM categories are then combined to perform a stage grouping. These are summarized in Table 1.2.1, 1.2.2, 1.2.3 and 1.2.4.

Classification T	**Thickness (mm)**	**Ulceration Status/Mitoses**
Tis (in situ)	NA (not applicable)	NA
T1	≤1,00	a : whiteout ulceration and mitoses < 1/mm^2
		b : with ulceration or mitoses ≥ 1/mm^2
T2	1,01 – 2,00	a : whiteout ulceration
		b : with ulceration
T3	2,01 – 4,00	a : whiteout ulceration
		b : with ulceration
T4	>4,00	a : whiteout ulceration
		b : with ulceration

Table 1.2.1– Tumour thickness classification. According to the 7th edition of the Melanoma staging system by the American Joint Commission on Cancer (AJCC).

Classification M	**Site**	**Serum LDH (lactate dehydrogenase)**
M0	No distant metastases	NA
M1a	Distant skin, subcutaneous or nodal metastases	Normal
M1b	Lung metastases	Normal
M1c	All other visceral metastases	Normal
	Any distant metastases	Elevated

Table 1.2.2 – Lymph nodes classification. According to the 7th edition of the Melanoma staging system by the American Joint Commission on Cancer (AJCC).

Classification N	No. of Metastatic Nodes	Nodal Metastatic Burden
N0	0	NA
N1	1	a : Micrometastasis
		b : Macrometastasis
N2	2 – 3	a : Micrometastasis
		b : Macrometastasis
		c : In transit metastases/satellites without metastatic nodes
N3	4 + metastatic nodes, or matted nodes, or in transit metastases/satellites with metastatic nodes	

Table 1.2.3 - Metastases classification. According to the 7th edition of the Melanoma staging system by the American Joint Commission on Cancer (AJCC).

Stage	Characteristics	Classification			5 year survival rate
		T	N	M	
0	Carcinoma in situ (in epidermis and has not spread to dermis)	Tis	N0	M0	99 – 100 %
I A/B	Lesions up to 2 mm but no nodal or distant metastases	T1a	N0	M0	A – 95% B –88 - 92 %
		T1b	N0	M0	
		T2a	N0	M0	
II A/B/C	Lesions greater than 2 mm, no positive nodes or distant metastases	T2b	N0	M0	A – 77 - 79 % B – 61 - 70% C – 43 - 45%
		T3a	N0	M0	
		T3b	N0	M0	
		T4a	N0	M0	
		T4b	N0	M0	
III A/B/C	Lesions of any size with positive lymph nodes	Tx	N1	M0	A – 57 – 73 % B – 41 – 57 % C – 20 – 34 %
		Tx	N2	M0	
		Tx	N3	M0	
IV	Lesions of any size with distant metastases	Tx	Nx	M1	5 – 22 %

Table1.2.4 – Melanoma staging. According to the 7th edition of the Melanoma staging system by the American Joint Commission on Cancer (AJCC) and respective five-year survival rates.

Of all diagnosed melanomas, 90 % are superficial spreading melanoma, nodular melanoma and lentigno malignant melanoma (that are common in the elderly) (10). The

remaining are acral lentiginous melanoma (palms of the hands and soles of the feet) or non-cutaneous melanomas (ocular, mucosal) (10).

The standard treatment for advance melanoma has for many years been Dacarbazine (DTIC) that was approved by the Food and Drug Administration (FDA) in 1975. Until 2011, DTIC used in combination with interleukin-2 (IL-2) was the only approved treatment for metastatic melanoma (4). Importantly, DTIC only has an average 12% response rate (RR). In Europe, some countries use fotemustine as a 1st line therapy because this nitrosoureas drug has shown a RR of 12-27% (4).

In 2011, Ipilimumab, a safer therapeutic has been approved. Ipilimumab is a recombinant monoclonal antibody raised against the cytotoxic T-lymphocyte associated antigen 4 (CTLA-4) that can help the immune response to tumour antigens (11). CTLA-4 acts as an "immune checkpoint" that downregulates T-cell activation and prevents auto-immunity (3). By blocking CTLA-4, Ipilimumab allows the re-establishment of the proper interaction between T-cell and the antigen presenting cell (10). Many clinical trials with Ipilimumab showed an increase in overall survival (OS) of patients independent of age, sex, stage of tumour or previous treatment(s) (4).

Another group of successful chemotherapeutics is signal transduction small molecule inhibitors such as Vemurafenib, Dabrafenib and Trametinib. The first two are inhibitors of oncogenic BRAF-V600 protein kinase approved by the FDA in 2011 and 2013, respectively (10). Since 40 – 50% of melanomas harbour a *BRAF* mutation, these drugs can oppose its oncogenic activities. Trametinib acts in similar way but it inhibits MEK, a substrate of BRAF (10). Despite good initial responses to these treatments, many tumours develop resistance to these inhibitors (4). Consequently, the investigation to increase the treatment "arsenal" and its many combinations remains imperative.

1.3- The PI3K/AKT pathway

Overall, DTIC has a very poor response rate in the majority of melanoma patients. As such, researchers are trying to identify common conserved mutations in deregulated signalling pathways in cancer that could be therapeutically targeted. One such pathway that has demonstrated a very high number of potential "drugable" molecules is the PI3K/AKT pathway.

The PI3K/AKT pathway is a highly complex, critical cellular network involved in cell proliferation and survival (schematically represented in Figure 1.3.1) (12). This pathway is one of the most frequently mutated pathways (for example, the loss of *PTEN*)

in many human cancers where there is the constitutive activation of phosphatidylinositol-3 kinase (PI3K). In non-transformed cells, following growth or other proliferative signals, PI3K phosphorylates inositol phospholipids generating phosphatidylinositol 3, 4, 5-trisphosphate, (PIP_3). PI3K is a heterodimer that is composed of a catalytic subunit (p110) and a regulatory subunit (p85) (13). Typically PI3K is activated by either a receptor protein tyrosine kinase (RPTK) or a G-protein coupled receptor (GPCR) (13). The conversion of the plasma membrane lipid PI(4,5)P2 (PIP_2) into PIP_3 by active PI3K is extremely rapid (normally within seconds) (12). Once generated, PIP_3 specifically binds to at least two distinct protein-lipid binding domains, principally the FYVE (Fab-1, YGLO23, Vps27 and EEA1) domain and/or pleckstrin homology (PH) domains (14). These PH domains are present in many proteins including the protein kinase B (PKB, also known as AKT) and the serine/threonine kinase 3'-phosphoinositide-dependent kinase 1 (PDK1) (12).

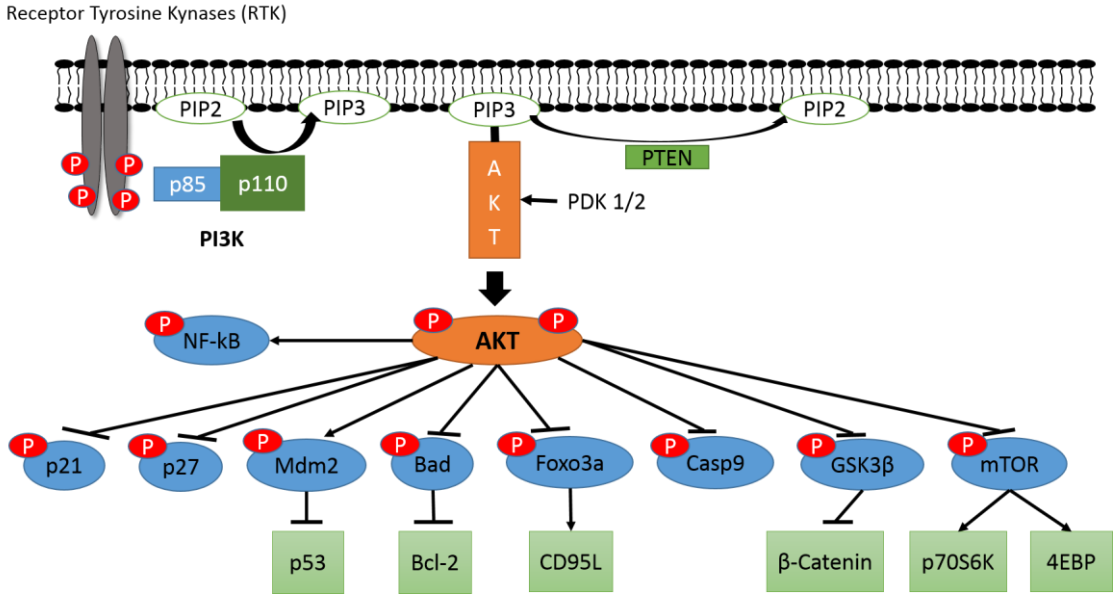

Figure 1.1.1 – Schematic of the PI3K/AKT pathway. Activation of RTK leads to recruitment of PI3K to the membrane and activation of the catalytic subunit. This initiates production of PIP3, which in turn recruits PDK1/2 and AKT. Activated AKT uses phosphorylation to activate and inhibit many different targets involved in cell survival, growth and proliferation. PTEN is a negative regulator of the pathway by converting PIP3 back to PIP2.

AKT is a 57 kilo-Dalton serine/threonine kinase that acts by the phosphorylation of downstream protein targets. Mammalian species possess 3 AKT genes: *AKT1*, *AKT2* and *AKT3* (15). However their protein expression varies in a tissue-specific manner. AKT1 expression is very high in brain, heart and lung. In contrast, AKT2 protein expression is highest in skeletal muscle and embryonic brown fat tissue (16). AKT3 is predominantly expressed in brain, kidney and embryonic heart(17).

Following AKT/PIP_3 binding, AKT is activated by PDK1 and is phosphorylated at the threonine 308 residue (Thr308) (18). A secondary phosphorylation occurs at serine 473 (Ser473) by the action of different kinases such as mammalian target of rapamycin complex 2 (mTORC2) and integrin-linked kinase (ILK) (19). Although a dual phosphorylation is necessary for a full activation of AKT, a Thr308 p-AKT is still capable of phosphorylate some but not all of its substrates.

The active AKT is translocated (by a currently unknown mechanism) from the cell membrane into the cytoplasm and from here, into many others cellular compartments (including the nucleus, Golgi, endoplasmic reticulum and mitochondria), where its target substrates are located (19,20). Once activated, AKT inhibits the GSK3 (glycogen synthase kinase 3) protein by direct phosphorylation (20). With GSK3 inhibition, its targets such as β-catenin are not phosphorylated, which impedes their degradation. This allows β-catenin to translocate to the nucleus, where it interacts (both directly and indirectly) with transcription factors to regulate the expression of several genes such as *cyclin D1*. Cyclins are proteins which are involved in cell cycle checkpoints, in combination with cyclin-dependent kinases (CDKs) to regulate the cell cycle (21). The cyclin D1 protein is very important because not only is it a positive regulator for the G_1/S checkpoint transition in the cell cycle, but it is also a direct target of GSK3β (22). Cyclin D1 binds to CDK4, forming a cyclin/CDK complex that phosphorylates the retinoblastoma protein (Rb). The phosphorylation of Rb leads to the activation of genes required for the cell cycle progression (23). As such, AKT can positively regulate G_1/S cell cycle progression through inactivation of GSK3β and nuclear accumulation of cyclin D1.

AKT can also stop the inhibition of Cyclin/CDK complexes by the phosphorylation of $p21^{Waf1/Cip1}$ (p21) and $p27^{Kip2}$ (p27) (24,25). Once phosphorylated, the p21 protein is retained in the cytoplasm and cannot inhibit the cyclin D-CDK4 complex while p27 is relocated from the nucleus into the cytoplasm, preventing p27-mediated inhibition of cyclin E-Cdk2 and cyclin A-Cdk2 (19).

AKT can also affect protein synthesis through regulation of mTOR (mammalian target of rapamycin). The mTOR protein is a serine/threonine kinase that exists in two different protein complexes: mTORC1 and mTORC2 (26). Among its components, a relevant difference between them is the Raptor (regulatory-associated protein of mTOR) accessory protein in complex 1 and Rictor (rapamycin-insensitive companion of mTOR) accessory protein in complex 2 (26). mTORC1 can elevate mRNA translation by

activating the p70 ribosomal protein S6 kinase (p70S6K1) and inhibiting the repressor eIF4E-binding protein (4E-BP) (27). The regulation of mTORC1 is by the tuberous sclerosis complex (TSC), a heterodimer of hamartin (TSC1) and tuberin (TSC2). The TSC acts as a GTPase-activating protein (GAP) that negatively regulates Rheb (RAS homolog enriched in brain), a small GTPase that is required for mTORC1 activation (27). AKT can phosphorylate TSC2, impeding the formation of the TSC complex and leading to the activation of mTORC1.

Another interesting interaction between AKT and mTOR is through the mTORC2. This complex can regulate metabolism, cytoskeleton (28) and it can also phosphorylate AKT at Ser473 (26,27). Additionally, mTORC2 can phosphorylate the Thr450 residue upon the translation of nascent AKT, implying that mTORC2 activity is regulated by signals that promote AKT translation (28).

AKT can also promote cell survival by activating the cyclic AMP-response element binding protein (CREB). Phosphorylation of CREB induces the binding of accessory proteins that are needed for the transcription of anti-apoptotic genes, including *Bcl-2* (B-cell lymphoma 2) and *Mcl-1* (myeloid cell leukaemia 1) (19). Related to this function, AKT can affect apoptosis by the phosphorylation of BAD (Bcl-2-associated death promoter). Bad controls the release of cytochrome c from mitochondria to initiate the caspase cascade, a process that is critical for the induction of apoptosis (12). BAD can also bind to Bcl-2 or Bcl-XL (B-cell lymphoma-extra-large), therefore blocking their anti-apoptotic activities (19). When phosphorylated by AKT, the BAD-Bcl-2/Bcl-XL complexes are disrupted and BAD is bound instead to the 14-3-3 chaperon protein, being sequestered into the cytosol. In addition, AKT will also phosphorylate BAX (Bcl-2-associated X protein), blocking its translocation to the mitochondria (19). Another way that AKT directly affects the apoptotic response is the inactivation of pro-caspase9, impeding the initiation of caspase cascade, and the phosphorylation of MDM2 (murine double minute 2), leading to the inhibition of p53-mediated apoptosis (19). A critical AKT protein target are the members of the FOXO (Forkhead box O) family of transcription factors including FOXO1a, FOXO3a and FOXO4 (19). These transcription factors have an essential role in promoting apoptosis and inducing cell cycle arrest. These (FOXOs and p53) are discussed in depth in section 1.4 and 1.5 respectively.

AKT can also activate the inhibitor of kappa B kinase-α (IKKα), leading to the phosphorylation of I-kappa-B (I-kB), marking it for degradation and stopping its inhibitory function over NF-kB (nuclear factor kappa-light-chain-enhancer of activated

B cells) (19). The free NF-kB can translocate to the nucleus and stimulate the transcription of pro-survival genes including the *inhibitor of apoptosis protein 1* (*IAP1*) and *IAP2* (19).

The PI3K/AKT pathway is negatively regulated by PI-3, 4, 5-P_3 phosphatases including the phosphatase and tensin homologue deleted on chromosome 10 (PTEN) (12,29). This phosphatase dephosphorylate PIP_3 into PIP_2, thus preventing the activation of AKT. Other phosphatases capable of regulating this pathway are protein phosphatase 2A (PP2A) and the pleckstrin homology domain leucine-rich repeat protein phosphatase (PHLPP) family (19). These phosphatases are able of dephosphorylating the thr308 and ser473 AKT residues respectively, thus inactivating the network.

1.4- FOXO proteins

The Forkhead box O (FOXO) family are transcription factors with a highly conserved DNA binding domain (30). In mammalian cells, four FOXOs have been identified: FOXO1, FOXO3a, FOXO4 and FOXO6. FOXOs can act either as transcriptional activators or as repressors, depending on additional co-factors recruited alongside them when they are bound to DNA (30). FOXOs are critical effectors of the PI3K pathway and when growth factors, cytokines or hormones activate the PI3K pathway, FOXOs are phosphorylated by AKT and are bound by the 14-3-3 chaperon protein (31,32). This FOXO/14-3-3 complex formation prevents FOXO-DNA binding and directs the cytoplasmic retention of FOXOs (30). Other kinases have been identified that are able to induce the cytoplasmic relocation of FOXO, such as serum- and glucocorticoid-inducible kinase (SGK), cyclin-dependent kinase- 2 (CDK2) and IκB kinase (33). By directing the cytoplasmic accumulation of FOXOs (and their subsequent ubiquitin-dependent proteomic degradation), activated AKT can prevent FOXO-dependent gene transcription preventing cell cycle arrest and apoptosis (summarized in figure 1.4.1).

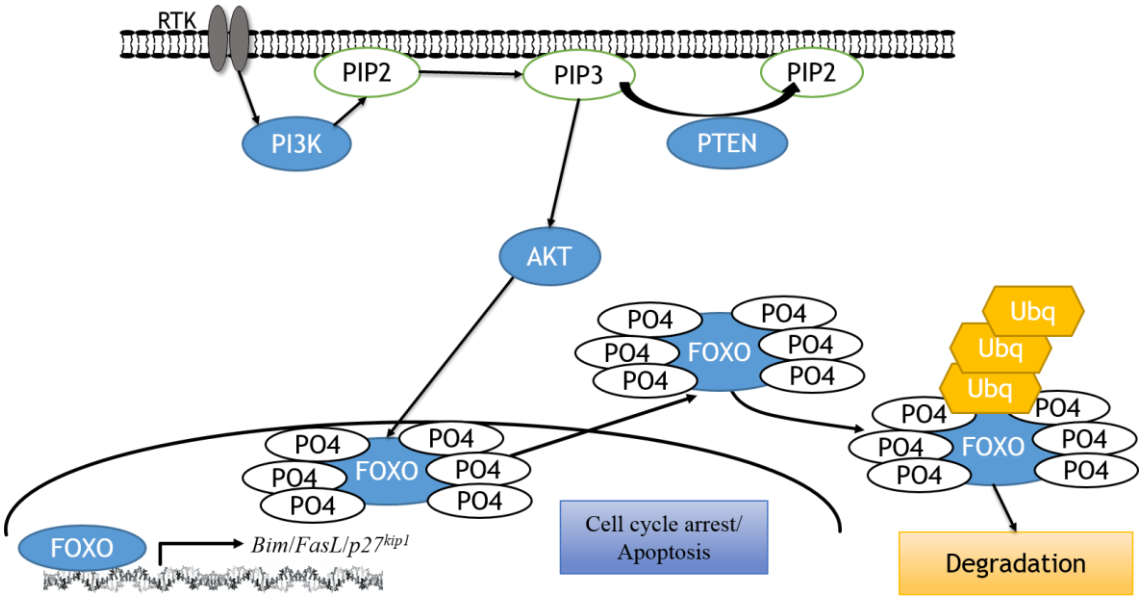

Figure 1.4.1 - Schematic of FOXO cytoplasmic translocation and sequential degradation.
Activated AKT translocate to the nucleus (unknown mechanism) and phosphorylates FOXO. FOXO is then translocated to the cytoplasm where it suffers polyubiquitination and subsequent degradation.

FOXOs have a major role in proliferation, apoptosis, metabolism, inflammation, differentiation and stress resistance (32). Amongst the genes currently known that are regulated by FOXOs are *p27*, *p21*, *p15* and *p19*. The p15 and p19 proteins are Cdk inhibitors that block the binding of cyclin D to CDK4 and CDK6 (30). As mentioned before, the p27 and p21 proteins are also CDK inhibitors necessary for cell cycle checkpoints regulation. Through the regulation of the expression of these genes/proteins, FOXOs are able to modulate the G1/S and G2/M transition of the cell cycle. In addition, it has been showed that activation of FOXO3 alone is sufficient for p27 upregulation and inhibition of proliferation (30).

During oxidative stress, FOXOs can coordinate the regulation of manganese superoxide dismutase (MnSOD) and catalase expression to decrease oxidative damage and increase cellular survival (30,34). Another way that FOXOs favours cell survival is by maintaining energy homeostasis through *Sestrin3* (Sesn3) and *Rictor* expression. Inducing the expression of these genes results in inhibition of mTORC1 activity (major energy consumer) and an increase of mTORC2 activity, leading to the activation of AKT (which increase energy metabolism) (27).

In regard to regulating apoptosis, FOXOs can modulate the expression of *BIM* (*Bcl-2 interacting mediator of cell death*, also known as *BCL2L11*), *PUMA* (*p53 upregulated modulator of apoptosis*) and *Bcl-6* to induce the intrinsic apoptotic pathway. Alternatively, FOXOs upregulate the death receptor ligands *FasL* (*Fas-ligand*, also

known as *CD95L*) and *TRAIL* (tumour necrosis factor-related apoptosis inducing ligand) to activate the extrinsic apoptotic pathway (30). FasL is the key death factor of receptor-triggered programmed cell death in immune cells (35,36). It has an important role in termination of immune responses, elimination of autoreactive cells and the establishment of immune privilege. Tumour cells that constitutively express FasL on their surface are able to generate a tumour-associated immune privilege, evading the immune surveillance and even kill tumour infiltrating lymphocytes (35). It has also been shown that FOXOs also play a role in preserving the self-renewal capacity of hematopoietic stem cells (33).

FOXO factors have been shown to be deregulated in many types of cancer such as breast, prostate, glioblastoma, rhabdomyosarcoma and leukaemia (33). Because of their role in regulating genes involved in apoptosis and cell cycle arrest, inactivation of FOXOs is an important step in tumorigenesis. As tumour suppressor genes, FOXOs are of extreme importance in the development of treatments against cancer. The study of how the many different signalling pathways affect the FOXO proteins have already shown that these factors are need for the current chemotherapeutics to have a cytostatic or cytotoxic effect on tumour cells (31,33). As such, FOXOs can be considered as biomarkers for treatment prognostics and risk assessment of patients. For example, cytoplasmic location of FOXO3a correlates with poor survival in breast cancer (33). New drugs that can influence the expression of FOXOs or that can affect their subcellular translocation will bring alternative approaches to chemotherapy. Combination treatments with drugs that activate FOXO can synergize with standard chemotherapeutics to sensitize tumour cells, opening new ways to counteract cancer resistance. However, the use of FOXO transcription factors must be well study because their ability to activate survival signalling and feedback mechanisms between FOXO family members may limit clinical utility.

The role of FOXOs on melanoma ranges from initial tumorigenesis all the way to treatment resistance. Melanoma is known to have the PI3K pathway constitutively active from either mutation of RTKs, PI3K or loss of PTEN. With AKT constantly active, the phosphorylation of FOXOs and its subsequent degradation will lead to uncontrolled proliferation. As for resistance, given that many current chemotherapeutics need FOXOs to exert their cytostatic/cytotoxic effect, tumour cells can counter treatments with cross-talk between signalling pathways that have FOXO as a common downstream target. For example, FOXO3a is a common target of three oncokinases: AKT, IKK and ERK (33). All three kinase-mediated phosphorylation induce FOXO3a ubiquitination and

subsequent degradation. Reverting their action over FOXO3a can re-sensitize tumour cells to chemotherapeutics.

1.5- The tumour suppressor p53

Similar to FOXO-family members, the tumour suppressor protein p53 is a transcription factor that regulates many genes involved in cell cycle arrest, apoptosis, senescence, autophagy and metabolism. Due to the importance of p53 in multiple cellular networks and preserving the cells genome, p53 is commonly referred to as "the guardian of the genome"(37).

Under normal cellular conditions, p53 exists in the cell bound to its negative regulator MDM2 (murine double minute 2) (schematically represented in Figure 1.5.1). In response to stress signals (for example DNA damage), p53 can be phosphorylated, abrogating the MDM2 interaction, allowing p53 levels to accumulate leading to the transcriptional induction of a vast array of target genes (37,38).

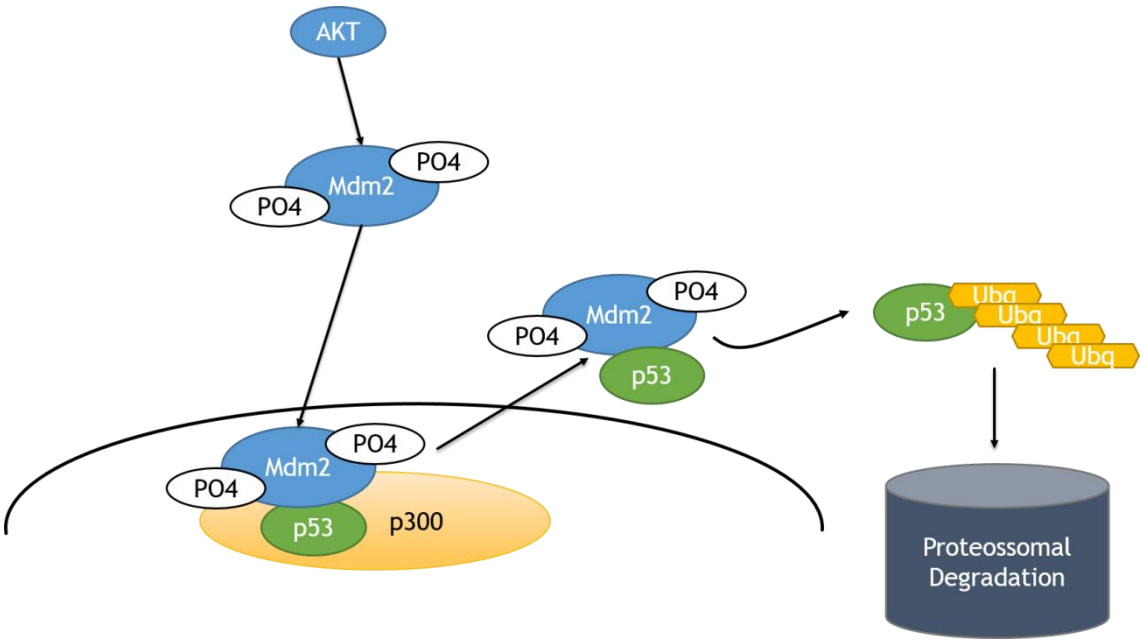

Figure 1.5.1 - Schematic of p53 degradation.
Activated AKT phosphorylates Mdm2, which in turn will bind to p53. P53 then suffers ubiquitination and is degraded by proteasomes.

When MDM2 is phosphorylated, it will shift the balance p53/MDM2 in three ways (37). First, it abrogates the transcriptional activity by binding to the N-terminal of the transactivation domain of p53. Second, it induces nuclear export of p53 through mono-ubiquitination. Lastly, it destabilizes p53 through poly-ubiquitination and subsequent proteasomal degradation (Figure 1.5.1).

As an E3 ubiquitin ligase, MDM2 has the ability to attach an ubiquitin chain of 76 amino acids to its target protein (38). This action is facilitated by MDM4, an E4 ligase (also known as ubiquitin chain elongating factors) that mediates the elongation of the ubiquitin chain previously established by MDM2 (38). Importantly, *Mdm2* is a transcriptional target of p53, creating a feedback loop between them. This loop is the primary mode through which p53 autoregulates its levels.

The p53 transcription factor has always been of major interest in the fight against cancer. Because of its diverse biological functions that thwart tumorigenesis, the status of p53 has become a standard evaluation in cancer patients. In fact, p53 is the most mutated gene in human cancer, with a mutation rate that varies from 5% to 95% according to tumour type (39). Most mutations occur in the DNA binding domain. Even if the tumour cells retain the wildtype p53, it is often non-functional through its regulation mechanisms being altered (40).

In chemotherapy, p53 has an important role in chemosensitization and radiosensitization of tumour cells. As such, drug development is focusing p53 in four different approaches 1) activate wildtype p53, 2) reactivate mutant p53, 3) selectively kill cells with mutant p53 and 4) temporally inhibit wildtype p53 for normal cell protection (40).

In the particular case of melanoma, p53 has a mutation frequency of 10-20%. This is curious given that the background mutational load of melanoma is one of the highest in human cancer, comparable to lung and colon cancer (39). Although melanoma retains a wildtype p53, its functions are inactivated by other means. One way is through the deletion of *CDKN2A* (*cyclin-dependent kinase inhibitor 2A*), which leads to the loss of $p14^{ARF}$, an inhibitor of MDM2 that prevents the targeting of p53 for degradation. Another mechanism is through the amplification of MDM2, leading to the destabilization of p53/MDM2 homeostasis (39,41).

Another possibility is the constitutive activation of the PI3K pathway. AKT phosphorylates MDM2 in both the nucleus and the cytoplasm, leading to the degradation of p53 through the methods described above. This link between p53 and AKT is of extreme importance in the development of new treatments for melanoma.

1.6- Novel Therapeutics in the Treatment of Melanoma

With modern drug development, many new drugs are being developed focusing in the cross-talk between different signalling pathways as a way to avoid resistance. As seen

with Vemurafenib, cancer cells can "counter-act" the inhibition of BRAF by, for example, re-activation of downstream targets such as ERK (4). A way to delay or circumvent the resistance to BRAF inhibitors is to combine them with MEK inhibitors such as Trametinib, which is being tested in clinical trials.

A key example of combined targeted therapies is the PI3K/AKT pathway. As this pathway interacts with and signals via RAS/RAF/MEK/ERK components at multiple points, resulting in cross-activation, cross-inhibition and pathway convergence, these targets could, in principle be individually targeted in combinational therapy to either restore drug sensitivity or to reduce the possibility of emerging resistant cancer cells(3). This is particularly noted in breast cancer resistance. Trastuzumab (marketed as Herceptin) is a recombinant monoclonal antibody that binds to the extracellular domain of HER2 (Human Epidermal growth factor Receptor 2) (42) and used to treat HER2+ breast cancers. Trastuzumab blocks the formation of HER2-HER3 heterodimers and also the binding of HER3 to PI3K (43). Many laboratory models of resistance have demonstrated that the loss of PTEN can reduce the anti-tumour effect of Trastuzumab as well as mutational activation of PI3K (42). As a consequence of this, many PI3K and AKT inhibitors are being tested in clinical trials as a means to reverse resistance to Trastuzumab in dual treatment regimens(43,44).

The PI3K, mTOR and AKT inhibitors can be used in many types of cancer, since they can target one of the most mutated pathways in human cancer. The mTOR inhibitors such as rapamycin and everolimus to test the PI3K signalling blockade in melanoma through inhibition of mTORC1 (45). Unfortunately, the efficacy of mTORC1 inhibitors is limited by dysregulation of negative feedback loops (45). PI3K inhibitors, such as wortmannin and LY294002 (46), and AKT inhibitors, such as afuresertib and MK2206 (44,47), showed positive results in pre-clinical models (47). Although positive, this results only confirmed that single-agent inhibition of the PI3K/AKT pathway is often cytostatic rather than cytotoxic, with activation of compensatory pathways (48).

The development of dual PI3K-mTOR inhibitors, such as NVP-BAG956, NVP-BBD130 and NVP-BEZ235, was an important step that showed impressive antiproliferative activity both in vitro and in vivo (45,46). In particular, BEZ235 is a potent pan-PI3K inhibitor that blocks mTOR by targeting the ATP-binding site of mTORC1/mTORC2 (46) and is currently in clinical trials (47,49). As mentioned before, cross-talking between signalling pathways has become a focus in the development of new therapies. The dual PI3K/mTOR inhibitors can synergize with BRAF and MEK

inhibitors, sensitizing back tumours who previously acquired resistance to this drugs (50–52). A prime example is the combination of Vemurafenib with BEZ235, currently being tested in pre-clinical studies but already showing promising results. More combinatorial targeted therapies are extensively reviewed in Grazia et al. (47).

Another approach is the improvement of immunotherapies and their combination with cytotoxic agents and/or targeted therapies. Nivolumab (BMS-936558, MDX – 1106) is a fully human IgG4 antibody that blocks the PD-1 (programmed death 1) receptor. PD-1 interacts with PD-L1 (Programmed death ligand 1), inhibiting T-cell proliferation and cytotoxic functions (4). The interaction PD-1/PD-L1 plays an important role in tumour-induced immunosuppression in many advanced malignancies. Nivolumab has demonstrated clinical activity in patients with melanoma, renal-cell carcinoma and non-small-cell lung cancer (NSCLC) (10). Currently, a combination of Ipilimumab and Nivolumab is being studied and already shows early phase results of rapid and deep response of 80% (NCT01783938; NCT01024231) (53).

An alternative to complement current therapies is the use of phytochemicals. These are naturally occurring chemical compounds such as flavonoids and phytoalexins that can be found in common food (peanuts, red wine, grapes, strawberries, etc.).Phytochemicals are remarkably nontoxic and have proven their ability in preventing the development of cutaneous malignancies (45). They are currently being studied as potential adjuvant therapies for metastatic melanoma (45).

1.7- The Tribble2 homolog

Originally identified as *tribbles* in *Drosophila*, TRIB2 is pseudokinase which functions as a signalling modulator and mediator (54). Mammalian cells possess three Trib homologs: Trib1, Trib2 and Trib3 (55). All three Trib have been associated with human malignancies by interacting with pathways involved in cell survival and apoptosis. Trib proteins interact with many signalling molecules and transcription factors such as activating transcription factor 4 (ATF4), p65, mitogen-activated protein kinase kinase (MAPKK), AKT and constitutive morphogenesis 1 (COP1) (55).

Like all Trib proteins, TRIB2 has three main domains: an N-terminal, a C-terminal and a kinase domain. It belongs to the pseudokinase family because its central region (kinase domain) possess high homology with serine/threonine kinases but deviations in the catalytic loop eliminates its catalytic activity (Figure 1.7.1). Although it is a phosphoprotein, it is theorized that TRIB2 is unable of autophosphorylate itself (55).

TRIB2 has two important motifs on its C-terminal domain: MEK1 and COP1 binding sites. Through the MEK1 motif, TRIB2 is able to interact with the RAS/MEK/ERK signalling pathway and enhance ERK phosphorylation (54). TRIB2 can bind to COP1, an E3 ubiquitin ligase, through the COP1-binding site and promote proteasome-mediated degradation (54). One known target is the C/EBP

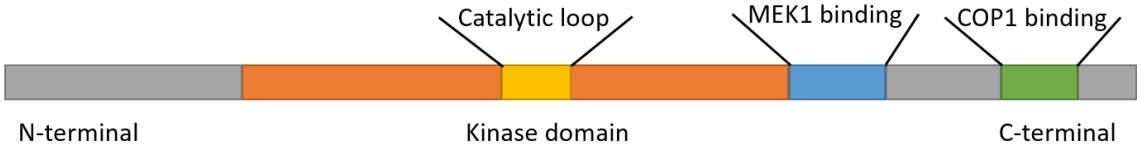

Figure 1.7.1 - Representation of TRIB2. Kinase domain and C-terminal are highly conserved, with two binding motifs for MEK1 and COP-1.

(CCAAT/enhancer-binding protein) family of transcription factors. By facilitating C/EBP-α degradation, TRIB2 aids in myeloid differentiation. This characteristic marked TRIB2 as an oncogene for acute myeloid leukaemia (AML). (54,56). Further studies brought to light that TRIB2 is commonly overexpress in many types of cancer such as lung adenocarcinoma, cervical carcinoma, liver cancer and malignant melanoma (55–59). In the case of melanoma, TRIB2 can be used as a biomarker since its expression correlates with the tumoral progression (60).

Another important fact is that TRIB2 was found to be a negative regulator of the FOXO family of transcription factors (59). TRIB2 can interact with AKT, leading to the inactivation and degradation of FOXO proteins. This implies that TRIB2 may be involved in mechanisms of cancer resistance.

Since TRIB2 is a pseudokinase, the mechanisms through which it exercises its functions is currently unknown. The main possibility is that TRIB2 acts as an adaptor that binds multiple proteins and brings them together. Given its proven role over FOXOs and in tumorigenesis, elucidation of how TRIB2 interacts and activates survival signalling can be an important step in cancer treatment.

1.8- Hypothesis

The previous work of our group showed that TRIB2 is a biomarker of diagnosis and progression of melanoma. Recent studies in our laboratory revealed that TRIB2 involved in mechanisms of drug resistance to many chemotherapeutics, including PI3K inhibitors currently in clinical trials. Based in our research, this work intends to characterize the TRIB2 pseudokinase following PI3K inhibition, its regulation, the domain responsible

for the activation of survival signalling molecules such as AKT and how it relates to drug resistance in cancer.

2. Materials and Methods

2.1- Cell lines and reagents

The human cell lines HEK293T (embryonic kidney cells), U2OS [p53+/+], were maintained in DMEM supplemented with 10% FBS (Sigma, PT) and antibiotics (Gibco, US). Antibodies used in my studies are shown in Table 2.1.1 and were used for our immunoblots. Signal visualization was achieved using a ChemidocXRS+ system (BioRad, PT). Dacarbazine (Sigma, PT), gemcitabine hydrochloride (Eli Lilly #VL7502), AKT inhibitor VIII (Calbiochem, US), BEZ235 (Novartis, US), BAY806946, BAY 1082439, BAY1001931 (a gift from Bayer Healthcare, Germany), rapamycin (Sigma, PT), actinomycin D (Sigma, PT), and cycloheximide (Sigma, PT) and MG132 (Sigma, PT) were used at the following concentrations (Actinomycin D (ActD) 5 μg/ml, Cycloheximide (CHX) 50 μg/ml, MG132 at 1 μM).

Primary Antibodies	Species	Information	Supplier
Actin	goat	I-19; sc-1616	Santa Cruz Biotechnology
Total AKT	goat	C-20; sc-1618	Santa Cruz Biotechnology
p-AKT	rabbit	Ser473; sc-7985	Santa Cruz Biotechnology
BIM	rabbit	H-191; sc-11425	Santa Cruz Biotechnology
P27	mouse	F-8; sc-1641	Santa Cruz Biotechnology
MDM2	rabbit	C-18; sc-812	Santa Cruz Biotechnology
p-MDM2	rabbit	Ser 166; sc-293105	Santa Cruz Biotechnology
p-Mdm2	rabbit	S166; 3521S	Cell Signalling Technology
Lamin A/C	mouse	N-18; sc-6215	Santa Cruz Biotechnology
TRIB2	rabbit	custom	Home-made, generated at CNIO (Madrid, Spain)
FasL	rabbit	C-178; sc-6237	Santa Cruz Biotechnology
Total Foxo3a (FKHRL1)	goat	N-16; sc-9813	Santa Cruz Biotechnology
p-Foxo3a (p-FKHRL1)	rabbit	Ser 253; sc-101683	Santa Cruz Biotechnology

Table 2.1.1- Primary antibodies used. Datasheets of each antibody are on Appendix A1-A11.

2.2- Western blot analysis

For the preparation of whole cell lysate, cells were harvested and lysed using RIPA buffer (50 mM Tris-HCl pH 7.4, 1% NP-40, 0.5% Na-deoxychlorate, 150 mM NaCl, 1

mM EDTA, 2 mM NaF, 2 mM NaVO4 and 1x protease inhibitor cocktail (PIC) (Sigma). We used the Bradford assay, with the Quick Start TM Bradford 1x Dye Reagent (Bio-Rad). We prepare PCR tubes with 99 µl of Bradford. We dilute 1 µl of sample in 10 µl of H_2O. We then add 1 µl of the dilution to the tubes. The blank tube was prepared with 100 µl of Bradford only. We analysed in the Nanodrop 2000/2000c Thermo Scientific by using 2 µl of each tube. For SDS–PAGE, protein samples were boiled for 5–10 min in protein sample buffer (50 mM Tris pH 6.8, 1% SDS, 10% glycerol, 0.01% Bromophenol Blue, β-mercaptoethanol [50 µL per 950 µL sample buffer]). Following electrophoresis, proteins were transferred onto nitrocellulose membrane (BioRad). The membrane was blocked for 1 hour at room temperature or overnight at 4°C 5% BSA 0.1% $tween_{20}$ blocking buffer. Primary antibodies were added to the membrane (Supplemental Table 1) overnight at 4°C or for 2 hours at room temperature. Secondary antibody was added (Supplemental Table 2) at typically 1:5000 dilution for 1 hour at room temperature. Visualization of signal was achieved using a ChemidocXRS+ Imaging System (BioRad).

Secondary Antibodies	**Species**	**Information**	**Supplier**
Anti-rabbit	goat	IgG-HRP; sc-2030	Santa Cruz Biotechnology
Anti-goat	donkey	IgG-HRP; sc-2020	Santa Cruz Biotechnology
Anti-mouse	goat	IgG-HRP; sc-2005	Santa Cruz Biotechnology
Anti-mouse	rabbit	IgG; A9044	Sigma

Table 2.2.1 – Secondary antibodies used. Datasheets of each antibody are on Appendix A12-A15.

2.3- Constructs

A 3062 bp fragment encoding the entire human Trib2 (hTRIB2) cDNA was sub-cloned into pEGFP-N1 or pIREPuro2 plasmids, (one co-expressing GFP, the other containing a V5 tag.). Full length human TRIB2 (hTRIB2, 1-343 aa), dN (63-343aa hTRIB2, dC (1-304 aa) hTRIB2, KD (63-304 aa) hTRIB2, NT (ΔCT, 1-250 aa) hTRIB2, CT (ΔNT, 270-343 aa) hTRIB2 and ΔCOP1 hTRIB2 were kindly provided by W.S. Pear and shown in Table 3. Each was cloned into pMigR1-myc plasmid (55). All cDNAs were sequenced in their entirety to verify there were no mutations in any of our constructs. Each construct was transfected (Polyplus Transfection jetPRIME® transfection reagent) following the manufacturers guidelines (Appendix B). After transfection, the plates were incubated for 24 hours or selection and screening initiated.

Plasmids constructs	Mutant
#1	Full length TRIB2
#2	Δ COP1
#3	Δ N
#4	Δ C
#5	Kinase domain
#6	C term
#7	N term

Table 2.3.1 – TRIB2 plasmids constructs used

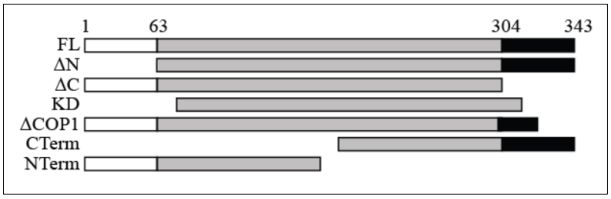

Figure 2.3.1 – Schematic of TRIB2 mutants. Different regions deleted in the TRIB2 plasmids constructs.

2.4- Flow cytometry cell cycle analysis

Cells were grown to 70% confluence. Cells were mock treated/exposed to each compound for the time points indicated. Samples were collected, washed (PBS) and fixed (70% ethanol). Ethanol was removed and samples were ressuspended in PBS. Propidium iodide (2.5 mg mL) was added to each sample. Samples were run on a Fluorescence Activated Cell Scanner (FACS) and the percentage populations (sub-G_1, G_1, S and G_2 phases) determined. 10,000 total events were scored per study Data was analysed using Infinicyt (Cytognos).

2.5- FACS sorting

Cells were grown to 70% confluence. Cells were mock treated/exposed to each compound for the time points indicated. Samples were collected, washed (PBS) and fixed (70% ethanol). Ethanol was removed and samples were ressuspended in PBS. Samples were run on a Fluorescence Activated Cell Sorter (FACS) and the GFP positive and GFP negative populations separated. 50,000 total events were scored per study. Data was analysed using Infinicyt (Cytognos). The sorted samples were stored at 4^0C until the following day prior to sample collection for immunoblotting.

2.6- Immunoprecipitation

The samples sorted by FACS were collected with 50 µl each of total protein lysis buffer (50 mM Tris pH 7.5, 1% NP-40, 0.1% Na-deoxychlorate, 130 mM NaCl, 5 mM EGTA, 10 mM NaF, 2,5 mM NaVO4 and 1x protease inhibitor cocktail (PIC)). Stored at -80^{0}C for 24 hours. On the following day, added to each sample 5 µl of antibody and left them spinning on the "end-over-end" overnight at 4^0C.

Prepared beads with Protein G Sepharose Fast Flow (20 µl/sample) and PBS. Spin for 2 minutes at 1.300 rpm. Ressuspended with 1ml PBS and spin again. Repeated the last step but added PBS in an equal amount to the total volume of beads. Added 20 µl of the beads solution prepared and 300 µl of PBS to each sample. Left the samples spinning in the "end-over-end" for 1 hour at room temperature. Centrifuged for 2 minutes at 1.300 rpm. Removed supernatant and kept the beads. Added 300 µl of PBS and repeated the spin. Removed the supernatant and prepared the samples with 30 µl of 2x laemmli buffer. Boiled the samples for 5 minutes at 98^0C. Proceeded by following the western blot protocol indicated above by loading 25 µl of each sample to the gel.

2.7- Co-Immunoprecipitation

Cells were harvested using total protein lysis buffer (50 mM Tris pH 7.5, 1% NP-40, 0.1% Na-deoxychlorate, 130 mM NaCl, 5 mM EGTA, 10 mM NaF, 2,5 mM NaVO4 and 1x protease inhibitor cocktail (PIC)). We used the Bradford assay and the Nanodrop 2000/2000c Thermo Scientific for protein quantification, as mentioned above.

Prepared α-GFP probes with Protein G Sepharose Fast Flow, antibody against GFP and PBS. Spin the probes for 1 h in the "end-over-end" at room temperature. Centrifuged for 1 minute at 1.300 rpm. Washed 2 times with PBS. Ressuspended with PBS.
Calculated amounts required for 250 µg of protein, probe and PBS for each sample. Add all to an Eppendorf and spin again in the "end-over-end" for 1h. Centrifuged for 1 minute at 1.300 rpm. Washed 2 times with 1 ml of PBS. Removed the supernatant and eluted with 50 µl of 2x Laemmli buffer. Boiled the samples for 5 minutes at 98^0C and stored them at -80^0C.

2.8- RNA extraction/First strand cDNA protocol

We used the TRI-reagent protocol from Sigma (Appendix C). The resulting RNA samples were then used to make first strand cDNA with NZY First-strand cDNA Synthesis Kit from Nzytech (Appendix E). Samples were stored at -18^0C.

2.9- qRT-PCR /DNA electrophoresis agarose gel (1 %)/Primer validation

We used the LuminoCt® SYBR® Green qPCR Ready Mix™ protocol from Sigma (Appendix F).

Primers	Supplier
GAPDH	Nzytech
TRIB2	Nzytech
PTEN	Nzytech
MDM2	Nzytech
FasL	Nzytech
P27	Nzytech
TRAIL	Nzytech
Cyclin D1	Nzytech
P19	Nzytech
BIM	Nzytech
P21	Nzytech

Table 2.9.1 – List of primers used

We then ran a 1% agarose electrophoresis gel to analyse the amplified products.

2.10- Chromatin Immunoprecipitation assay (ChIP)

The plates were washed with ice-cold 1x PBS twice and added a 1% formaldehyde/PBS solution to each for cross-linking the proteins with the DNA. Plates were incubated at 37^0C for 10 minutes and washed again with ice-cold 1x PBS twice. The plates were scraped with 1 ml Scrape buffer (1M Tris-HCL with 10 mM DTT), collected in eppendorfs and incubated in water bath at 30^0C for 15 minutes. The tubes were centrifuged and washed with ice-cold 1x PBS, Buffer I (10% Triton X-100, 100 mM EDTA, 100 mM EGTA, 0,5 M HEPES) and Buffer II (100 mM EDTA, 100 mM EGTA, 0,5 M HEPES in 5M NaCl) . The pellets were ressuspended with Lysis buffer (10 % SDS, EDTA, Tris pH 8.0) prepared with PIC (protease inhibitor complex). The samples were sonicated 5-6 times, 10 seconds each, to break the DNA into approximately 250 base pairs fragments. The samples were then centrifuged at 15.000 rpm, 4^0C for 10 minutes.

The supernatant was transferred to new eppendorfs and we added 300 µl of Buffer D (10% Triton X-100, 100 mM EDTA, Tris pH 8.0, NaCl) with PIC. We then removed 100 µl to the input eppendorfs. These input samples were left in the heat block at 65^0C overnight (to reverse the cross-link). To the remaining samples we added antibody (5µl per sample) and left overnight at 4^0C.

On the following day, we removed the input samples from the heat block and stored them at -20^0C. Added protein G-fast flow beads (Sigma) to samples (10µl per sample)

and rotated for 1 hour at room temperature. Washed samples with TSE I (10% SDS, 1% Triton X-100, 100 mM EDTA, 3% NaCl (5M) in Tris pH 8.0), TSE II (10% SDS, 1% Triton X-100, 100 mM EDTA, 16% NaCl (5M) in Tris pH 8.0) and TSE III (1% NP-40, 100 mM EDTA, 10% Tris pH 8.0, 1% deoxycholate in LiCl (1M)) with rotation and centrifugation between washes. Washed 3 times with ice-cold TE buffer. Added a solution of SDS and NaCHO3 to each sample and rotated for 1 hour at room temperature. Transferred the supernatant to new eppendorfs, left them overnight on the heat block at 65^0C and stored them at -20^0C on the next day.

We used the NzyGelpure purification kit (Appendix D) to "clean" the previous ChIP and input samples. We used 1 ml of binding buffer on step 1 and 30 µl of dH_2O on step 5 instead of the manufacturer indications. The purified DNA was stored at -20^0C.

3. Results

3.1- TRIB2 protein levels increase in the presence of PI3K inhibitors

Our group has previously demonstrated that TRIB2 is a biomarker for malignant melanoma (60) and is a negative regulator of FOXO3a (59). As such, we know that TRIB2 is integrated within the PI3K pathway but where within this network and specifically how TRIB2 can regulate FOXO3a is unknown. We have previously generated a range of isogenic TRIB2 expressing cell lines and obtained a number of novel PI3K pathway inhibitors (summarized in Figure 3.1.1). We first questioned if there were any effects on the TRIB2 protein before and after PI3K inhibition within our isogenic cell lines. Using an immunoblotting approach, we found a discernible increase in TRIB2 protein in both the endogenous U2OS-Empty and the U2OS-TRIB2 cell lines (Figure 3.1.2).

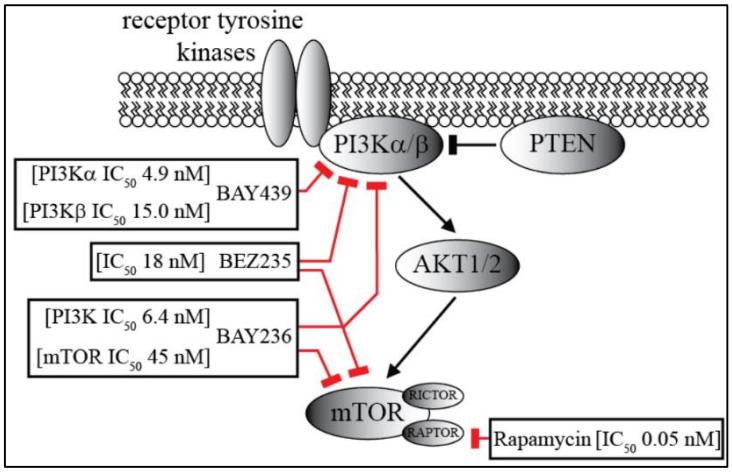

Figure 3.1.1- PI3K pathway inhibitors.
Squematic of PI3K pathway and how the inhibitors target its components.

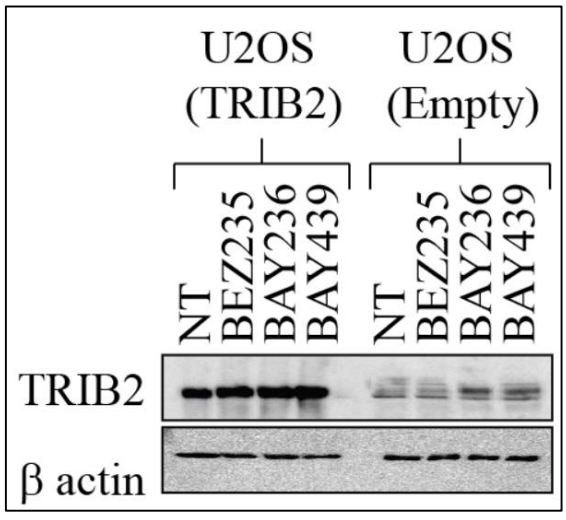

Figure 3.1.2- TRIB2 protein levels increase following PI3K inhibition.
Representative western blot of isogenic osteosarcoma cell lines with over expression of TRIB2 (U2OS-TRIB2) and endogenous TRIB2 protein expression (U2OS-Empty). Cell lines were treated with 100nM of each indicated compound and 50µg of total protein lysate was loaded per lane. β-actin is shown to indicate protein loading. .

3.2- PI3K inhibition does not result in an increase in *TRIB2* transcription

We next questioned what the mechanism was for this increase in TRIB2 protein expression following PI3K inhibition. To answer this question, we treated cells with each of our novel PI3K inhibitors and 12 hours post exposure, collected total RNA (described in materials and methods). Once we had our RNA extracted, we generated cDNA and conducted quantitative real time PCR (qRT-PCR) analysis (Figure 3.2.1). Interestingly, we note that there was no significant increase in the level of *TRIB2* transcription following PI3K treatment in either of our isogenic U2OS cell lines. As we would expect, our U2OS-TRIB2 cells show an almost 6 fold increase in *TRIB2* expression compared to endogenous U2OS-Empty cells. From this study, we can conclude that the increase we note in TRIB2 protein levels post-PI3K inhibition was independent of transcription.

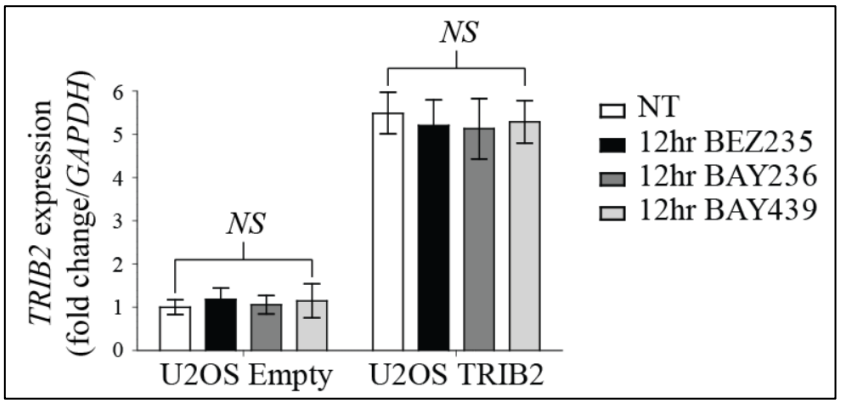

Figure 3.2.1- PI3K inhibition does not change levels of TRIB2 expression qRT-PCR of our isogenic osteosarcoma cell lines following PI3K inhibitor exposure. TRIB2 transcription was evaluated and normalized to GAPDH using the $2^{-\Delta\Delta CT}$ methodology. N = 6. Statistical analysis was carried out using a 2-tailed analysis of variance (ANOVA) approach.

3.3- TRIB2 keeps mRNA and protein stability in the presence of PI3K inhibitors

Having observed no significant difference in *TRIB2* transcription following PI3K inhibition, we next questioned if the increase in TRIB2 protein levels after PI3K inhibition was the result of a change in mRNA stability. We conducted an actinomycin D (ActD) time course study following exposure to our PI3K inhibitors. Actinomycin D is a drug that binds to the

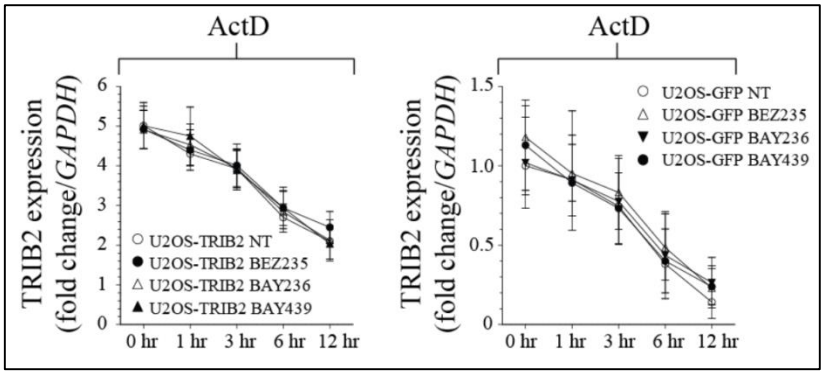

Figure 3.3.1- PI3K inhibition does not alter TRIB2 mRNA synthesis
Left) qRT-PCR of U2OS-TRIB2 cells treated with Actinomycin D and PI3K inhibitors. **Right)** qRT-PCR of U2OS-Empty cells treated with Actinomycin D and Pi3K inhibitors. TRIB2 transcription was evaluated and normalized to GAPDH using the $2^{-\Delta\Delta CT}$ methodology. N = 6. Statistical analysis was carried out using a 2-tailed analysis of variance (ANOVA) approach.

DNA and blocks RNA synthesis (61). Collecting total RNA from each isogenic cell line at 1hr, 3hr 6hr and 12 hr (Figure 3.3.1). We generated cDNA from the total RNA at each time post ActD exposure and conducted qRT-PCR analysis. It is important to note here that the time point indicated in each graph shown in Figure 3.3.1 is the time **post ActD addition** and that at the time point 0 hr, the cell lines have been incubated in the presence of each PI3K inhibitor for 3 hours. Consequently, when the 12 hour time point is reached (12 hours post ActD addition) the respective cell lines have been in the presence of each PI3K inhibitor for 15 hours. We saw no difference in the amounts of *TRIB2* mRNA at each time point in the presence of each PI3K inhibitor and ActD indicating that there was no change in *TRIB2* mRNA stability post PI3K inhibition.

Having observed no significant difference between either *TRIB2* transcription or *TRIB2* mRNA stability, we questioned if the TRIB2 protein stability was effected following PI3K inhibition. Similarly to our ActD studies, we treated our isogenic cell line with each PI3K inhibitor in the presence of cycloheximide (CHX) (an inhibitor of protein synthesis) (62) (Figure 3.3.2). It is important to note here that the time point indicated in each graph shown in Figure 3.3.2 is the time **post CHX addition** and that at the time point 0 hr, the cell lines have been incubated in the presence of each PI3K inhibitor for 12 hours. Consequently, when the 12 hour time point is reached (12 hours post CHX addition) the respective cell lines have been in the presence of each PI3K inhibitor for 24 hours. In the case of the 1 hour time point (this is 13 hours with each PI3K inhibitor), 3 hr (is 15 hours in the presence of the inhibitors) and 6 hr represents 18 hours in the presence of the PI3K inhibitors. In both U2OS-TRIB2 and U2OS-Empty cells, we note that there is a significantly higher amount of TRIB2 protein in the presence of each PI3K inhibitor tested.

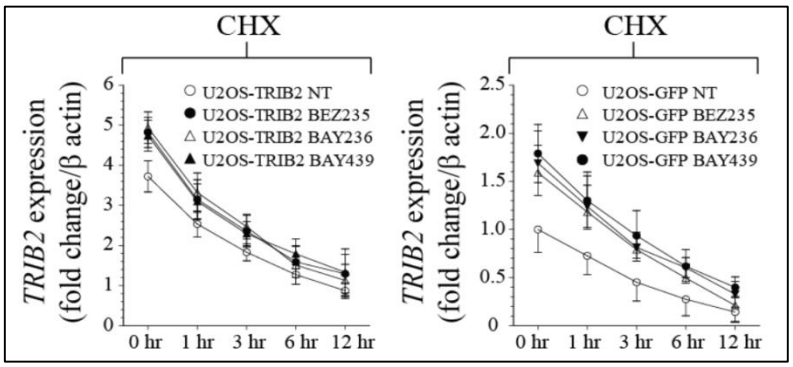

Figure 3.3.2- PI3K inhibition does not affect protein synthesis. Western blot quantification of U2OS-TRIB2 and U2OS-Empty cells incubated with cycloheximide (CHX) for the time points shown. At the time the CHX time course was initiated (0hr), the cells have already been incubated in the presence of each specific PI3K inhibitor for 12 hours. **Left)** U2OS-TRIB2 treated cells. **Right)** U2OS-empty treated cells. qRT-PCR of U2OS-Empty cells treated with Actinomycin D and Pi3K inhibitors. TRIB2 protein levels were evaluated and normalized to β-actin (applying the $2^{-\Delta\Delta CT}$ normalization methodology). N = 3.

However, irrespective of the compound tested, there was no statistically significant difference in the gradient of each graph for total TRIB2 amount. Therefore, while there is a clear increase in the amount of total TRIB2 protein following incubation with each PI3K (independent of whether this was endogenous or exogenous TRIB2), there is no significant difference in TRIB2 protein stability post PI3K-inhibition.

3.4- PI3K treatment significantly reduces proteasome-dependent degradation of TRIB2

Having questioned if the increase in total TRIB2 protein was the result of a change in *TRIB2* transcription, *TRIB2* mRNA stability or TRIB2 protein stability, we investigated if there was a change in proteasome-dependent degradation. We treated our isogenic cell lines with MG132, a small peptide that acts as a proteasome inhibitor (63). We found that when incubated in the presence of MG132, there was no longer an increase in TRIB2 protein levels post PI3K inhibition (Figure 3.4.1).

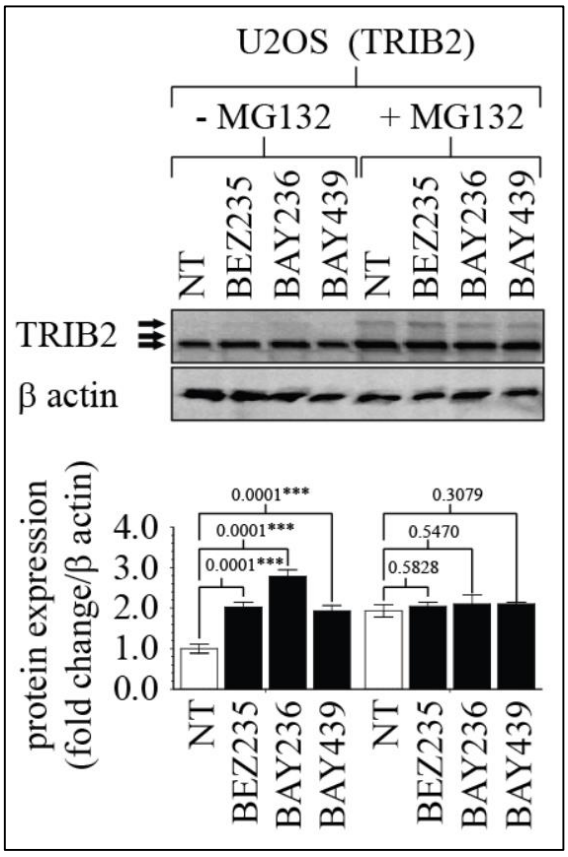

Figure 3.4.1– PI3K inhibition reduces TRIB2 degradation
Top) Western blot of U2OS-TRIB2 cells treated with each PI3K inhibitor in the absence/presence of MG132. 50 □g of total protein lysate was loaded per lane. **Bottom)** Quantification of multiple (3) western blots for TRIB2 following PI3K incubation -/+ MG132. Statistical analysis was carried out using a $2^{-\Delta\Delta CT}$ methodology, normalized to β-actin. In the presence of MG132 we notice the accumulation of 2 larger (higher) TRIB2 protein bands.

3.5- TRIB2 protein expression correlates with increased total AKT and significantly elevated pSer473-AKT.

Previous data from our group indicated that in a range of isogenic cell lines and *in vitro* models that, in the presence of high TRIB2 protein, there is a significantly higher level of active pSer473-AKT (*Figure 3.5.1; kindly provided by Dr Richard Hill*).

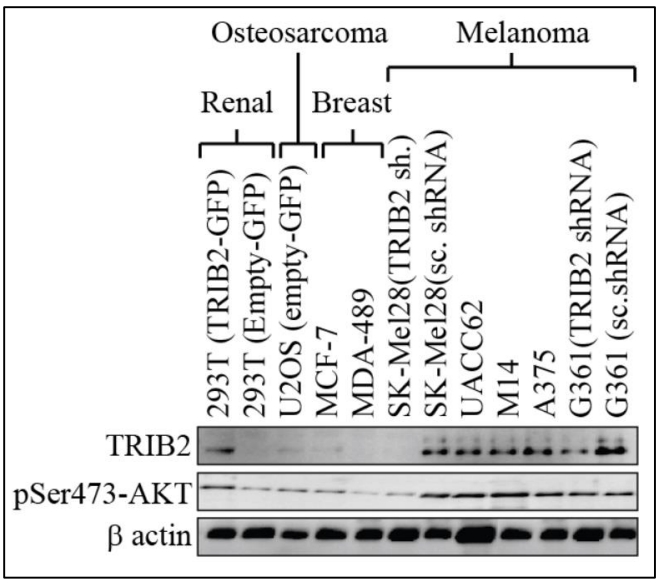

Figure 3.5.12- TRIB2 protein expression correlates with pSer473-AKT.
TRIB2 protein levels correlate with AKT-Ser473 phosphorylation in a broad range of model in vitro models. Representative images showing 100 µg (TRIB2), 50 µg (AKT-Ser473) total protein loaded per lane separated by 10% SDS-PAGE. sc indicates scramble shRNA within the indicated cell lines.

3.6- COP1 domain is the crucial region required for pSer473 AKT post-translational modification

Data (unpublished) from our group has revealed that the TRIB2 protein is capable to bind and activate AKT. However, the specific region of TRIB2 that is responsible for that action is unknown. To address this we used a range of mutant TRIB2 constructs (Figure 3.6.1). We transfected 2 µg of each plasmid into human 293T renal carcinoma cells. 24 hours post transfection we screened transfected cells by immunoblotting for pSer473-AKT, pSer253-FOXO3a, pSer166-MDM2 and GFP (Figure 3.6.2). Mutants that retained the COP1-binding domain showed phosphorylation of downstream members of the PI3K pathway. We included GFP in this study as each construct was tagged with GFP. This served as a control for our studies as neither of our α-TRIB2 antibodies (CNIO or Santa Cruz Biotechnology) would recognise all of these constructs (data not shown).

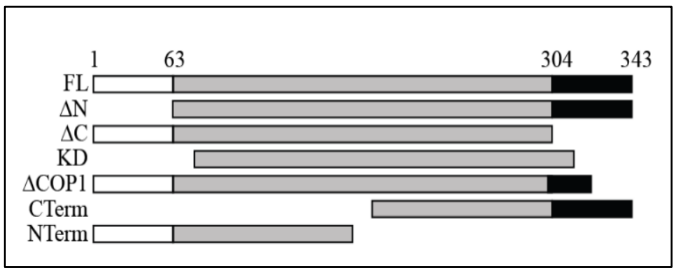

Figure 3.6.1- TRIB2 mutant constructs. Schematic figure of various TRIB2 mutant constructs used in our studies (kindly provided by Dr. Stephen Pear).

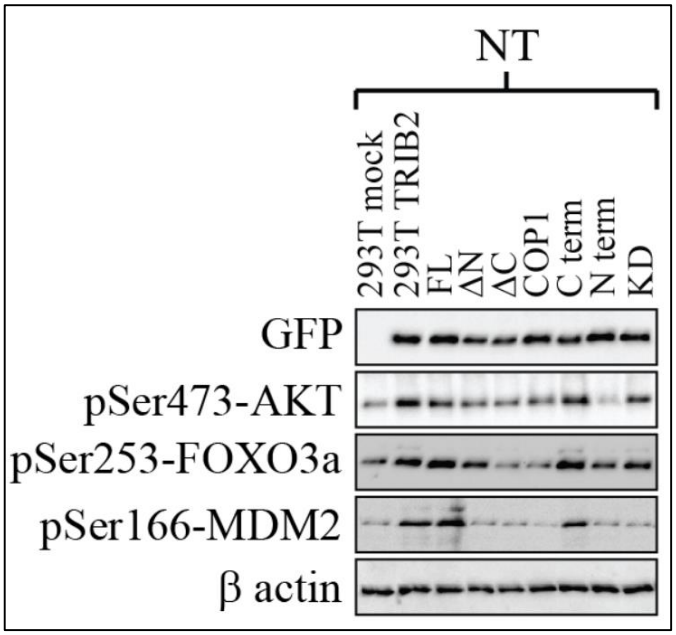

Figure 3.6.2- TRIB2 acts through the COP1 domain. Western blot with HEK293T cell lines transfected with the mutant constructs. 50 µg of lysate used in each lane.

3.7- Low levels of FOXO3a-mediated genes transcription correlate with increased AKT activity

To further analyse if the COP1 domain is in fact responsible for the activation of AKT, we studied the gene expression levels of target genes of FOXO3a. In particular, we focused on *p27* and *FasLG* to attest how cell cycle arrest and apoptosis were affected following transient reinfection with each TRIB2 construct. As mentioned before, *p27* is affected by the PI3K/AKT pathway because it needs FOXO3a to be expressed. AKT directs the post-translational modification of FOXO3a phosphorylating it at the Ser253 residue following which, FOXO3a is trafficked out of the nucleus into the cytoplasm for polyubiquitination and degradation. Consequently, high levels of phosphorylated AKT are indicative of low levels of FOXO3a and by consequence, low levels of p27 (at both the transcript and protein level). The same "chain-of-events" applies to FasLG. These transfection studies indicated that TRIB2 proteins that contained the COP1 domain had low levels *p27* and *FasLG* transcription (Figure 3.7.1, 3.7.2), supporting our immunoblot data where we note AKT and FOXO3a phosphorylation.

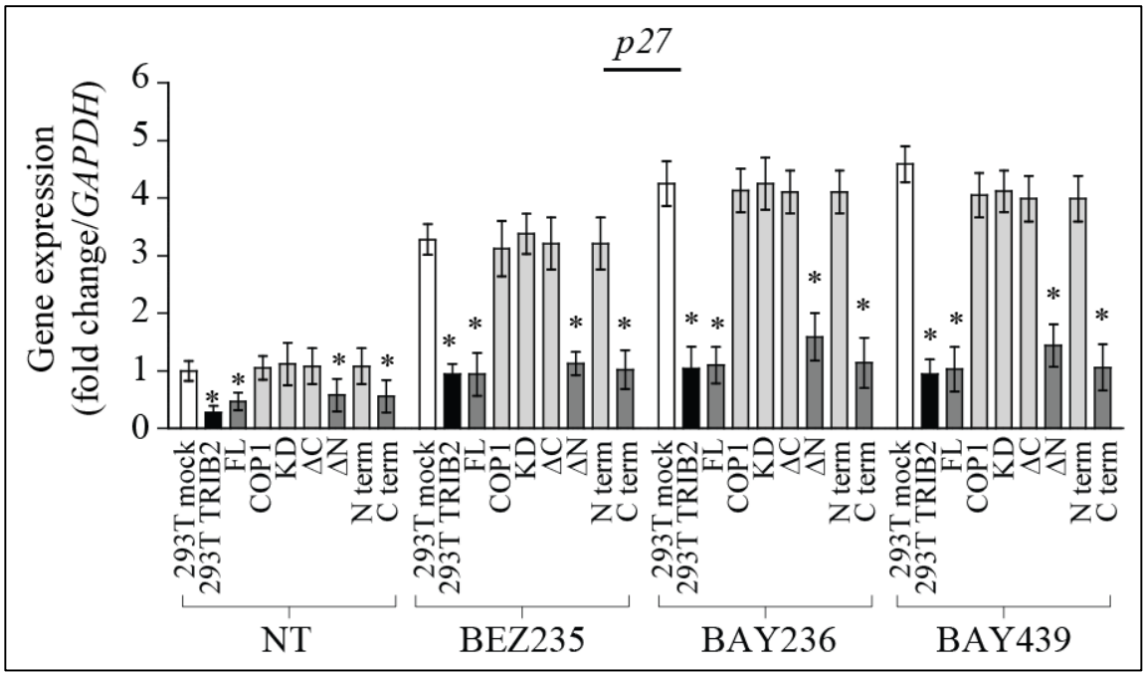

Figure 3.7.1- Low levels of p27 gene expression in mutants still possessing the COP1-binding domain. qRT-PCR of HEK293T cell lines transfected with mutant constructs.

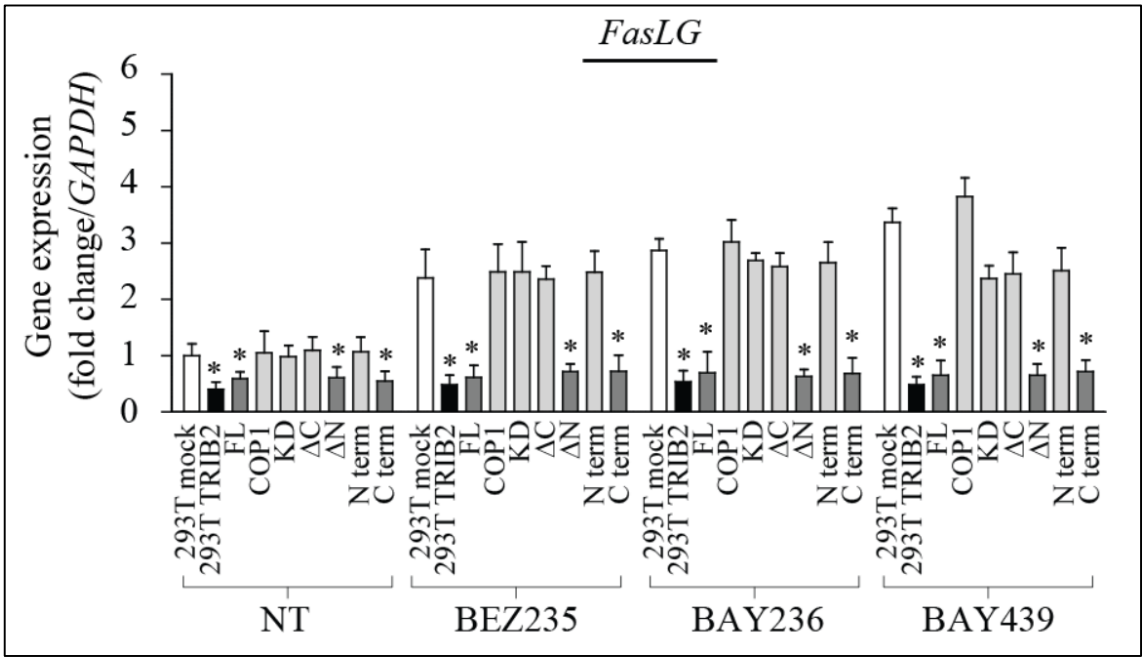

Figure 3.7.2- Low levels of FasLG gene expression in mutants still possessing the COP1-binding domain. qRT-PCR of HEK293T cell lines transfected with mutant constructs.

We next questioned if our transcription results for *p27* and *FasLG* were conserved at the protein level (i.e. in TRIB2-mutant construct transfected cells if there was p27 and FasLG protein induction following PI3K exposure). Following transient transfection of each construct and exposure to BEZ235 (a dual PI3K/mTOR inhibitor) we analysed by immunoblot, the protein levels of p27 and FasLG (Figure 3.7.3). The results correlate, with same mutants with low levels of gene expression showing low levels of protein expression of p27 and FasLG (Figure 3.7.3).

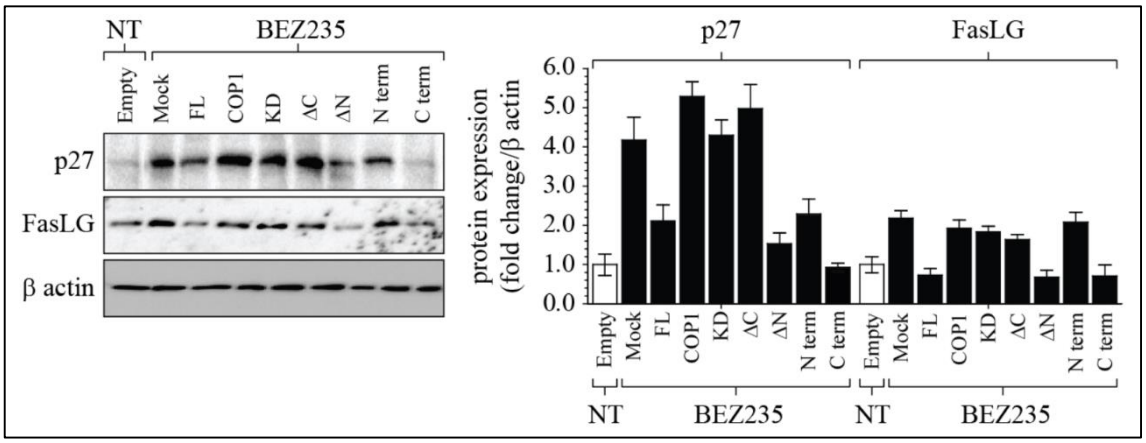

Figure 3.7.3- Low levels of protein expression of p27 and FasLG in mutant constructs still possessing the COP1-binding domain. Left) Western blot of U2OS-TRIB2 cells treated with PI3K inhibitor BEZ235. 50 µg of total protein lysate was loaded per lane. **Right)** Quantification of multiple (3) western blots for TRIB2 following PI3K inhibition. Statistical analysis was carried out using a $2^{-\Delta\Delta CT}$ methodology, normalized to β-actin.

These results also support our studies demonstrating that TRIB2 is actively involved in mechanisms of drug resistance in various cancers (metastatic melanoma, colon and pancreatic to name a few). Through the COP1-binding domain within the protein, TRIB2 is activating AKT and promoting cell survival by suppressing FOXO3a (directly) and p53 (indirectly).

To further prove the role of TRIB2 in activating AKT and chemotherapeutic resistance, we used FACS scanning (described in materials and methods) of the transfected 293T cell line after treatment with each specific PI3K inhibitor. Following transient transfection and PI3K inhibitor exposure, we measured the percentage of $SubG_1$ cells in each population (i.e. the percentage of dead/non-viable cells). The results revealed that the cells transfected with the TRIB2 mutants containing the COP-1 binding domain were no longer more resistant to various novel PI3K inhibitors and that they displayed significant increases in the percentage of SubG1 cells (Figure 3.7.4).

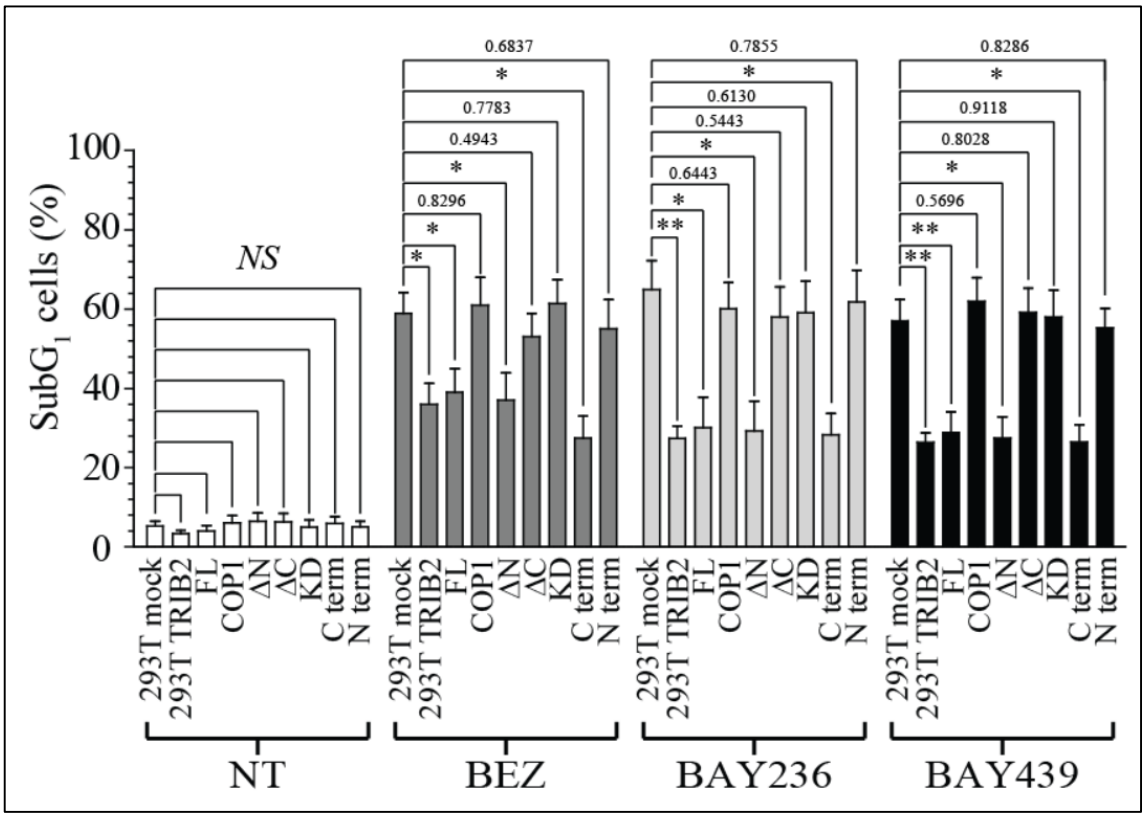

Figure 3.7.4- Cells with TRIB2 mutants possessing COP1-binding domain can transition the G1 checkpoint. 10,000 total events were scored per study. Data was analysed using Infinicyt (Cytognos).

The previous studies were obtained in transient transfected 293T cells with a mixed population. As a result, we hypothesised that there would be cells within this mixed population with high plasmid expression and those which did not take up the plasmid. Each construct was tagged with GFP so we asked if we could FACS sort the transfected cells following BEZ235 treatment into GFP positive and GFP negative. Upon obtaining the two populations, we extracted the proteins and with these sorted populations, we analysed the levels of protein expression of p27 (Figure 3.7.5) and BIM (Figure 3.7.6).

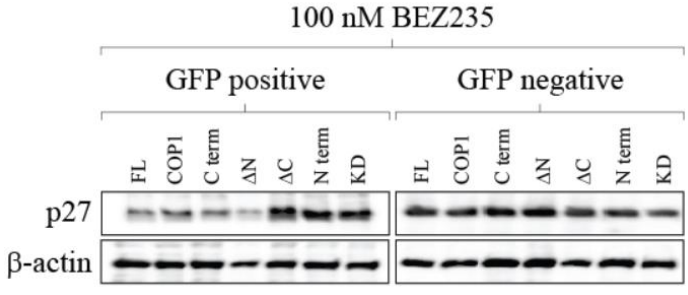

Figure 3.7.5-Protein expression of p27 in GFP$^+$ and GFP$^-$ populations. Representative immunoblot image for p27 or β-actin following FAC-sorting post transient transfection and 100 nM BEZ235 treatment. Cell populations were sorted using our FACS-Aria II sorter and the total protein extracted from each population. 50 µg total protein lysate was run on 10% SDS-PAGE gels and probed for p27 or β-actin (n=2).

Strikingly, our FAC-sorting data correlated with our previous findings and that GFP positive cells from the FL, ΔN and CTerm constructs could not

repress p27 or BIM expression but that within these sorted populations, the GFP negative population lost this ability. Irrespective of GFP status, the other constructs could not repress p27 or BIM induction. An important caveat of this study was that each study required the transient transfection of individual constructs in different passages of 293T cells. Consequently, the transfection efficiency could vary. In addition, we only sorted cells that had an extremely high GFP signal. Consequently, within each mixed population, there were cells with low GFP signals that could have been incorporated/sorted within the GFP negative pool. This could account for the repression profile that while attenuated, can still be observed (somewhat) in our samples evaluated for BIM (Figure 3.7.6). As such, these studies need to be expanded and repeated.

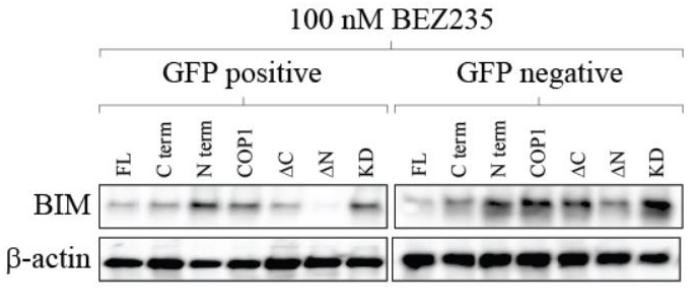

Figure 3.7.6- Protein expression of BIM in GFP^{+} and GFP^{-} populations. Representative immunoblot image for BIM or β-actin following FAC-sorting post transient transfection and 100 nM BEZ235 treatment. Cell populations were sorted using our FACS-Aria II sorter and the total protein extracted from each population. 50 µg total protein lysate was run on 10% SDS-PAGE gels and probed for p27 or β-actin (n=2).

4. Conclusion

TRIB2 has been established as a FOXO repressor protein with oncogenic capacity in melanoma. Previous work from our group has found that TRIB2 is a melanoma biomarker for diagnosis, progression and patient response to conventional first line chemotherapy. This capacity arises from its ability to interact with the PI3K/AKT pathway, a key signalling pathway for cell survival. Intriguingly, the TRIB2 protein levels have been found to be increased upon treatment with PI3K inhibitors. The present study reveals that TRIB2 protein levels increase post PI3K inhibition due to a decrease in proteasomal degradation. Proteasomal degradation is a mechanism for cells to get rid of unnecessary or damaged proteins, keeping homeostasis. For degradation to be initiated, the target proteins must be "tagged" through post-translational modifications such as ubiquitination (64).

Our results imply that the degradation of TRIB2 is regulated by the PI3K pathway. When PI3K inhibitors block the activation of the pathway, they appear to be affecting the "tagging" of TRIB2 for degradation. As such, we hypothesise that a downstream target that is activated upon PI3K/AKT signalling is responsible for the post-translational modification that "tags" TRIB2 for proteasomal degradation. Obvious candidates include MDM2 (Hill and Link, unpublished data) and COP1 (55), both E3 ubiquitin ligases that interact with TRIB2. MDM2 is also a known target of AKT. These E3 ubiquitin ligases may be responsible for the ubiquitination of TRIB2. However, the precise underlying mechanism remains to be determined. A recent study reports other candidates responsible for the degradation of TRIB2 (65). The authors show that p70S6K can phosphorylate TRIB2, inducing the SMAD ubiquitination regulatory factor 1 (Smurf1) to polyubiquitinate TRIB2 (65). They also showed that impairing any of these modifications stabilizes TRIB2 and enhances its carcinogenic properties in liver cancer cells (65). These data are very intriguing as p70S6K can be activated by PI3K/AKT signalling. Therefore we hypothesise that the inhibition of PI3K might reduce MDM2 or Smurf1 activity and in turn decrease proteasomal degradation of TRIB2.

These are extremely relevant observations for cancer treatment, specifically for drug resistance. In clinical practice, patients with tumours that overexpress TRIB2 will have an intrinsic resistance to the use of PI3K inhibitors. Furthermore, patients with lower levels of TRIB2, if treated with PI3K inhibitors, might acquire resistance through the stabilization of TRIB2 protein levels.

Further studies will be required to establish the underlying mechanism of TRIB2 degradation and how it affects cancer chemotherapies.

The present work also shows that TRIB2 is able to bind and activate AKT and that this interaction is mediated by its COP1-binding domain. AKT is activated by phosphorylation on two different residues, Threonine 308 and Serine 473. As shown here TRIB2 expression increases phosphorylation of Ser473, a residue known to be phosphorylated by the mTORC2 complex. There is very recent evidence in our lab that TRIB2 does not affect the PDK-1 mediated phosphorylation of Thr308 (currently under review). This data suggests that TRIB2 functions as an adaptor protein that facilitates the phosphorylation of the Serine 473. We hypothesise that TRIB2 binds to AKT and recruits mTORC2, which is known to phosphorylate the Ser473 residue. Another interesting possibility emerges from a recent study by Velasco *et al.* on the role ofTRIB3 in cancer. This group shows that TRIB3 possesses a tumour inhibitory role through the regulation of the activity of the AKT pathway in breast cancer cells (66). They also show that inhibition of TRIB3 increases tumorigenesis due to enhanced phosphorylation of AKT by the mTORC2 complex and subsequent inactivation of FOXO3 (66). Their results and our data suggest that TRIB2 and TRIB3 may compete for AKT binding, with opposing functions.

Another recent seminal work showed that TRIB2 can bind to ATP and autophosphorylate in a metal-independent manner (67) suggesting that TRIB2 could act as a kinase. They proved *in vitro* that ATP binds with low affinity to the Lys90 residue of the catalytic site of TRIB2. They also show that targeting that site with small molecules may be a viable pursuit for development of novel chemotherapeutics (67).

4.1- Future Directions

The findings presented in this study provide the groundwork for future basic and translational research. The mechanism of by which TRIB2 protein levels are regulated, in particular the identification of the molecular mechanism of its proteasomal degradation and the involved players would shed light on the influence of PI3K/AKT signalling on this process. As mentioned above this could be a mechanism for both acquired and intrinsic resistance against anti-cancer drugs that interfere with the PI3K/AKT signalling network. Expanding our studies to *in vivo* or clinical samples could establish TRIB2 as a predictive biomarker capable of stratifying cancer patients into responders and non-responders to these agents. The result showing the interaction of TRIB2 and AKT via its

COP1 domain suggests several testable hypotheses, including the competition of TRIB2 and TRIB3 for AKT binding or the direct recruitment of the mTORC2 complex by TRIB2/AKT. A further understanding of the exact mechanism how TRIB2 activates AKT is of key importance for the development of therapies aimed at interfering with the activation of AKT and to overcome TRIB2 mediated drug resistance.

This work only tested for a few downstream targets of the FOXO and p53 transcription factors. These factors are known to regulate the transcription of a vast array of genes. As predicted, our results of ChIP assays showed a suppression of FOXO3a and p53 target gene expression upon increased TRIB2 levels. These data was not presented in this work for they were preliminary results and further experiments are required. The identification of targets that are critically involved in TRIB2 mediated drug resistance would further increase the mechanistic insight into this clinically relevant process.

.

5. References

1. Hanahan D, Weinberg RA. Hallmarks of cancer: The next generation. Cell. 2011. p. 646–74.

2. Siegel RL, Miller KD, Jemal A. Cancer Statistics, 2015. CA Cancer J Clin. 2015;65(1):5–29.

3. Russo A, Ficili B, Candido S, Pezzino FM, Guarneri C, Biondi A, et al. Emerging targeted therapies for melanoma treatment (Review). Int J Oncol. 2014;45(2):516–24.

4. Shah DJ, Dronca RS. Latest advances in chemotherapeutic, targeted, and immune approaches in the treatment of metastatic melanoma. Mayo Clin Proc [Internet]. Elsevier Inc; 2014;89(4):504–19. Available from: http://dx.doi.org/10.1016/j.mayocp.2014.02.002

5. Bello DM, Ariyan CE, Carvajal RD. Melanoma mutagenesis and aberrant cell signaling. Cancer Control. 2013;20(4):261–81.

6. Shtivelman E, Davies MQ a, Hwu P, Yang J, Lotem M, Oren M, et al. Pathways and therapeutic targets in melanoma. Oncotarget [Internet]. 2014;5(7):1701–52. Available from: http://www.pubmedcentral.nih.gov/articlerender.fcgi?artid=4039128&tool=pmcentrez&rendertype=abstract

7. Tas F. Metastatic behavior in melanoma: Timing, pattern, survival, and influencing factors. J Oncol. 2012;2012.

8. Tuong W, Cheng LS, Armstrong AW. Melanoma: Epidemiology, Diagnosis, Treatment, and Outcomes. Dermatol Clin [Internet]. Elsevier Inc; 2012;30(1):113–24. Available from: http://dx.doi.org/10.1016/j.det.2011.08.006

9. Balch CM, Gershenwald JE, Soong SJ, Thompson JF, Atkins MB, Byrd DR, et al. Final version of 2009 AJCC melanoma staging and classification. J Clin Oncol. 2009;27(36):6199–206.

10. Olszanski AJ. Current and future roles of targeted therapy and immunotherapy in advanced melanoma. J Manag Care Pharm [Internet]. 2014;20(4):346–56. Available from: http://www.ncbi.nlm.nih.gov/pubmed/24684639

11. Griewank KG, Scolyer R a., Thompson JF, Flaherty KT, Schadendorf D, Murali R. Genetic alterations and personalized medicine in melanoma: progress and future prospects. J Natl Cancer Inst. 2014;106(2).

12. Osaki M, Oshimura M, Ito H. PI3K-Akt pathway: its functions and alterations in human cancer. Apoptosis. 2004;9(6):667–76.

13. Fresno Vara JA, Casado E, de Castro J, Cejas P, Belda-Iniesta C, González-Barón M. PI3K/Akt signalling pathway and cancer. Cancer Treat Rev. 2004;30(2):193–204.

14. Pawson T, Nash P. Protein − protein interactions define specificity in signal transduction Protein – protein interactions define specificity in signal transduction. 2000;(416):1027–47.

15. Datta SR, Brunet A, Greenberg ME. Cellular survival: A play in three akts. Genes Dev. 1999;13(22):2905–27.

16. Coffer PJ, Woodgett JR. Molecular cloning and characterisation of a novel putative protein-serine kinase related to the cAMP-dependent and protein kinase C families. Eur J Biochem. 1991;201(2):475–81.

17. Brodbeck D, Cron P, Hemmings B a. A human protein kinase B?? with regulatory phosphorylation sites in the activation loop and in the C-terminal hydrophobic domain. J Biol Chem. 1999;274(14):9133–6.

18. Blume-Jensen P, Hunter T. Oncogenic kinase signalling. Nature. 2001;411(6835):355–65.

19. Martelli AM, Tabellini G, Bressanin D, Ognibene A, Goto K, Cocco L, et al. The emerging multiple roles of nuclear Akt. Biochim Biophys Acta - Mol Cell Res [Internet]. Elsevier B.V.; 2012;1823(12):2168–78. Available from: http://dx.doi.org/10.1016/j.bbamcr.2012.08.017

20. Cross D a, Alessi DR, Cohen P, Andjelkovich M, Hemmings B a. Inhibition of glycogen synthase kinase-3 by insulin mediated by protein kinase B. Nature [Internet]. 1995;378(6559):785–9. Available from: http://www.ncbi.nlm.nih.gov/pubmed/8524413

21. Shimura T, Fukumoto M, Kunugita N. The role of cyclin D1 in response to longterm exposure to ionizing radiation. Cell Cycle. 2013;12(17):2738–43.

22. Shimura T. Acquired Radioresistance of Cancer and the AKT/GSK3β/cyclin D1 Overexpression Cycle. J Radiat Res [Internet]. 2011;52(5):539–44. Available from: https://www.jstage.jst.go.jp/article/jrr/52/5/52_11098/_pdf

23. Pestell RG. New roles of cyclin D1. Am J Pathol [Internet]. American Society for Investigative Pathology; 2013;183(1):3–9. Available from: http://www.pubmedcentral.nih.gov/articlerender.fcgi?artid=3702737&tool=pmcentrez&rendertype=abstract

24. Liang J, Zubovitz J, Petrocelli T, Kotchetkov R, Connor MK, Han K, et al. PKB/Akt phosphorylates p27, impairs nuclear import of p27 and opposes p27-mediated G1 arrest. Nat Med. 2002;8(10):1153–60.

25. Zhou BP, Liao Y, Xia W, Spohn B, Lee MH, Hung MC. Cytoplasmic localization of p21Cip1/WAF1 by Akt-induced phosphorylation in HER-2/neu-overexpressing cells. Nat Cell Biol. 2001;3(3):245–52.

26. Guertin D a, Guertin D a, Sabatini DM, Sabatini DM. An expanding role for mTOR in cancer. Trends Mol Med [Internet]. 2005;11(8):353–61. Available from: http://www.ncbi.nlm.nih.gov/pubmed/16002336

27. Chen CC, Jeon SM, Bhaskar PT, Nogueira V, Sundararajan D, Tonic I, et al. FoxOs Inhibit mTORC1 and Activate Akt by Inducing the Expression of Sestrin3 and Rictor. Dev Cell [Internet]. Elsevier Ltd; 2010;18(4):592–604. Available from: http://dx.doi.org/10.1016/j.devcel.2010.03.008

28. Oh WJ, Jacinto E. mTOR complex 2 signaling and functions. Cell Cycle. 2011;10(14):2305–16.

29. Chang F, Lee JT, Navolanic PM, Steelman LS, Shelton JG, Blalock WL, et al. Involvement of PI3K/Akt pathway in cell cycle progression, apoptosis, and neoplastic transformation: a target for cancer chemotherapy. Leuk Off J Leuk Soc Am Leuk Res Fund, UK. 2003;17(3):590–603.

30. Van der Vos KE, Coffer PJ. The extending network of FOXO transcriptional target genes. Antioxid Redox Signal. 2011;14(4):579–92.

31. Maiese K, Zhao ZC, Yan CS, Hou J. Clever cancer strategies with FoxO transcription factors. Cell Cycle. 2008;7(24):3829–39.

32. Bouck DC, Shu P, Cui J, Shelat A, Chen T. A high-content screen identifies inhibitors of nuclear export of forkhead transcription factors. J Biomol Screen Off J Soc Biomol Screen. 2011;16(4):394–404.

33. Yang J-Y, Hung M-C. Deciphering the Role of Forkhead Transcription Factors in Cancer Therapy. Curr Drug Targets [Internet]. 2011 Aug 1;12(9):1284–90. Available from: http://www.eurekaselect.com/openurl/content.php?genre=article&issn=1389-4501&volume=12&issue=9&spage=1284

34. Luo H, Yang Y, Duan J, Wu P, Jiang Q, Xu C. PTEN-regulated AKT/FoxO3a/Bim signaling contributes to reactive oxygen species-mediated apoptosis in selenite-treated colorectal cancer cells. Cell Death Dis [Internet]. 2013;4:e481. Available from: http://www.pubmedcentral.nih.gov/articlerender.fcgi?artid=3734838&tool=pmcentrez&rendertype=abstract

35. Lettau M, Paulsen M, Schmidt H, Janssen O. Insights into the molecular regulation of FasL (CD178) biology. Eur J Cell Biol [Internet]. Elsevier GmbH.; 2011;90(6-7):456–66. Available from: http://dx.doi.org/10.1016/j.ejcb.2010.10.006

36. Waring P, Müllbacher A. Cell death induced by the Fas/Fas ligand pathway and its role in pathology. Immunol Cell Biol. 1999;77(4):312–7.

37. Hao Q, Cho W. Battle Against Cancer: An Everlasting Saga of p53. Int J Mol Sci [Internet]. 2014;15(12):22109–27. Available from: http://www.mdpi.com/1422-0067/15/12/22109/

38. Pant V, Lozano G. Limiting the power of p53 through the ubiquitin proteasome pathway. Genes Dev. 2014;28(16):1739–51.

39. Lu M, Miller P, Lu X. Restoring the tumour suppressive function of p53 as a parallel strategy in melanoma therapy. FEBS Lett [Internet]. Federation of European Biochemical Societies; 2014;588(16):2616–21. Available from: http://dx.doi.org/10.1016/j.febslet.2014.05.008

40. Wang Z, Sun Y. Targeting p53 for Novel Anticancer Therapy. Transl Oncol. 2010;3(1):1–12.

41. Jochemsen AG. Reactivation of p53 as therapeutic intervention for malignant melanoma. Curr Opin Oncol [Internet]. 2014;26(1):114–9. Available from: http://www.ncbi.nlm.nih.gov/pubmed/24275854

42. Chandarlapaty S, Sakr R a., Giri D, Patil S, Heguy A, Morrow M, et al. Frequent mutational activation of the PI3K-AKT pathway in trastuzumab-resistant breast cancer. Clin Cancer Res. 2012;18(24):6784–91.

43. Chen X, Wang H, Xie F, Wu J. Research on drug resistance mechanism of trastuzumab caused by activation of the PI3K / Akt signaling pathway. 2013;3–9.

44. Bhutani J, Sheikh A, Niazi AK. Akt inhibitors: mechanism of action and implications for anticancer therapeutics. Infect Agent Cancer [Internet]. 2013;8(1):49. Available from: http://www.pubmedcentral.nih.gov/articlerender.fcgi?artid=4028840&tool=pmcentrez&rendertype=abstract

45. Strickland LR, Pal HC, Elmets C a., Afaq F. Targeting drivers of melanoma with synthetic small molecules and phytochemicals. Cancer Lett [Internet]. Elsevier Ireland Ltd; 2015;359(1):20–35. Available from: http://linkinghub.elsevier.com/retrieve/pii/S0304383515000385

46. Marone R, Erhart D, Mertz AC, Bohnacker T, Schnell C, Cmiljanovic V, et al. Targeting melanoma with dual phosphoinositide 3-kinase/mammalian target of rapamycin inhibitors. Mol Cancer Res. 2009;7(4):601–13.

47. Grazia G, Penna I, Perotti V, Anichini A, Tassi E. Towards combinatorial targeted therapy in melanoma: From pre-clinical evidence to clinical application (Review). Int J Oncol. 2014;45(3):929–49.

48. Janku F, Hong DS, Fu S, Piha-Paul S a., Naing A, Falchook GS, et al. Assessing PIK3CA and PTEN in early-phase trials with PI3K/AKT/mTOR inhibitors. Cell

Rep [Internet]. The Authors; 2014;6(2):377–87. Available from: http://dx.doi.org/10.1016/j.celrep.2013.12.035

49. Bendell JC, Kurkjian C, Infante JR, Bauer TM, Burris H a., Greco FA, et al. A phase 1 study of the sachet formulation of the oral dual PI3K/mTOR inhibitor BEZ235 given twice daily (BID) in patients with advanced solid tumors. Invest New Drugs [Internet]. 2015;235:463–71. Available from: http://link.springer.com/10.1007/s10637-015-0218-6

50. Hao M, Song F, Du X, Wang G, Yang Y, Chen K, et al. Advances in targeted therapy for unresectable melanoma: New drugs and combinations. Cancer Lett [Internet]. Elsevier Ireland Ltd; 2015;359(1):1–8. Available from: http://linkinghub.elsevier.com/retrieve/pii/S0304383515000038

51. Grazia G, Vegetti C, Benigni F, Penna I, Perotti V, Tassi E, et al. Synergistic anti-tumor activity and inhibition of angiogenesis by cotargeting of oncogenic and death receptor pathways in human melanoma. Cell Death Dis [Internet]. Nature Publishing Group; 2014;5(10):e1434. Available from: http://www.nature.com/doifinder/10.1038/cddis.2014.410

52. Sweetlove M, Wrightson E, Kolekar S, Rewcastle GW, Baguley BC, Shepherd PR, et al. Inhibitors of pan-PI3K Signaling Synergize with BRAF or MEK Inhibitors to Prevent BRAF-Mutant Melanoma Cell Growth. Front Oncol [Internet]. 2015;5(June):1–14. Available from: http://journal.frontiersin.org/Article/10.3389/fonc.2015.00135/abstract

53. Wolchok JD, Kluger H, Callahan MK, Postow M a, Rizvi N a, Lesokhin AM, et al. Nivolumab plus ipilimumab in advanced melanoma. N Engl J Med [Internet]. 2013;369(2):122–33. Available from: http://www.ncbi.nlm.nih.gov/pubmed/23724867

54. Yokoyama T, Nakamura T. Tribbles in disease: Signaling pathways important for cellular function and neoplastic transformation. Cancer Sci. 2011;102(6):1115–22.

55. Keeshan K, Bailis W, Dedhia PH, Vega ME, Shestova O, Xu L, et al. Transformation by Tribbles homolog 2 (Trib2) requires both the Trib2 kinase domain and COP1 binding. Blood. 2010;116(23):4948–57.

56. Grandinetti KB, Stevens TA, Ha S, Salamone RJ, Walker JR, Zhang J, et al. Overexpression of TRIB2 in human lung cancers contributes to tumorigenesis through downregulation of C/EBPα. Oncogene [Internet]. 2011 Jul 28;30(30):3328–35. Available from: http://www.nature.com/doifinder/10.1038/onc.2011.57

57. Wang J, Park JS, Wei Y, Rajurkar M, Cotton J, Fan Q, et al. TRIB2 acts downstream of Wnt/TCF in liver cancer cells to regulate YAP and C/EBPα function. Mol Cell [Internet]. Elsevier Inc.; 2013;51(2):211–25. Available from: http://dx.doi.org/10.1016/j.molcel.2013.05.013

58. Xin JX, Yue Z, Zhang S, Jiang ZH, Wang PY, Li YJ, et al. miR-99 inhibits cervical carcinoma cell proliferation by targeting TRIB2. Oncol Lett. 2013;6(4):1025–30.

59. Zanella F, Renner O, García B, Callejas S, Dopazo a, Peregrina S, et al. Human TRIB2 is a repressor of FOXO that contributes to the malignant phenotype of melanoma cells. Oncogene. 2010;29(20):2973–82.

60. Hill R, Kalathur RKR, Colaco L, Brandao R, Ugurel S, Futschik M, et al. TRIB2 as a biomarker for diagnosis and progression of melanoma. Carcinogenesis [Internet]. 2015 Apr 1;36(4):469–77. Available from: http://www.carcin.oxfordjournals.org/cgi/doi/10.1093/carcin/bgv002

61. Hill CR, Cole M, Errington J, Malik G, Boddy a V, Veal GJ. Characterisation of the clinical pharmacokinetics of actinomycin D and the influence of ABCB1 pharmacogenetic variation on actinomycin D disposition in children with cancer. Clin Pharmacokinet [Internet]. 2014;53(8):741–51. Available from: http://www.scopus.com/inward/record.url?eid=2-s2.0-84905040303&partnerID=40&md5=a0ca1675c4a80a631151715df29daf79

62. Rehfeldt F, Engler AJ, Eckhardt A, Ahmed F, Discher DE. Cell responses to the mechanochemical microenvironment-Implications for regenerative medicine and drug delivery. Adv Drug Deliv Rev. 2007;59(13):1329–39.

63. Cui W, Bai Y, Luo P, Miao L, Cai L. Preventive and therapeutic effects of mg132 by activating nrf2-are signaling pathway on oxidative stress-induced cardiovascular and renal injury. Oxid Med Cell Longev. 2013;2013.

64. Lecker SH, Goldberg AL, Mitch WE. Protein degradation by the ubiquitin-proteasome pathway in normal and disease states. J Am Soc Nephrol. 2006;17(7):1807–19.

65. Wang J, Zhang Y, Weng W, Qiao Y, Ma L, Xiao W, et al. Impaired phosphorylation and ubiquitination by p70 S6 kinase (p70S6K) and smad ubiquitination regulatory factor 1 (Smurf1) promote tribbles homolog 2 (TRIB2) stability and carcinogenic property in liver cancer. J Biol Chem. 2013;288(47):33667–81.

66. Salazar M, Lorente M, Garcia-Taboada E, Perez Gomez E, Davila D, Zuniga-Garcia P, et al. Loss of Tribbles pseudokinase-3 promotes AKT-driven tumorigenesis via selective FoxO inactivation. Cell Death Differ. 2015;in press:131–44.

67. Bailey FP, Byrne DP, Oruganty K, Eyers CE, Novotny CJ, Shokat KM, et al. The Tribbles 2 (TRB2) pseudokinase binds to ATP and autophosphorylates in a metal-independent manner. Biochem J. 2015;467:47–62.

6. Appendix

SANTA CRUZ BIOTECHNOLOGY, INC.

p-Akt1/2/3 (Ser 473)-R: sc-7985-R

SANTA CRUZ BIOTECHNOLOGY

The Power to Question

BACKGROUND

The serine/threonine kinase Akt family contains several members, including Akt1 (also designated PKB or RacPK), Akt2 (also designated PKBβ or RacPK-β) and Akt 3 (also designated PKBγ or thyoma viral proto-oncogene 3), which exhibit sequence homology with the protein kinase A and C families and are encoded by the c-Akt proto-oncogene. All members of the Akt family have a Pleckstrin homology domain. Akt1 and Akt2 are activated by PDGF stimulation. This activation is dependent on PDGFR-β tyrosine residues 740 and 751, which bind the subunit of the phosphatidylinositol 3-kinase (PI 3-kinase) complex. Activation of Akt1 by Insulin or Insulin-growth factor-1(IGF-1) results in phosphorylation of both Thr 308 and Ser 473. Akt proteins become phosphorylated and activated in Insulin/IGF-1-stimulated cells by an upstream kinase(s), and the activation of Akt1 and Akt2 is inhibited by the PI kinase inhibitor Wortmannin. Taken together, this data strongly suggests that the protein signals downstream of the PI kinases. Akt3 is phosphorylated on a serine residue in response to Insulin. However, the activation of Akt3 by Insulin is inhibited by prior activation of protein kinase C via a mechanism that does not require the presence of the PH domain. Akt3 is expressed in 3T3-L1 fibroblasts, adipocytes and skeletal muscle and may be involved in various biological processes, including adipocyte and muscle differentiation, glycogen synthesis, glucose uptake, apoptosis and cellular proliferation.

SOURCE

p-Akt1/2/3 (Ser 473)-R is a rabbit polyclonal antibody raised against a short amino acid sequence containing Ser 473 phosphorylated Akt1 of human origin.

PRODUCT

Each vial contains 200 µg IgG in 1.0 ml of PBS with < 0.1% sodium azide and 0.1% gelatin.

Blocking peptide available for competition studies, sc-7985 P, (100 µg peptide in 0.5 ml PBS containing < 0.1% sodium azide and 0.2% BSA).

APPLICATIONS

p-Akt1/2/3 (Ser 473)-R is recommended for detection of Ser 473 phosphorylated Akt1 and correspondingly Ser 474 phosphorylated Akt2 and correspondingly Ser 472 phosporylated Akt3 of mouse, rat, human and *Xenopus laevis* origin by Western Blotting (starting dilution 1:200, dilution range 1:100-1:1000), immunoprecipitation [1-2 µg per 100-500 µg of total protein (1 ml of cell lysate)], immunofluorescence (starting dilution 1:50, dilution range 1:50-1:500) and solid phase ELISA (starting dilution 1:30, dilution range 1:30-1:3000).

p-Akt1/2/3 (Ser 473)-R is also recommended for detection of correspondingly phosphorylated Akt1, Akt2 and Akt3 in additional species, including bovine, porcine and avian.

Molecular Weight of p-Akt1: 62 kDa.

Molecular Weight of p-Akt2: 56 kDa.

Molecular Weight of p-Akt3: 62 kDa.

Positive Controls: A-431 whole cell lysate: sc-2201, Jurkat whole cell lysate: sc-2204 or HeLa + heat shock cell lysate: sc-2272.

STORAGE

Store at 4° C, **DO NOT FREEZE**. Stable for one year from the date of shipment. Non-hazardous. No MSDS required.

DATA

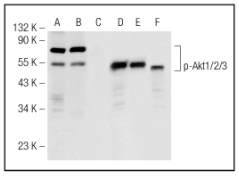

Western blot analysis of Akt1/2/3 phosphorylation in untreated (**A**,**D**), calyculin treated (**B**,**E**) and calyculin and lambda protein phosphatase (sc-200312A) treated (**C**,**F**) Jurkat whole cell lysates. Antibodies tested include p-Akt1/2/3 (Ser 473)-R: sc-7985-R (**A**,**B**,**C**) and Akt1 (C-20): sc-1618 (**D**,**E**,**F**).

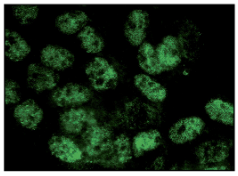

p-Akt1/2/3 (Ser 473)-R: sc-7985-R. Immunofluorescence staining of methanol-fixed A-431 cells showing nuclear localization.

SELECT PRODUCT CITATIONS

1. Contos, J.J., et al. 2002. Characterization of lpa_2 (EDG-4) and lpa_1/lpa_2 (EDG-2/EDG-4) lysophosphatidic acid receptor knockout mice: signaling deficits without obvious phenotypic abnormality attributable to lpa_2. Mol. Cell. Biol. 22: 6921-6929.
2. He, Y.Y., et al. 2003. Epidermal growth factor receptor downregulation induced by UVA in human keratinocytes does not require the receptor kinase activity. J. Biol. Chem. 278: 42457-42465.
3. Singh, M.K., et al. 2003. High-fat diet and leptin treatment alter skeletal muscle Insulin-stimulated phosphatidylinositol 3-kinase activity and glucose transport. Metab. Clin. Exp. 52: 1196-1205.
4. Yaspelkis, B.B., III, et al. 2004. Chronic leptin treatment enhances Insulin-stimulated glucose disposal in skeletal muscle of high-fat fed rodents. Life Sci. 74: 1801-1816.
5. De Souza, C.T., et al. 2005. Short-term inhibition of peroxisome proliferator-activated receptor-γ coactivator-1α expression reverses diet-induced diabetes mellitus and hepatic steatosis in mice. Diabetologia 48: 1860-1871.
6. Singleton, P.A., et al. 2006. Transactivation of sphingosine 1-phosphate receptors is essential for vascular barrier regulation. Novel role for hyaluronan and CD44 receptor family. J. Biol. Chem. 281: 34381-34393.
7. Nincheri, P., et al. 2010. Sphingosine kinase-1/S1P1 signalling axis negatively regulates mitogenic response elicited by PDGF in mouse myoblasts. Cell. Signal. 22: 1688-1699.
8. Alexandru, N., et al. 2011. Platelet activation in hypertension associated with hypercholesterolemia: effects of irbesartan. J. Thromb. Haemost. 9: 173-184.

RESEARCH USE

For research use only, not for use in diagnostic procedures.

Santa Cruz Biotechnology, Inc. 1.800.457.3801 831.457.3800 fax 831.457.3801 **Europe** +00800 4573 8000 49 6221 4503 0 ***www.scbt.com***

Figure A.1: Datasheet of phospho-AKT antibody (hhttp://www.scbt.com/)

SANTA CRUZ BIOTECHNOLOGY, INC.

Akt1 (C-20): sc-1618

SANTA CRUZ BIOTECHNOLOGY

The Power to Question

BACKGROUND

The serine/threonine kinase Akt family contains several members, including Akt1 (also designated PKB or RacPK), Akt2 (also designated PKBβ or RacPK-β) and Akt3 (also designated PKBγ or thyoma viral proto-oncogene 3), which exhibit sequence homology with the protein kinase A and C families and are encoded by the c-Akt proto-oncogene. All members of the Akt family have a Pleckstrin homology domain. Akt1 and Akt2 are activated by PDGF stimulation. This activation is dependent on PDGFR-β tyrosine residues 740 and 751, which bind the subunit of the phosphatidylinositol 3-kinase (PI 3-kinase) complex. Activation of Akt1 by Insulin or Insulin-growth factor-1 (IGF-1) results in phosphorylation of both Thr 308 and Ser 473. Phosphorylation of both residues is important to generate a high level of Akt1 activity, and the phosphorylation of Thr 308 is not dependent on phosphorylation of Ser 473 *in vivo*. Thus, Akt proteins become phosphorylated and activated in Insulin/IGF-1-stimulated cells by an upstream kinase(s). The activation of Akt1 and Akt2 is inhibited by the PI kinase inhibitor Wortmannin, suggesting that the protein signals downstream of the PI kinases.

SOURCE

Akt1 (C-20) is available as either goat (sc-1618) or rabbit (sc-1618-R) polyclonal affinity purified antibody raised against a peptide mapping at the C-terminus of Akt1 of human origin.

PRODUCT

Each vial contains 200 µg IgG in 1.0 ml of PBS with < 0.1% sodium azide and 0.1% gelatin.

Blocking peptide available for competition studies, sc-1618 P, (100 µg peptide in 0.5 ml PBS containing < 0.1% sodium azide and 0.2% BSA).

Available as phycoerythrin conjugate for flow cytometry, sc-1618 PE, 100 tests; and as agarose conjugate for immunoprecipitation, sc-1618 AC, 500 µg/0.25 ml agarose in 1 ml.

APPLICATIONS

Akt1 (C-20) is recommended for detection of Akt1 and, to a lesser extent, Akt2 and Akt3 of mouse, rat, human and *Xenopus laevis* origin by Western Blotting (starting dilution 1:200, dilution range 1:100-1:1000), immunoprecipitation [1-2 µg per 100-500 µg of total protein (1 ml of cell lysate)], immunofluorescence (starting dilution 1:50, dilution range 1:50-1:500), flow cytometry (1 µg per 1 x 10^6 cells) and solid phase ELISA (starting dilution 1:30, dilution range 1:30-1:3000).

Akt1 (C-20) is also recommended for detection of Akt1 and, to a lesser extent, Akt2 and Akt3 in additional species, including equine, canine, bovine, porcine and avian.

Molecular Weight of Akt1: 62 kDa.

Positive Controls: Akt1 (h): 293T Lysate: sc-158248, HeLa whole cell lysate: sc-2200 or IMR-32 cell lysate: sc-2409.

STORAGE

Store at 4° C, **DO NOT FREEZE**. Stable for one year from the date of shipment. Non-hazardous. No MSDS required.

RESEARCH USE

For research use only, not for use in diagnostic procedures.

DATA

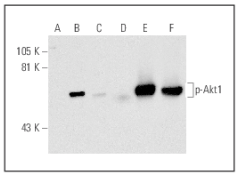

Western blot analysis of Akt1 phosphorylation in non-transfected: sc-117752 (**A,D**), untreated human Akt1 transfected: sc-158248 (**B,E**) and lambda protein phosphatase (sc-200312A) treated human Akt1 transfected: sc-158248 (**C,F**) 293T whole cell lysates. Antibodies tested include p-Akt1 (Thr 308): sc-135650 (**A-C**) and Akt1 (C-20): sc-1618 (**D-F**).

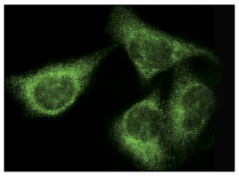

Akt1 (C-20): sc-1618. Immunofluorescence staining of methanol-fixed HeLa cells showing cytoplasmic localization.

SELECT PRODUCT CITATIONS

1. Datta, S.R., et al. 1997. Akt phosphorylation of Bad couples survival signals to the cell intrinsic death machinery. Cell 91: 231-241.
2. Sun, S., et al. 2012. The ATP-P2X7 signaling axis is dispensable for obesity-associated inflammasome activation in adipose tissue. Diabetes 61: 1471-1478.
3. Li, M., et al. 2012. HBcAg induces PD-1 upregulation on $CD4^+$T cells through activation of JNK, ERK and PI3K/AKT pathways in chronic hepatitis-B-infected patients. Lab. Invest. 92: 295-304.
4. Razolli, D.S., et al. 2012. Hypothalamic action of glutamate leads to body mass reduction through a mechanism partially dependent on JAK2. J. Cell. Biochem. 113: 1182-1189.
5. Urtasun, R., et al. 2012. Osteopontin, an oxidant stress sensitive cytokine, up-regulates collagen-I via integrin $\alpha_V\beta_3$ engagement and PI3K/pAkt/NFκB signaling. Hepatology 55: 594-608.
6. Cintra, D.E., et al. 2012. Unsaturated fatty acids revert diet-induced hypothalamic inflammation in obesity. PLoS ONE 7: e30571.
7. Ramis, G., et al. 2012. EGFR inhibition in glioma cells modulates Rho signaling to inhibit cell motility and invasion and cooperates with temozolomide to reduce cell growth. PLoS ONE 7: e38770.
8. Sarró, E., et al. 2012. A pharmacologically-based array to identify targets of cyclosporine A-induced toxicity in cultured renal proximal tubule cells. Toxicol. Appl. Pharmacol. 258: 275-287.
9. Jang, J.Y., et al. 2012. Aqueous fraction from *Cuscuta japonica* seed suppresses melanin synthesis through inhibition of the p38 mitogen-activated protein kinase signaling pathway in B16F10 cells. J. Ethnopharmacol. 141: 338-344.
10. Jia, Y. 2012. Endogenous erythropoietin signaling facilitates skeletal muscle repair and recovery following pharmacologically induced damage. FASEB J. 26: 2847-2858.

Santa Cruz Biotechnology, Inc. 1.800.457.3801 831.457.3800 fax 831.457.3801 **Europe** +00800 4573 8000 49 6221 4503 0 ***www.scbt.com***

Figure A.2: Datasheet of Total AKT antibody (hhttp://www.scbt.com/)

SANTA CRUZ BIOTECHNOLOGY, INC.

FKHRL1 (N-16): sc-9813

SANTA CRUZ BIOTECHNOLOGY
The Power to Question

BACKGROUND

FKHRL1 (forkhead in rhabdomyosarcoma-like 1), also known as FOXO3 (forkhead box O3) or FOXO3A, is a 673 amino acid transcriptional activator that belongs to the FKHR subfamily of forkhead transcription factors. Transcriptional activation of FKHR proteins is regulated by the serine/threonine kinase Akt1, which phosphorylates FKHRL1 at Threonine 32 and Serine 253. Phosphorylation by Akt1 negatively regulates FKHRL1 by promoting its export from the nucleus. Phosphorylated FKHRL1 associates with 14-3-3 proteins and this complex is retained in the cytoplasm. Growth factor withdrawal stimulates FKHRL1 dephosphorylation and nuclear translocation, leading to FKHR-induced gene-specific transcriptional activation. Within the nucleus, dephosphorylated FKHRL1 triggers apoptosis by inducing the expression of genes that are critical for cell death.

CHROMOSOMAL LOCATION

Genetic locus: FOXO3 (human) mapping to 6q21; Foxo3 (mouse) mapping to 10 B2.

SOURCE

FKHRL1 (N-16) is an affinity purified goat polyclonal antibody raised against a peptide mapping at the N-terminus of FKHRL1 of human origin.

PRODUCT

Each vial contains 200 µg IgG in 1.0 ml of PBS with < 0.1% sodium azide and 0.1% gelatin.

Blocking peptide available for competition studies, sc-9813 P, (100 µg peptide in 0.5 ml PBS containing < 0.1% sodium azide and 0.2% BSA).

Available as TransCruz reagent for Gel Supershift and ChIP applications, sc-9813 X, 200 µg/0.1 ml.

APPLICATIONS

FKHRL1 (N-16) is recommended for detection of FKHRL1 of mouse, rat and human origin by Western Blotting (starting dilution 1:200, dilution range 1:100-1:1000), immunoprecipitation [1-2 µg per 100-500 µg of total protein (1 ml of cell lysate)], immunofluorescence (starting dilution 1:50, dilution range 1:50-1:500), immunohistochemistry (including paraffin-embedded sections) (starting dilution 1:50, dilution range 1:50-1:500) and solid phase ELISA (starting dilution 1:30, dilution range 1:30-1:3000).

FKHRL1 (N-16) is also recommended for detection of FKHRL1 in additional species, including bovine and porcine.

Suitable for use as control antibody for FKHRL1 siRNA (h): sc-37887, FKHRL1 siRNA (m): sc-37888, FKHRL1 shRNA Plasmid (h): sc-37887-SH, FKHRL1 shRNA Plasmid (m): sc-37888-SH, FKHRL1 shRNA (h) Lentiviral Particles: sc-37887-V and FKHRL1 shRNA (m) Lentiviral Particles: sc-37888-V.

FKHRL1 (N-16) X TransCruz antibody is recommended for Gel Supershift and ChIP applications.

Molecular Weight (predicted) of FKHRL1: 71 kDa.

Molecular Weight (observed) of FKHRL1: 87-99 kDa.

STORAGE

Store at 4° C, **DO NOT FREEZE**. Stable for one year from the date of shipment. Non-hazardous. No MSDS required.

DATA

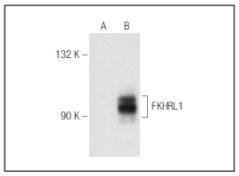

FKHRL1 (N-16): sc-9813. Western blot analysis of FKHRL1 expression in non-transfected: sc-117752 (**A**) and mouse FKHRL1 transfected: sc-178817 (**B**) 293T whole cell lysates.

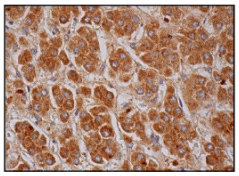

FKHRL1 (N-16): sc-9813. Immunoperoxidase staining of formalin fixed, paraffin-embedded human adrenal gland tissue showing cytoplasmic staining of glandular cells.

SELECT PRODUCT CITATIONS

1. Ghosh, A.K., et al. 2001. A nucleoprotein complex containing CCAAT/enhancer-binding protein β interacts with an insulin response sequence in the insulin-like growth factor-binding protein-1 gene and contributes to insulin-regulated gene expression. J. Biol. Chem. 276: 8507-8515.
2. Nadal, A., et al. 2002. Down-regulation of the mitochondrial 3-hydroxy-3-methylglutaryl-CoA synthase gene by insulin: the role of the forkhead transcription factor FKHRL1. Biochem. J. 366: 289-297.
3. Li, L., et al. 2003. Caveolin-1 maintains activated Akt in prostate cancer cells through scaffolding domain binding site interactions with and inhibition of serine/threonine protein phosphatases PP1 and PP2A. Mol. Cell. Biol. 23: 9389-9404.
4. Xiang, Y., et al. 2012. Calorie restriction increases primordial follicle reserve in mature female chemotherapy-treated rats. Gene 493: 77-82.
5. Kornfeld, S.F., et al. 2012. Differential expression of mature microRNAs involved in muscle maintenance of hibernating little brown bats, *Myotis lucifugus*: a model of muscle atrophy resistance. Genomics Proteomics Bioinformatics 10: 295-301.

RESEARCH USE

For research use only, not for use in diagnostic procedures.

PROTOCOLS

See our web site at www.scbt.com or our catalog for detailed protocols and support products.

Santa Cruz Biotechnology, Inc. 1.800.457.3801 831.457.3800 fax 831.457.3801 **Europe** +00800 4573 8000 49 6221 4503 0 ***www.scbt.com***

Figure A.3: Datasheet of Total FOXO antibody (hhttp://www.scbt.com/)

SANTA CRUZ BIOTECHNOLOGY, INC.

Actin (I-19): sc-1616

SANTA CRUZ BIOTECHNOLOGY

The Power to Question

BACKGROUND

All eukaryotic cells express Actin, which often constitutes as much as 50% of total cellular protein. Actin filaments can form both stable and labile structures and are crucial components of microvilli and the contractile apparatus of muscle cells. While lower eukaryotes, such as yeast, have only one Actin gene, higher eukaryotes have several isoforms encoded by a family of genes. At least six types of Actin are present in mammalian tissues and fall into three classes. α Actin expression is limited to various types of muscle, whereas β and γ are the principle constituents of filaments in other tissues. Members of the small GTPase family regulate the organization of the Actin cytoskeleton. Rho controls the assembly of Actin stress fibers and focal adhesion, Rac regulates Actin filament accumulation at the plasma membrane and Cdc42 stimulates formation of filopodia.

SOURCE

Actin (I-19) is available as either goat (sc-1616) or rabbit (sc-1616-R) polyclonal affinity purified antibody raised against a peptide mapping at the C-terminus of Actin of human origin.

PRODUCT

Each vial contains 200 µg IgG in 1.0 ml of PBS with < 0.1% sodium azide and 0.1% gelatin.

Blocking peptide available for competition studies, sc-1615 P, (100 µg peptide in 0.5 ml PBS containing < 0.1% sodium azide and 0.2% BSA).

Available as TransCruz reagent for ChIP application, sc-1615 X, 200 µg/0.1 ml; as agarose conjugate for immunoprecipitation, sc-1615 AC, 500 µg/0.25 ml agarose in 1 ml; as HRP conjugate for Western blotting, sc-1615 HRP, 200 µg/1 ml; as rhodamine (sc-1615 TRITC) conjugate for immunofluorescence, 200 µg/1 ml; as phycoerythrin (sc-1615 PE) or fluorescein (sc-1615 FITC) conjugates for flow cytometry, 100 tests; and as Alexa Fluor® 405 (sc-1615 AF405), Alexa Fluor® 488 (sc-1615 AF488) or Alexa Fluor® 647 (sc-1615 AF647) conjugates for flow cytometry or immunofluorescence; 100 µg/2 ml.

Alexa Fluor® is a trademark of Molecular Probes, Inc., Oregon, USA

APPLICATIONS

Actin (I-19) is recommended for detection of a broad range of Actin isoforms of mouse, rat, human, *Drosophila melanogaster, Xenopus laevis*, zebrafish and *Caenorhabditis elegans* origin by Western Blotting (starting dilution 1:200, dilution range 1:100-1:1000), immunoprecipitation [1-2 µg per 100-500 µg of total protein (1 ml of cell lysate)], immunofluorescence (starting dilution 1:50, dilution range 1:50-1:500), flow cytometry (1 µg per 1 x 10^6 cells) and solid phase ELISA (starting dilution 1:30, dilution range 1:30-1:3000).

Actin (I-19) is also recommended for detection of a broad range of Actin isoforms in additional species, including equine, canine, bovine, porcine and avian.

Molecular Weight of Actin: 43 kDa.

STORAGE

Store at 4° C, **DO NOT FREEZE**. Stable for one year from the date of shipment. Non-hazardous. No MSDS required.

RESEARCH USE

For research use only, not for use in diagnostic procedures.

DATA

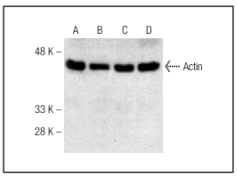

Actin (I-19): sc-1616. Western blot analysis of Actin expression in C32 (**A**), BC_3HI (**B**), Sol 8 (**C**) and L8 (**D**) whole cell lysates.

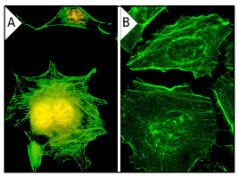

Actin (I-19): sc-1616. Immunofluorescence staining of methanol-fixed NIH/3T3 cells showing cytoskeletal fluorescein immunostaining of actin filaments. Note nuclear rhodamine immunostaining with PCNA (PC-10): sc-56 (**A**). Immunofluorescence staining of methanol-fixed HeLa cells showing cytoskeletal localization (**B**).

SELECT PRODUCT CITATIONS

1. Pogorzelska, E., et al. 1990. Modification of the test for determining bacterial capacity for nitrate reduction. Rocz. Panstw. Zakl. Hig. 41: 58-62.
2. Chung, L.C., et al. 2012. L-Mimosine blocks cell proliferation via upregulation of B-cell translocation gene 2 and N-myc downstream regulated gene 1 in prostate carcinoma cells. Am. J. Physiol., Cell Physiol. 302: C676-C685.
3. Scotti, L., et al. 2013. Involvement of the ANGPTs/Tie-2 system in ovarian hyperstimulation syndrome (OHSS). Mol. Cell. Endocrinol. 365: 223-230.
4. Alvarez, Z., et al. 2013. The effect of the composition of PLA films and lactate release on glial and neuronal maturation and the maintenance of the neuronal progenitor niche. Biomaterials 34: 2221-2233.
5. Garcia-Yague, A.J., et al. 2013. Nuclear import and export signals control the subcellular localization of Nurr1 in response to oxidative stress. J. Biol. Chem. 288: 5506-5517.
6. Kaur, J. and Tikoo, K. 2013. Evaluating cell specific cytotoxicity of differentially charged silver nanoparticles. Food Chem. Toxicol. 51: 1-14.
7. Miranda-Goncalves, V., et al. 2013. Monocarboxylate transporters (MCTs) in gliomas: expression and exploitation as therapeutic targets. Neuro Oncol. 15: 172-188.
8. Faouzi, M., et al. 2013. ORAI3 silencing alters cell proliferation and cell cycle progression via c-myc pathway in breast cancer cells. Biochim. Biophys. Acta 1833: 752-760.
9. Lutz, D., et al. 2013. Generation and nuclear translocation of sumoylated transmembrane fragment of cell adhesion molecule L1. J. Biol. Chem. 287: 17161-17175.
10. García-Corzo, L., et al. 2013. Dysfunctional Coq9 protein causes predominant encephalomyopathy associated with CoQ deficiency. Hum. Mol. Genet. 22: 1233-1248.

Santa Cruz Biotechnology, Inc. 1.800.457.3801 831.457.3800 fax 831.457.3801 **Europe** +00800 4573 8000 49 6221 4503 0 ***www.scbt.com***

Figure A.4: Datasheet of Actin antibody (hhttp://www.scbt.com/)

SANTA CRUZ BIOTECHNOLOGY, INC.

MDM2 (C-18): sc-812

SANTA CRUZ BIOTECHNOLOGY
The Power to Question

BACKGROUND

p53 is the most commonly mutated gene in human cancer identified to date. Expression of p53 leads to inhibition of cell growth by preventing progression of cells from G_1 to S phase of the cell cycle. Most importantly, p53 functions to cause arrest of cells in the G_1 phase of the cell cycle following any exposure of cells to DNA-damaging agents. The MDM2 (murine double minute-2) protein was initially identified as an oncogene in a murine transformation system. MDM2 functions to bind p53 and block p53-mediated transactivation of cotransfected reporter constructs. The MDM2 gene is amplified in a high percentage of human sarcomas that retain wildtype p53 and tumor cells that overexpress MDM2 can tolerate high levels of p53 expression. These findings argue that MDM2 overexpression represents at least one mechanism by which p53 function can be abrogated during tumorigenesis.

CHROMOSOMAL LOCATION

Genetic locus: MDM2 (human) mapping to 12q15; Mdm2 (mouse) mapping to 10 D2.

SOURCE

MDM2 (C-18) is an affinity purified rabbit polyclonal antibody raised against a peptide mapping within the C-terminus of MDM2 of human origin.

PRODUCT

Each vial contains 200 µg IgG in 1.0 ml of PBS with < 0.1% sodium azide and 0.1% gelatin.

Blocking peptide available for competition studies, sc-812 P, (100 µg peptide in 0.5 ml PBS containing < 0.1% sodium azide and 0.2% BSA).

APPLICATIONS

MDM2 (C-18) is recommended for detection of MDM2 of mouse, rat and human origin by Western Blotting (starting dilution 1:100, dilution range 1:50-1:500), immunoprecipitation [1-2 µg per 100-500 µg of total protein (1 ml of cell lysate)], immunofluorescence (starting dilution 1:25, dilution range 1:25-1:250) and solid phase ELISA (starting dilution 1:30, dilution range 1:30-1:3000).

MDM2 (C-18) is also recommended for detection of MDM2 in additional species, including equine, canine, bovine, porcine, avian and feline.

Suitable for use as control antibody for MDM2 siRNA (h): sc-29394, MDM2 siRNA (m): sc-37263, MDM2 shRNA Plasmid (h): sc-29394-SH, MDM2 shRNA Plasmid (m): sc-37263-SH, MDM2 shRNA (h) Lentiviral Particles: sc-29394-V and MDM2 shRNA (m) Lentiviral Particles: sc-37263-V.

Molecular Weight of MDM2: 90 kDa.

Molecular Weight of MDM2 cleavage product: 60 kDa.

Positive Controls: A-673 cell lysate: sc-2414, RAW 264.7 whole cell lysate: sc-2211 or MCF7 whole cell lysate: sc-2206.

STORAGE

Store at 4° C, **DO NOT FREEZE**. Stable for one year from the date of shipment. Non-hazardous. No MSDS required.

RESEARCH USE

For research use only, not for use in diagnostic procedures.

DATA

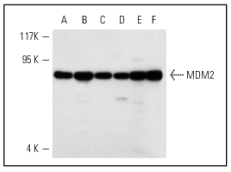

MDM2 (C-18): sc-812. Western blot analysis of MDM2 expression in MCF7 (**A**), V-205 (**B**), A-673 (**C**), RAW 264.7 (**D**), Jurkat (**E**) and MDA-MB-468 (**F**) whole cell lysates.

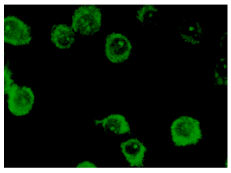

MDM2 (C-18): sc-812. Immunofluorescence staining of methanol-fixed RAW 264.7 cells showing cytoplasmic localization.

SELECT PRODUCT CITATIONS

1. Carroll, P.E., et al. 1999. Centrosome hyperamplification in human cancer: chromosome instability by p53 mutation and/or MDM2 overexpression. Oncogene 18: 1935-1944.
2. Eischen, C.M., et al. 2001. Bax loss impairs Myc-induced apoptosis and circumvents the selection of p53 mutations during Myc-mediated lymphomagenesis. Mol. Cell. Biol. 21: 7653-7662.
3. Samuels-Lev, Y., et al. 2001. ASPP proteins specifically stimulate the apoptotic function of p53. Mol. Cell 8: 781-794.
4. Steinman, H.A., et al. 2004. An alternative splice form of MDM2 induces p53-independent cell growth and tumorigenesis. J. Biol. Chem. 279: 4877-4886.
5. Perucca-Lostanlen, D., et al. 2004. Distinct MDM2 and p14 ARF expression and centrosome amplification in well-differentiated liposarcomas. Genes Chromosomes Cancer 39: 99-109.
6. Eischen, C.M., et al. 2004. Loss of one allele of ARF rescues MDM2 haploinsufficiency effects on apoptosis and lymphoma development. Oncogene 23: 8931-8940.
7. Gladden, A.B., et al. 2006. Expression of constitutively nuclear cyclin D1 in murine lymphocytes induces B-cell lymphoma. Oncogene 25: 998-1007.
8. Gorrini, C., et al. 2007. Tip60 is a haplo-insufficient tumour suppressor required for an oncogene-induced DNA damage response. Nature 448: 1063-1067.
9. Kulikov, R., et al. 2010. Mdm2 facilitates the association of p53 with the proteasome. Proc. Natl. Acad. Sci. USA 107: 10038-10043.
10. Arrate, M.P., et al. 2010. MicroRNA biogenesis is required for Myc-induced B-cell lymphoma development and survival. Cancer Res. 70: 6083-6092.
11. Ta, V.B., et al. 2010. Malignant transformation of Slp65-deficient pre-B cells involves disruption of the Arf-Mdm2-p53 tumor suppressor pathway. Blood 115: 1385-1393.

Santa Cruz Biotechnology, Inc. 1.800.457.3801 831.457.3800 fax 831.457.3801 **Europe** +00800 4573 8000 49 6221 4503 0 ***www.scbt.com***

Figure A.5: Datasheet of MDM2 antibody (hhttp://www.scbt.com/)

SANTA CRUZ BIOTECHNOLOGY, INC.

Bim (H-191): sc-11425

SANTA CRUZ BIOTECHNOLOGY
The Power to Question

BACKGROUND

Pro-apototic Bcl-2 family members promote cell death by neutralizing their anti-apoptotic relatives, which otherwise maintain cell viability by regulating caspase activity. Bim belongs to the BH3-only subgroup of Bcl-2 related proteins and exists in three distinct isoforms, Bim_S (short), Bim_L (long) and Bim_{EL} (extra long). ERK1/2 phosphorylates Bim_{EL}, resulting in rapid degradation of the isoform via the proteasome pathway. At least three sites for ERK1/2 phosphorylation exist on Bim_{EL}, whereas ERK1/2 does not effect Bim_S or Bim_L, implying a unique role for Bim_{EL} in cell survival signaling.

CHROMOSOMAL LOCATION

Genetic locus: BCL2L11 (human) mapping to 2q13; Bcl2l11 (mouse) mapping to 2 F1.

SOURCE

Bim (H-191) is a rabbit polyclonal antibody raised against amino acids 4-195 of Bim_{EL} of human origin.

PRODUCT

Each vial contains 200 µg IgG in 1.0 ml of PBS with < 0.1% sodium azide and 0.1% gelatin.

APPLICATIONS

Bim (H-191) is recommended for detection of Bim_{EL}, Bim_L and Bim_S of mouse, rat and human origin by Western Blotting (starting dilution 1:200, dilution range 1:100-1:1000), immunoprecipitation [1-2 µg per 100-500 µg of total protein (1 ml of cell lysate)], immunofluorescence (starting dilution 1:50, dilution range 1:50-1:500), immunohistochemistry (including paraffin-embedded sections) (starting dilution 1:50, dilution range 1:50-1:500) and solid phase ELISA (starting dilution 1:30, dilution range 1:30-1:3000).

Suitable for use as control antibody for Bim siRNA (h): sc-29802, Bim siRNA (m): sc-29803, Bim shRNA Plasmid (h): sc-29802-SH, Bim shRNA Plasmid (m): sc-29803-SH, Bim shRNA (h) Lentiviral Particles: sc-29802-V and Bim shRNA (m) Lentiviral Particles: sc-29803-V.

Molecular Weight of Bim_S: 19 kDa.

Molecular Weight of Bim_L: 21 kDa.

Molecular Weight of Bim_{EL}: 24 kDa.

Positive Controls: HuT 78 whole cell lysate: sc-2208 or HL-60 whole cell lysate: sc-2209.

STORAGE

Store at 4° C, **DO NOT FREEZE**. Stable for one year from the date of shipment. Non-hazardous. No MSDS required.

PROTOCOLS

See our web site at www.scbt.com or our catalog for detailed protocols and support products.

RESEARCH USE

For research use only, not for use in diagnostic procedures.

DATA

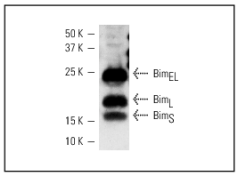

Bim (FL-198): sc-11425. Western blot analysis of Bim isoform expression in HuT 78 whole cell lysate.

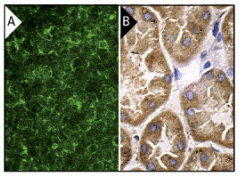

Bim (H-191): sc-11425. Immunofluorescence staining of normal mouse lymph node frozen section showing cytoplasmic staining (**A**). Immunoperoxidase staining of formalin fixed, paraffin-embedded human kidney tissue showing cytoplasmic staining of cells in tubules (**B**).

SELECT PRODUCT CITATIONS

1. Qin, J.Z., et al. 2004. p53-independent NOXA induction overcomes apoptotic resistance of malignant melanomas. Mol. Cancer Ther. 3: 895-902.
2. Castera, L., et al. 2009. Apoptosis-related mitochondrial dysfunction defines human monocyte-derived dendritic cells with impaired immuno-stimulatory capacities. J. Cell. Mol. Med. 13: 1321-1335.
3. Tong, D.D., et al. 2009. RUNX3 inhibits cell proliferation and induces apoptosis by TGF-β-dependent and -independent mechanisms in human colon carcinoma cells. Pathobiology 76: 163-169.
4. Yu, C.Z., et al. 2009. Neuroprotection against transient focal cerebral ischemia and oxygen-glucose deprivation by interference with GluR6-PSD95 protein interaction. Neurochem. Res. 34: 2008-2021.
5. Di Leva, G., et al. 2010. MicroRNA cluster 221-222 and estrogen receptor α interactions in breast cancer. J. Natl. Cancer Inst. 102: 706-721.
6. Lai, K.W., et al. 2010. MicroRNA-130β regulates the tumour suppressor RUNX3 in gastric cancer. Eur. J. Cancer 46: 1456-1463.
7. Wood, K.L., et al. 2010. The small heat shock protein 27 is a key regulator of $CD8^+$ $CD57^+$ lymphocyte survival. J. Immunol. 184: 5582-5588.
8. Latré de Laté, P., et al. 2010. Glucocorticoid-induced leucine zipper (GILZ) promotes the nuclear exclusion of FOXO3 in a Crm1-dependent manner. J. Biol. Chem. 285: 5594-5605.
9. Stühmer, T., et al. 2010. Preclinical anti-myeloma activity of the novel HDAC-inhibitor JNJ-26481585. Br. J. Haematol. 149: 529-536.
10. Kim, K.D., et al. 2011. ORAI1 deficiency impairs activated T cell death and enhances T cell survival. J. Immunol. 187: 3620-3630.
11. Essafi, M., et al. 2011. Cell-penetrating TAT-FOXO3 fusion proteins induce apoptotic cell death in leukemic cells. Mol. Cancer Ther. 10: 37-46.
12. Liao, M., et al. 2011. Role of bile salt in regulating Mcl-1 phosphorylation and chemoresistance in hepatocellular carcinoma cells. Mol. Cancer 10: 44.

Santa Cruz Biotechnology, Inc. 1.800.457.3801 831.457.3800 fax 831.457.3801 **Europe** +00800 4573 8000 49 6221 4503 0 ***www.scbt.com***

Figure A.6: Datasheet of BIM antibody (hhttp://www.scbt.com/)

SANTA CRUZ BIOTECHNOLOGY, INC.

FAS-L (C-178): sc-6237

SANTA CRUZ BIOTECHNOLOGY

The Power to Question

BACKGROUND

Cytotoxic T lymphocyte (CTL)-mediated cytotoxicity constitutes an important component of specific effector mechanisms in immuno-surveillance against virus-infected or transformed cells. Two mechanisms appear to account for this activity, one of which is the perforin-based process. Independently, a FAS-based mechanism involves the transducing molecule FAS (also designated Apo-1) and its ligand (FAS-L). The human FAS protein is a cell surface glycoprotein that belongs to a family of receptors that includes CD40, nerve growth factor receptors and tumor necrosis factor receptors. The FAS antigen is expressed on a broad range of lymphoid cell lines, certain of which undergo apoptosis in response to treatment with antibody to FAS. These findings strongly imply that targeted cell death is potentially mediated by the intercellular interactions of FAS with its ligand or effectors, and that FAS may be critically involved in CTL-mediated cytotoxicity.

CHROMOSOMAL LOCATION

Genetic locus: FASLG (human) mapping to 1q24.3; Fasl (mouse) mapping to 1 H2.1.

SOURCE

FAS-L (C-178) is a rabbit polyclonal antibody raised against amino acids 100-278 mapping at the C-terminus of FAS-L of rat origin.

PRODUCT

Each vial contains 200 µg IgG in 1.0 ml of PBS with < 0.1% sodium azide and 0.1% gelatin.

Available as agarose conjugate for immunoprecipitation, sc-6237 AC, 500 µg/0.25 ml agarose in 1 ml.

APPLICATIONS

FAS-L (C-178) is recommended for detection of FAS-L of mouse, rat and human origin by Western Blotting (starting dilution 1:200, dilution range 1:100-1:1000), immunoprecipitation [1-2 µg per 100-500 µg of total protein (1 ml of cell lysate)], immunofluorescence (starting dilution 1:50, dilution range 1:50-1:500) and solid phase ELISA (starting dilution 1:30, dilution range 1:30-1:3000).

Suitable for use as control antibody for FAS-L siRNA (h): sc-29313, FAS-L siRNA (m): sc-35358, FAS-L shRNA Plasmid (h): sc-29313-SH, FAS-L shRNA Plasmid (m): sc-35358-SH, FAS-L shRNA (h) Lentiviral Particles: sc-29313-V and FAS-L shRNA (m) Lentiviral Particles: sc-35358-V.

Molecular Weight of soluble FAS-L: 26 kDa.

Molecular Weight of FAS-L membrane: 40 kDa.

Positive Controls: HL-60 whole cell lysate: sc-2209, Jurkat whole cell lysate: sc-2204 or K-562 whole cell lysate: sc-2203.

STORAGE

Store at 4° C, **DO NOT FREEZE**. Stable for one year from the date of shipment. Non-hazardous. No MSDS required.

RESEARCH USE

For research use only, not for use in diagnostic procedures.

DATA

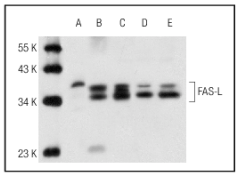

FAS-L (C-178): sc-6237. Western blot analysis of FAS-L expression in AML-193 (**A**), HL-60 (**B**), K-562 (**C**), CCRF-CEM (**D**) and Jurkat (**E**) whole cell lysates.

SELECT PRODUCT CITATIONS

1. Chen, M.K., et al. 1999. FAS-mediated induction of hepatocyte apoptosis in a neurobalstoma and hepatocyte coculture model. J. Surg. Res. 84: 82-87.
2. Wang, Y., et al. 2008. Protective effect of a standardized Ginkgo extract (ginaton) on renal ischemia/reperfusion injury via suppressing the activation of JNK signal pathway. Phytomedicine 15: 923-931.
3. Liu, Q.B., et al. 2010. The induction of reactive oxygen species and loss of mitochondrial Omi/HtrA2 is associated with S-nitrosoglutathione-induced apoptosis in human endothelial cells. Toxicol. Appl. Pharmacol. 244: 374-384.
4. Williams, K.E., et al. 2010. Lumican reduces tumor growth via induction of fas-mediated endothelial cell apoptosis. Cancer Microenviron. 4: 115-126.
5. Pan, J., et al. 2010. Small peptide inhibitor of JNKs protects against MPTP-induced nigral dopaminergic injury via inhibiting the JNK-signaling pathway. Lab. Invest. 90: 156-167.
6. Qi, S.H., et al. 2010. Neuroprotection of ethanol against ischemia/reperfusion-induced brain injury through decreasing c-Jun N-terminal kinase 3 (JNK3) activation by enhancing GABA release. Neuroscience 167: 1125-1137.
7. Jin, X., et al. 2010. Apoptosis-inducing activity of the antimicrobial peptide cecropin of *Musca domestica* in human hepatocellular carcinoma cell line BEL-7402 and the possible mechanism. Acta Biochim. Biophys. Sin. 42: 259-265.
8. Li, C., et al. 2010. Coactivation of GABA receptors inhibits the JNK3 apoptotic pathway via disassembly of GluR6-PSD-95-MLK3 signaling module in KA-induced seizure. Epilepsia 51: 391-403.
9. Zhang, J., et al. 2011. Activation of GluR6-containing kainate receptors induces ubiquitin-dependent Bcl-2 degradation via denitrosylation in the rat hippocampus after kainate treatment. J. Biol. Chem. 286: 7669-7680.

Santa Cruz Biotechnology, Inc. 1.800.457.3801 831.457.3800 fax 831.457.3801 **Europe** +00800 4573 8000 49 6221 4503 0 ***www.scbt.com***

Figure A.7: Datasheet of FasLG antibody (hhttp://www.scbt.com/)

SANTA CRUZ BIOTECHNOLOGY, INC.

p27 (F-8): sc-1641

BACKGROUND

Cell cycle progression is regulated by a series of cyclin-dependent kinases that consist of catalytic subunits, designated Cdks, and activating subunits, designated cyclins. Orderly progression through the cell cycle requires the activation and inactivation of different cyclin-Cdks at appropriate times. A series of proteins has been recently described that function as "mitotic inhibitors." These include p21, the levels of which are elevated upon DNA damage in G_1 in a p53-dependent manner, p16 and a more recently described p16 related inhibitor designated p15. A p21 related protein, p27, has been described as a negative regulator of G_1 progression and has been speculated to function as a possible mediator of TGFβ-induced G_1 arrest. p27 interacts strongly with D-type cyclins and Cdk4 *in vitro* and to a lesser extent with cyclin E and Cdk2.

CHROMOSOMAL LOCATION

Genetic locus: CDKN1B (human) mapping to 12p13.1; Cdkn1b (mouse) mapping to 6 G1.

SOURCE

p27 (F-8) is a mouse monoclonal antibody raised against amino acids 1-197 representing full length p27 of mouse origin.

PRODUCT

Each vial contains 200 µg IgG_1 in 1.0 ml of PBS with < 0.1% sodium azide and 0.1% gelatin.

Available as agarose conjugate for immunoprecipitation, sc-1641 AC, 500 µg/0.25 ml agarose in 1 ml; fluorescein (sc-1641 FITC) or rhodamine (sc-1641 TRITC) conjugates for immunofluorescence, 200 µg/ml; Alexa Fluor® 405 (sc-1641 AF405), Alexa Fluor® 488 (sc-1641 AF488) or Alexa Fluor® 647 (sc-1641 AF647) conjugates for flow cytometry or immunofluorescence; 100 µg/2 ml.

Alexa Fluor® is a trademark of Molecular Probes, Inc., Oregon, USA.

APPLICATIONS

p27 (F-8) is recommended for detection of p27 of mouse, rat and human origin by Western Blotting (starting dilution 1:200, dilution range 1:100-1:1000), immunoprecipitation [1-2 µg per 100-500 µg of total protein (1 ml of cell lysate)], immunofluorescence (starting dilution 1:50, dilution range 1:50-1:500), immunohistochemistry (including paraffin-embedded sections) (starting dilution 1:50, dilution range 1:50-1:500), flow cytometry (1 µg per 1 x 10^6 cells) and solid phase ELISA (starting dilution 1:30, dilution range 1:30-1:3000).

Suitable for use as control antibody for p27 siRNA (h): sc-29429, p27 siRNA (m): sc-29430, p27 shRNA Plasmid (h): sc-29429-SH, p27 shRNA Plasmid (m): sc-29430-SH, p27 shRNA (h) Lentiviral Particles: sc-29429-V and p27 shRNA (m) Lentiviral Particles: sc-29430-V.

Molecular Weight of p27: 27 kDa.

Positive Controls: MM-142 cell lysate: sc-2246, MCF7 whole cell lysate: sc-2206 or KNRK whole cell lysate: sc-2214.

STORAGE

Store at 4° C, **DO NOT FREEZE**. Stable for one year from the date of shipment. Non-hazardous. No MSDS required.

DATA

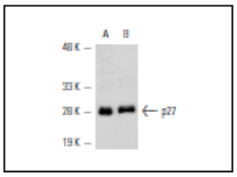

p27 (F-8): sc-1641. Western blot analysis of p27 expression in MM-142 (**A**) and KNRK (**B**) whole cell lysates.

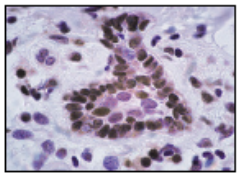

p27 (F-8): sc-1641. Immunoperoxidase staining of formalin-fixed, paraffin-embedded human breast carcinoma tissue showing nuclear localization of p27.

SELECT PRODUCT CITATIONS

1. Reynoud, E., et al. 1999. $p57^{Kip2}$ stabilizes the MyoD protein by inhibiting cyclin E-Cdk2 kinase activity in growing myoblasts. Mol. Cell. Biol. 19: 7621-7629.
2. Sane, A.T. and Bertrand, R. 1999. Caspase inhibition in camptothecin-treated U-937 cells is coupled with a shift from apoptosis to transient G_1 arrest followed by necrotic cell death. Cancer Res. 59: 3565-3569.
3. Kato, K., et al. 2011. Sodium butyrate inhibits the self-renewal capacity of endometrial tumor side-population cells by inducing a DNA damage response. Mol. Cancer Ther. 10: 1430-1439.
4. Kollmann, K., et al. 2011. c-JUN promotes BCR-ABL-induced lymphoid leukemia by inhibiting methylation of the 5' region of Cdk6. Blood 117: 4065-4075.
5. Bonfili, L., et al. 2011. Identification of an EGCG oxidation derivative with proteasome modulatory activity. Biochimie 93: 931-940.
6. Hsu, J.D., et al. 2011. Gallic acid induces G_2/M phase arrest of breast cancer cell MCF-7 through stabilization of $p27^{Kip1}$ attributed to disruption of $p27^{Kip1}$/Skp2 complex. J. Agric. Food Chem. 59: 1996-2003.
7. Li, L., et al. 2011. SIRT1 acts as a modulator of neointima formation following vascular injury in mice. Circ. Res. 108: 1180-1189.
8. Musumeci, G., et al. 2011. Mineral fibre toxicity: expression of retinoblastoma (Rb) and phospho-retinoblastoma (pRb) protein in alveolar epithelial and mesothelial cell lines exposed to fluoro-edenite fibres. Cell Biol. Toxicol. 27: 217-225.
9. Freije, A., et al. 2012. Cyclin E drives human keratinocyte growth into differentiation. Oncogene 31: 5180-5192.
10. Bonfili, L., et al. 2012. Arene-Ru^{II} complexes of curcumin exert antitumor activity via proteasome inhibition and apoptosis induction. ChemMedChem 7: 2010-2020.

RESEARCH USE

For research use only, not for use in diagnostic procedures.

Figure A.8: Datasheet of p27 antibody (hhttp://www.scbt.com/)

SANTA CRUZ BIOTECHNOLOGY, INC.

p-FKHRL1 (Ser 253): sc-101683

BACKGROUND

FKHRL1 (for forkhead in rhabdomyosarcoma) is a member of the FKHR subfamily of forkhead transcription factors. Transcriptional activation of FKHR proteins is regulated by the serine/threonine kinase Akt1, which phosphorylates FKHRL1 at Threonine 32 and Serine 253. Phosphorylation by Akt1 negatively regulates FKHRL1 by promoting its export from the nucleus. Phosphorylated FKHRL1 associates with 14-3-3 proteins and this complex is retained in the cytoplasm. Growth factor withdrawal stimulates FKHRL1 dephosphorylation and nuclear translocation, leading to FKHR-induced gene-specific transcriptional activation. Within the nucleus, dephosphorylated FKHRL1 triggers apoptosis by inducing the expression of genes that are critical for cell death.

REFERENCES

1. Galili, N., Davis, R.J., Fredericks, W.J., Mukhopadhyay, S., Rauscher, F.J. III, Emanuel, B.S., Rovera, G. and Barr, F.G. 1993. Fusion of a forkhead domain gene to Pax-3 in the solid tumour alveolar rhabdomyosarcoma. Nat. Genet. 5: 230-235.
2. Anderson, M.J., Viars, C.S., Czekay, S., Cavenee, W.K. and Arden, K.C. 1998. Cloning and characterization of three human forkhead genes that comprise an FKHR-like gene subfamily. Genomics 47: 187-199.
3. Biggs, W.H. III, Meisenhelder, J., Hunter, T., Cavenee, W.K. and Arden, K.C. 1999. Protein kinase B/Akt-mediated phosphorylation promotes nuclear exclusion of the winged helix transcription factor FKHR1. Proc. Natl. Acad. Sci. USA 96: 7421-7426.
4. Brunet, A., Bonni, A., Zigmond, M.J., Lin, M.Z., Juo, P., Hu, L.S., Anderson, M.J., Arden, K.C., Blenis, J. and Greenberg, M.E. 1999. Akt promotes cell survival by phosphorylating and inhibiting a forkhead transcription factor. Cell 96: 857-868.
5. Tang, E.D., Nunez, G., Barr, F.G. and Guan, K.L. 1999. Negative regulation of the forkhead transcription factor FKHR by Akt. J. Biol. Chem. 274: 16741-16746.

CHROMOSOMAL LOCATION

Genetic locus: FOXO3A (human) mapping to 6q21; Foxo3a (mouse) mapping to 10 B2.

SOURCE

p-FKHRL1 (Ser 253) is a rabbit polyclonal antibody raised against a short amino acid sequence containing phosphorylated Ser 253 of FKHRL1 of human origin.

PRODUCT

Each vial contains 100 µg IgG in 1.0 ml of PBS with < 0.1% sodium azide and 0.1% gelatin.

STORAGE

Store at 4° C, **DO NOT FREEZE**. Stable for one year from the date of shipment. Non-hazardous. No MSDS required.

APPLICATIONS

p-FKHRL1 (Ser 253) is recommended for detection of Ser 253 phosphorylated FKHRL1 of human origin and correspondingly phosphorylated Ser 253 of mouse and rat origin by Western Blotting (starting dilution 1:200, dilution range 1:100-1:1000), immunoprecipitation [1-2 µg per 100-500 µg of total protein (1 ml of cell lysate)], immunofluorescence and immunohistochemistry (including paraffin-embedded sections) (starting dilution 1:50, dilution range 1:50-1:500).

Suitable for use as control antibody for FKHRL1 siRNA (h): sc-37887, FKHRL1 siRNA (m): sc-37888, FKHRL1 shRNA Plasmid (h): sc-37887-SH, FKHRL1 shRNA Plasmid (m): sc-37888-SH, FKHRL1 shRNA (h) Lentiviral Particles: sc-37887-V and FKHRL1 shRNA (m) Lentiviral Particles: sc-37888-V.

Molecular Weight of p-FKHRL1: 97 kDa.

Positive Controls: NIH/3T3 + serum cell lysate: sc-2248, NIH/3T3 + serum cell lysate: sc-2248 or HeLa + serum-starved cell lysate: sc-24693.

DATA

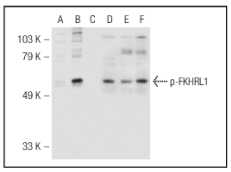

Western blot analysis of FKHRL1 phosphorylation in untreated (**A**,**D**), serum starved and serum treated (**B**,**E**) and serum starved, serum treated and lambda protein phosphatase (sc-200312A) treated (**C**,**F**) HeLa whole cell lysates. Antibodies tested include p-FKHRL1 (Ser 253): sc-101683 (**A**,**B**,**C**) and FKHRL1 (H-144): sc-11351 (**D**,**E**,**F**).

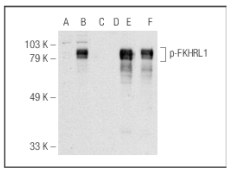

Western blot analysis of FKHRL1 phosphorylation in non-transfected: sc-117752 (**A**,**D**), untreated mouse FKHRL1 transfected: sc-178617 (**B**,**E**) and lambda protein phosphatase (sc-200312A) treated mouse FKHRL1 transfected: sc-178617 (**C**,**F**) 293T whole cell lysates. Antibodies tested include p-FKHRL1 (Ser 253): sc-101683 (**A**,**B**,**C**) and FKHRL1 (m): 293T Lysate: sc-11351 (**D**,**E**,**F**).

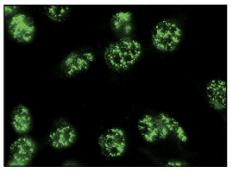

p-FKHRL1 (Ser 253): sc-101683. Immunofluorescence staining of methanol-fixed NIH/3T3 cells showing nuclear localization.

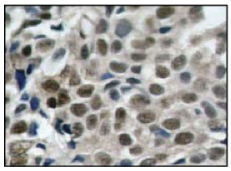

p-FKHRL1 (Ser 253): sc-101683. Immunoperoxidase staining of formalin-fixed, paraffin-embedded human breast carcinoma tissue showing nuclear staining.

RESEARCH USE

For research use only, not for use in diagnostic procedures.

PROTOCOLS

See our web site at www.scbt.com or our catalog for detailed protocols and support products.

Santa Cruz Biotechnology, Inc. 1.800.457.3801 831.457.3800 fax 831.457.3801 **Europe** +00800 4573 8000 49 6221 4503 0 ***www.scbt.com***

Figure A.9: Datasheet of phospho-FOXO antibody (hhttp://www.scbt.com/)

SANTA CRUZ BIOTECHNOLOGY, INC.

Lamin A/C (N-18): sc-6215

BACKGROUND

A unique family of cysteine proteases has been described that differs in sequence, structure and substrate specificity from any previously described protease family. This family, termed Ced-3/ICE, is comprised of ICE, CPP32, ICH-1/Nedd-2, Tx, Mch2, Mch3 (ICE-LAP3 or CMH-1), Mch4 and ICE-LAP6. Ced-3/ICE family members function as key components of the apoptotic machinery and act to destroy specific target proteins which are critical to cellular longevity. Nuclear lamins are critical to maintaining the integrity of the nuclear envelope and cellular morphology. The nuclear Lamin A is cleaved by Mch2, but not CPP32. Nuclear Lamin B is fragmented as a consequence of apoptosis by an unidentified member of the ICE family. Lamin C is a splice variant of Lamin A, differing only at the carboxy-terminus. Lamins A and C are identical for the first 566 amino acids, with Lamin C differing only in 6 unique carboxy-terminal amino acids.

CHROMOSOMAL LOCATION

Genetic locus: LMNA (human) mapping to 1q22; Lmna (mouse) mapping to 3 F1.

SOURCE

Lamin A/C (N-18) is an affinity purified goat polyclonal antibody raised against a peptide mapping at the N-terminus of Lamin A/C of human origin.

PRODUCT

Each vial contains 100 µg IgG in 1.0 ml of PBS with < 0.1% sodium azide and 0.1% gelatin.

Blocking peptide available for competition studies, sc-6215 P, (100 µg peptide in 0.5 ml PBS containing < 0.1% sodium azide and 0.2% BSA).

APPLICATIONS

Lamin A/C (N-18) is recommended for detection of Lamin A and Lamin C of mouse, rat and human origin by Western Blotting (starting dilution 1:200, dilution range 1:100-1:1000), immunoprecipitation [1-2 µg per 100-500 µg of total protein (1 ml of cell lysate)], immunofluorescence (starting dilution 1:50, dilution range 1:50-1:500) and solid phase ELISA (starting dilution 1:30, dilution range 1:30-1:3000).

Lamin A/C (N-18) is also recommended for detection of Lamin A and Lamin C in additional species, including equine, canine, bovine and porcine.

Suitable for use as control antibody for Lamin A/C siRNA (h): sc-35776, Lamin A/C siRNA (m): sc-29385, Lamin A/C shRNA Plasmid (h): sc-35776-SH, Lamin A/C shRNA Plasmid (m): sc-29385-SH, Lamin A/C shRNA (h) Lentiviral Particles: sc-35776-V and Lamin A/C shRNA (m) Lentiviral Particles: sc-29385-V.

Molecular Weight of Lamin A/C: 69/62 kDa.

STORAGE

Store at 4° C, **DO NOT FREEZE**. Stable for one year from the date of shipment. Non-hazardous. No MSDS required.

RESEARCH USE

For research use only, not for use in diagnostic procedures.

DATA

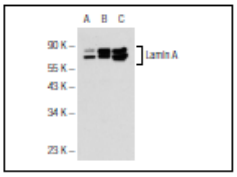

Lamin A/C (N-18): sc-6215. Western blot analysis of Lamin A expression in non-transfected 293T: sc-117752 (**A**), human Lamin A transfected 293T: sc-177452 (**B**) and HeLa (**C**) whole cell lysates.

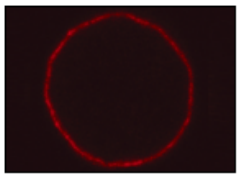

Lamin A/C (N-18): sc-6215. Immunofluorescence staining of transgenic *Drosophila* salivary gland nucleus expressing human Lamin A. Confocal section shows nuclear rim localization. Courtesy of Schulze, S.R. and Wallrath, L.L.W. unpublished.

SELECT PRODUCT CITATIONS

1. Barboro, P., et al. 2002. Unraveling the organization of the internal nuclear matrix: RNA-dependent anchoring of NuMA to a lamin scaffold. Exp. Cell Res. 279: 202-218.
2. Liu, G.H., et al. 2011. Recapitulation of premature ageing with iPSCs from Hutchinson-Gilford progeria syndrome. Nature 472: 221-225.
3. Bertrand, A.T., et al. 2012. DelK32-lamin A/C has abnormal location and induces incomplete tissue maturation and severe metabolic defects leading to premature death. Hum. Mol. Genet. 21: 1037-1048.
4. Orr, S.J., et al. 2012. Proteomic and protein interaction network analysis of human T lymphocytes during cell-cycle entry. Mol. Syst. Biol. 8: 573.
5. Magagnotti, C., et al. 2012. Protein profiling reveals energy metabolism and cytoskeletal protein alterations in LMNA mutation carriers. Biochim. Biophys. Acta 1822: 970-979.
6. Adriana, R., et al. 2012. Melanocortin 5 receptor signaling and internalization: role of MAPK/ERK pathway and β-arrestins 1/2. Mol. Cell. Endocrinol. 361: 69-79.
7. Capanni, C., et al. 2012. Familial partial lipodystrophy, mandibuloacral dysplasia and restrictive dermopathy feature barrier-to-autointegration factor (BAF) nuclear redistribution. Cell Cycle 11: 3568-3577.
8. Madureira, P.A., et al. 2012. Genotoxic agents promote the nuclear accumulation of annexin A2: role of annexin A2 in mitigating DNA damage. PLoS ONE 7: e50591.
9. Perrin, S., et al. 2012. HIV protease inhibitors do not cause the accumulation of prelamin A in PBMCs from patients receiving first line therapy: the ANRS EP45 "aging" study. PLoS ONE 7: e53035.
10. Kula, A., et al. 2013. HIV-1 pre-mRNA commitment to Rev mediated export through PSF and Matrin 3. Virology 435: 329-340.
11. Garcia-Corzo, L., et al. 2013. Dysfunctional Coq9 protein causes predominant encephalomyopathy associated with CoQ deficiency. Hum. Mol. Genet. 22: 1233-1248.

Santa Cruz Biotechnology, Inc. 1.800.457.3801 831.457.3800 fax 831.457.3801 **Europe** +00800 4573 8000 49 6221 4503 0 ***www.scbt.com***

Figure A.10: Datasheet of Lamin antibody (hhttp://www.scbt.com/)

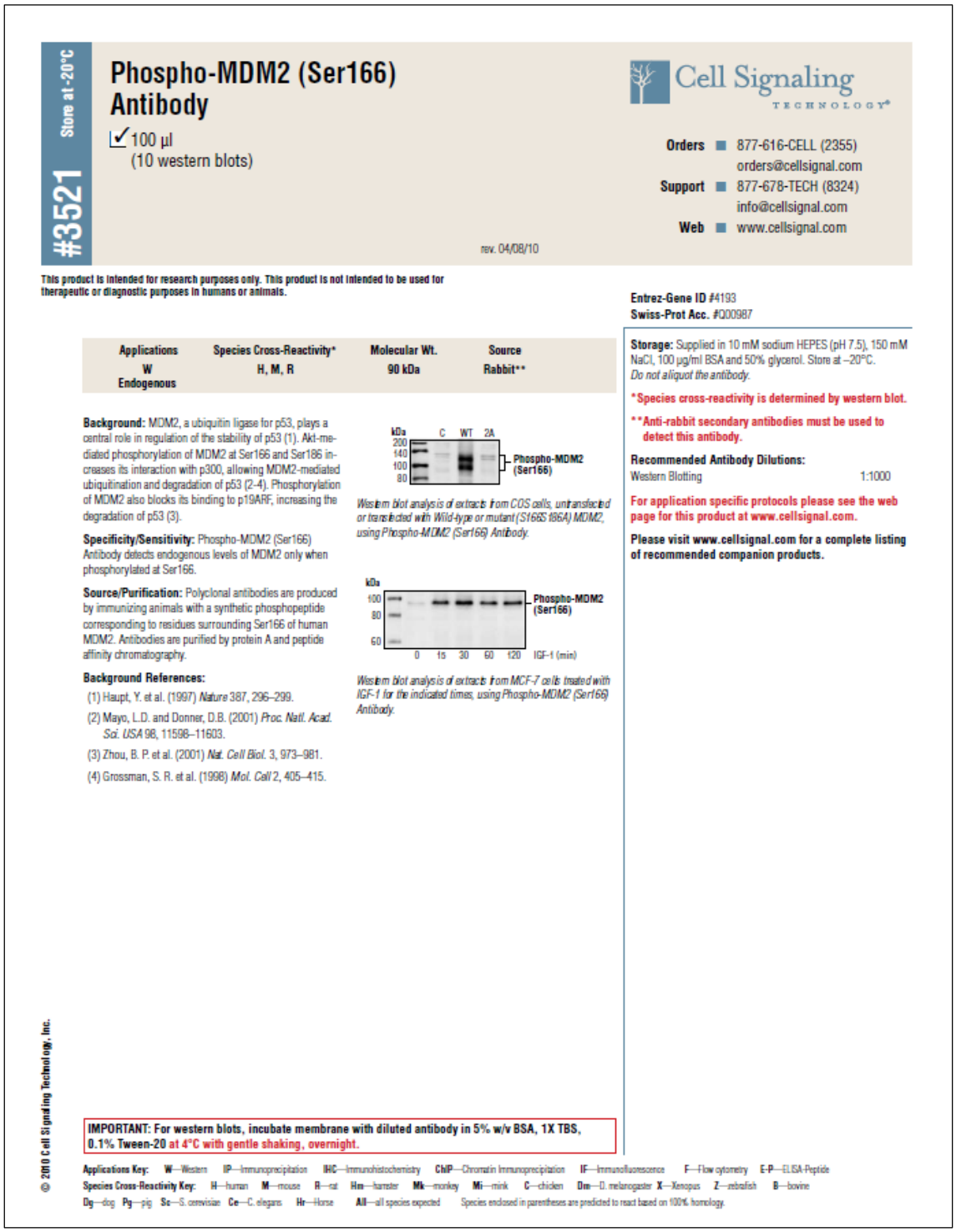

Phospho-MDM2 (Ser166) Antibody

#3521 Store at -20°C

☑ 100 µl
(10 western blots)

Cell Signaling TECHNOLOGY®

Orders ■ 877-616-CELL (2355)
orders@cellsignal.com
Support ■ 877-678-TECH (8324)
info@cellsignal.com
Web ■ www.cellsignal.com

rev. 04/08/10

This product is intended for research purposes only. This product is not intended to be used for therapeutic or diagnostic purposes in humans or animals.

Entrez-Gene ID #4193
Swiss-Prot Acc. #Q00987

Applications	Species Cross-Reactivity*	Molecular Wt.	Source
W Endogenous	H, M, R	90 kDa	Rabbit**

Background: MDM2, a ubiquitin ligase for p53, plays a central role in regulation of the stability of p53 (1). Akt-mediated phosphorylation of MDM2 at Ser166 and Ser186 increases its interaction with p300, allowing MDM2-mediated ubiquitination and degradation of p53 (2-4). Phosphorylation of MDM2 also blocks its binding to p19ARF, increasing the degradation of p53 (3).

Specificity/Sensitivity: Phospho-MDM2 (Ser166) Antibody detects endogenous levels of MDM2 only when phosphorylated at Ser166.

Source/Purification: Polyclonal antibodies are produced by immunizing animals with a synthetic phosphopeptide corresponding to residues surrounding Ser166 of human MDM2. Antibodies are purified by protein A and peptide affinity chromatography.

Background References:

(1) Haupt, Y. et al. (1997) *Nature* 387, 296–299.
(2) Mayo, L.D. and Donner, D.B. (2001) *Proc. Natl. Acad. Sci. USA* 98, 11598–11603.
(3) Zhou, B. P. et al. (2001) *Nat. Cell Biol.* 3, 973–981.
(4) Grossman, S. R. et al. (1998) *Mol. Cell* 2, 405–415.

Western blot analysis of extracts from COS cells, untransfected or transfected with Wild-type or mutant (S166S186A) MDM2, using Phospho-MDM2 (Ser166) Antibody.

Western blot analysis of extracts from MCF-7 cells treated with IGF-1 for the indicated times, using Phospho-MDM2 (Ser166) Antibody.

Storage: Supplied in 10 mM sodium HEPES (pH 7.5), 150 mM NaCl, 100 µg/ml BSA and 50% glycerol. Store at –20°C. *Do not aliquot the antibody.*

***Species cross-reactivity is determined by western blot.**

****Anti-rabbit secondary antibodies must be used to detect this antibody.**

Recommended Antibody Dilutions:

Western Blotting	1:1000

For application specific protocols please see the web page for this product at www.cellsignal.com.

Please visit www.cellsignal.com for a complete listing of recommended companion products.

IMPORTANT: For western blots, incubate membrane with diluted antibody in 5% w/v BSA, 1X TBS, 0.1% Tween-20 at 4°C with gentle shaking, overnight.

Applications Key: W—Western IP—Immunoprecipitation IHC—Immunohistochemistry ChIP—Chromatin Immunoprecipitation IF—Immunofluorescence F—Flow cytometry E-P—ELISA-Peptide
Species Cross-Reactivity Key: H—human M—mouse R—rat Hm—hamster Mk—monkey Mi—mink C—chicken Dm—D. melanogaster X—Xenopus Z—zebrafish B—bovine Dg—dog Pg—pig Sc—S. cerevisiae Ce—C. elegans Hr—Horse All—all species expected Species enclosed in parentheses are predicted to react based on 100% homology.

Figure A.11: Datasheet of phospho-MDM2 antibody (hhttp://www.cellsignal.com/)

SANTA CRUZ BIOTECHNOLOGY, INC.

goat anti-rabbit IgG-HRP: sc-2030

BACKGROUND

Santa Cruz Biotechnology's secondary antibodies are available conjugated to either an enzyme, biotin or fluorophore for use in a variety of antibody-based applications including Western Blot, immunostaining, flow cytometry and ELISA. We offer Cruz Marker™ compatible secondary antibodies, which are used in conjunction with Santa Cruz Biotechnology's Cruz Marker™ molecular weight standards. Cruz Marker™ compatible secondary antibodies recognize an epitope common to each of the Cruz Marker™ molecular weight standards and are provided as horseradish peroxidase (HRP) and alkaline phosphatase (AP) conjugated secondary antibodies for detection of mouse, goat, rabbit and rat primary antibodies. Pre-adsorbed HRP and AP conjugated Cruz Marker™ compatible secondary antibodies are also available and are recommended for use with immunoglobulin-rich samples.

SOURCE

goat anti-rabbit IgG-HRP is a CruzMarker™ compatible, affinity purified secondary antibody raised in goat against rabbit IgG and conjugated to HRP (horseradish peroxidase).

PRODUCT

Each vial contains 200 µg IgG in 0.5 ml of 1X PBS containing 40% glycerol.

APPLICATIONS

goat anti-rabbit IgG-HRP is recommended for detection of rabbit IgG by Western Blotting (starting dilution: 1:5000, dilution range 1:5000-1:10000; starting dilution to be determined by titration).

RECOMMENDED SUPPORT PRODUCTS

- UltraCruz™ Tissue Culture Dish, 100 mm polystyrene dish: sc-200286
- UltraCruz™ Cell Scrapers, 25 cm, sterile, 100 per case: sc-213229
- RIPA Lysis Buffer, 50 ml, cell lysis buffer with protease inhibitors: sc-24948
- Complete™ Protease Inhibitor Cocktail Tablet, 20 tablets: sc-29130
- Electrophoresis Sample Buffer, 2X, 25 ml, reducing buffer: sc-24945
- UltraCruz™ PVDF Transfer membrane, 0.45 µm, 30 cm x 3 m roll: sc-3723
- UltraCruz™ Nitrocellulose Pure Transfer Membrane, 0.22 µm, 30 cm x 3 m roll: sc-3718
- Cruz Blot-A: sc-3901 (Western blotting membrane with human cell line extracts from 10 different cell types)
- Running Buffer, 10X, 1 L, TRIS-Glycine WB running buffer, pH 8.3: sc-24949
- Towbin, with SDS, 10X, 1 L, WB transfer buffer pH 8.3: sc-24954
- Bovine Serum Albumin (BSA), 100 g, blocking/incubation agent: sc-2323
- TBS Blotto A, lyophilized powder in single-use bottle: sc-2333
- Western Blotting Luminol Reagent, for 2,000 cm^2 membrane area: sc-2048
- UltraCruz™ Electrophoresis Cell: sc-201625: runs up to 10 or 15 sample by SDS – PAGE protein electrophoresis
- UltraCruz™ Autoradiography Film, Blue, 8 x 1, 100 sheets: sc-201697
- Cruz Marker™ Molecular Weight Standards, for 50 gels: sc-2035

STORAGE

Store at 4° C, **DO NOT FREEZE**. Stable for one year from the date of shipment. Non-hazardous. No MSDS required.

DATA

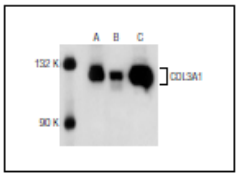

goat anti-rabbit IgG-HRP: sc-2030. Western blot analysis of COL3A1 expression in HeBl (**A**), HeLa (**B**) and Arc5 CA (**C**) whole cell lysates. Antibody tested: COL3A1 (S-17)-R: sc-8780-R.

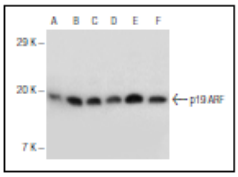

goat anti-rabbit IgG-HRP: sc-2030. Western blot analysis of p19 ARF expression in C3H/10T1/2 (**A**), NIH/3T3 (**B**), 3T3-L1 (**C**), MH-S (**D**), AMJ2-C8 (**E**) and L-11.15 (**F**) whole cell lysates. Antibody tested: p19 ARF (M-80): sc-22784.

SELECT PRODUCT CITATIONS

1. Mehlmann, L.M., et al. 1998. SH2 domain-mediated activation of phospholipase Cγ is not required to initiate Ca^{2+} release at fertilization of mouse eggs. Dev. Biol. 203: 221-232.
2. Tikoo, K., et al. 2011. Tannic acid ameliorates doxorubicin-induced cardiotoxicity and potentiates its anti-cancer activity: potential role of tannins in cancer chemotherapy. Toxicol. Appl. Pharmacol. 251: 191-200.
3. Surse, V.M., et al. 2011. Esculatin induced changes in Mmp13 and Bmp6 gene expression and histone H3 modifications attenuate development of glomerulosclerosis in diabetic rats. J. Mol. Endocrinol. 46: 245-254.
4. Chien, C.C., et al. 2012. Naloxonazine, a specific µ-opioid receptor antagonist, attenuates the increment of locomotor activity induced by acute methamphetamine in mice. Toxicol. Lett. 212: 61-65.
5. Lesueur, C., et al. 2012. Glutamine induces nuclear degradation of the NFκB p65 subunit in Caco-2/TC7 cells. Biochimie 94: 806-815.
6. Sundin, T., et al. 2012. The isoprenoid perillyl alcohol inhibits telomerase activity in prostate cancer cells. Biochimie 94: 2639-2648.
7. Gangoso, E., et al. 2012. Reduced connexin43 expression correlates with c-Src activation, proliferation, and glucose uptake in reactive astrocytes after an excitotoxic insult. Glia 60: 2040-2049.
8. Wang, K.C., et al. 2013. µ-opioid receptor knockout mice are more sensitive to chlordiazepoxide-induced anxiolytic behavior. Brain Res. Bull. 90: 137-141.
9. Sundin, T., et al. 2013. Disruption of an hTERT-mTOR-RAPTOR protein complex by a phytochemical perillyl alcohol and rapamycin. Mol. Cell. Biochem. 375: 97-104.

RESEARCH USE

For research use only, not for use in diagnostic procedures.

Figure A.12: Datasheet of goat anti-rabbit secondary antibody (hhttp://www.scbt.com/)

SANTA CRUZ BIOTECHNOLOGY, INC.

donkey anti-goat IgG-HRP: sc-2020

BACKGROUND

Santa Cruz Biotechnology's secondary antibodies are available conjugated to either an enzyme, biotin or fluorophore for use in a variety of antibody-based applications including Western Blot, immunostaining, flow cytometry and ELISA. We offer conventional horseradish peroxidase (HRP) and alkaline phosphatase (AP) conjugated secondary antibodies for detection of mouse, goat, rabbit, bovine, chicken, guinea pig, horse, sheep, swine, Syrian hamster, Armenian hamster and turkey immunoglobulin in Western Blot and ELISA. Pre-adsorbed HRP and AP secondary antibodies are also available and are recommended for use with immunoglobulin-rich samples.

SOURCE

donkey anti-goat IgG-HRP is an affinity purified secondary antibody raised in donkey against whole goat IgG and conjugated to HRP (horseradish peroxidase).

PRODUCT

Each vial contains 200 µg IgG in 0.5 ml of 1X PBS containing 40% glycerol.

APPLICATIONS

donkey anti-goat IgG-HRP is recommended for detection of goat IgG by Western Blotting (starting dilution: 1:5000, dilution range 1:5000-1:10000; optimal dilution to be determined by titration).

RECOMMENDED SUPPORT PRODUCTS

- Western Blotting Luminol Reagent, for 2,000 cm² membrane area: sc-2048
- RIPA Lysis Buffer, 50 ml, cell lysis buffer with protease inhibitors: sc-24948
- Electrophoresis Sample Buffer, 2X, 25 ml, reducing buffer: sc-24945
- Complete™ Protease Inhibitor Cocktail Tablet, 20 tablets: sc-29130
- Running Buffer, 10X, 1 L, TRIS-Glycine WB running buffer, pH 8.3: sc-24949
- Towbin, with SDS, 10X, 1 L, WB transfer buffer pH 8.3: sc-24954
- Bovine Serum Albumin (BSA), 100 g, blocking/incubation agent: sc-2323
- TBS Blotto A, lyophilized powder in single-use bottle: sc-2333
- UltraCruz™ PVDF Transfer Membrane, 0.45 µm, 30 cm x 3 m roll: sc-3723
- UltraCruz™ Nitrocellulose Pure Transfer Membrane, 0.22 µm, 30 cm x 3 m roll: sc-3718
- UltraCruz™ Tissue Culture Dish, 100 mm polystyrene dish: sc-200286
- UltraCruz™ Cell Scrapers, 25 cm, sterile, 100 per case: sc-213229
- UltraCruz™ Electrophoresis Cell: sc-201625: runs up to 10 or 15 sample by SDS – PAGE protein electrophoresis
- UltraCruz™ Autoradiography Film, Blue, 8 x 1, 100 sheets: sc-201697
- UltraCruz™ Gel Incubation Trays, 100 per pack: sc-201755 (blue), sc-201756 (green), sc-201757 (pink), sc-201758 (yellow), sc-201759 (orange)

STORAGE

Store at 4° C, **DO NOT FREEZE**. Stable for one year from the date of shipment.

RESEARCH USE

For research use only, not for use in diagnostic procedures.

DATA

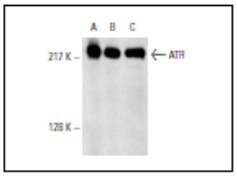

donkey anti-goat IgG-HRP: sc-2020. Western blot analysis of ATR expression in HeLa (**A**), A-431 (**B**) and K-562 (**C**) whole cell lysates. Antibody tested: ATR (N-19): sc-1887.

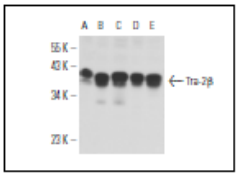

donkey anti-goat IgG-HRP: sc-2020. Western blot analysis of Tra-2β expression in HeLa (**A**), IMR-32 (**B**), SK-N-MC (**C**), K-562 (**D**) and HL-60 (**E**) nuclear extracts. Antibody tested: Tra-2β (S-18): sc-33318.

SELECT PRODUCT CITATIONS

1. Wang, S., et al. 1998. Alterations of the PPP2R1B gene in human lung and colon cancer. Science 282: 284-287.
2. Lappano, R., et al. 2012. MIBE acts as antagonist ligand of both estrogen receptor α and GPER in breast cancer cells. Breast Cancer Res. 14: R12.
3. Lappano, R., et al. 2012. Two novel GPER agonists induce gene expression changes and growth effects in cancer cells. Curr. Cancer Drug Targets 12: 531-542.
4. Loei, H., et al. 2012. Mining the gastric cancer secretome: identification of GRN as a potential diagnostic marker for early gastric cancer. J. Proteome Res. 11: 1759-1772.
5. Billing, A.M., et al. 2012. Proteomic profiling of rapid non-genomic and concomitant genomic effects of acute restraint stress on rat thymocytes. J. Proteomics 75: 2064-2079.
6. Zhang, L., et al. 2012. Alteration of striatal dopaminergic neurotransmission in a mouse model of DYT11 myoclonus-dystonia. PLoS ONE 7: e33669.
7. Huck, B., et al. 2012. GIT1 phosphorylation on serine 46 by PKD3 regulates paxillin trafficking and cellular protrusive activity. J. Biol. Chem. 287: 34604-34613.
8. Biasi, F., et al. 2012. Evidence of cell damage induced by major components of a diet-compatible mixture of oxysterols in human colon cancer CaCo-2 cell line. Biochimie 95: 632-640.
9. Kaja, S., et al. 2012. Homer-1a immediate early gene expression correlates with better cognitive performance in aging. Age. E-published.
10. Lakota, K., et al. 2012. International cohort study of 73 anti-Ku-positive patients: association of p70/p80 anti-Ku antibodies with joint/bone features and differentiation of disease populations by using principal-components analysis. Arthritis Res. Ther. 14: R2.

Santa Cruz Biotechnology, Inc. 1.800.457.3801 831.457.3800 fax 831.457.3801 **Europe** +00800 4573 8000 49 6221 4503 0 ***www.scbt.com***

Figure A.13: Datasheet of donkey anti-goat secondary antibody (hhttp://www.scbt.com/)

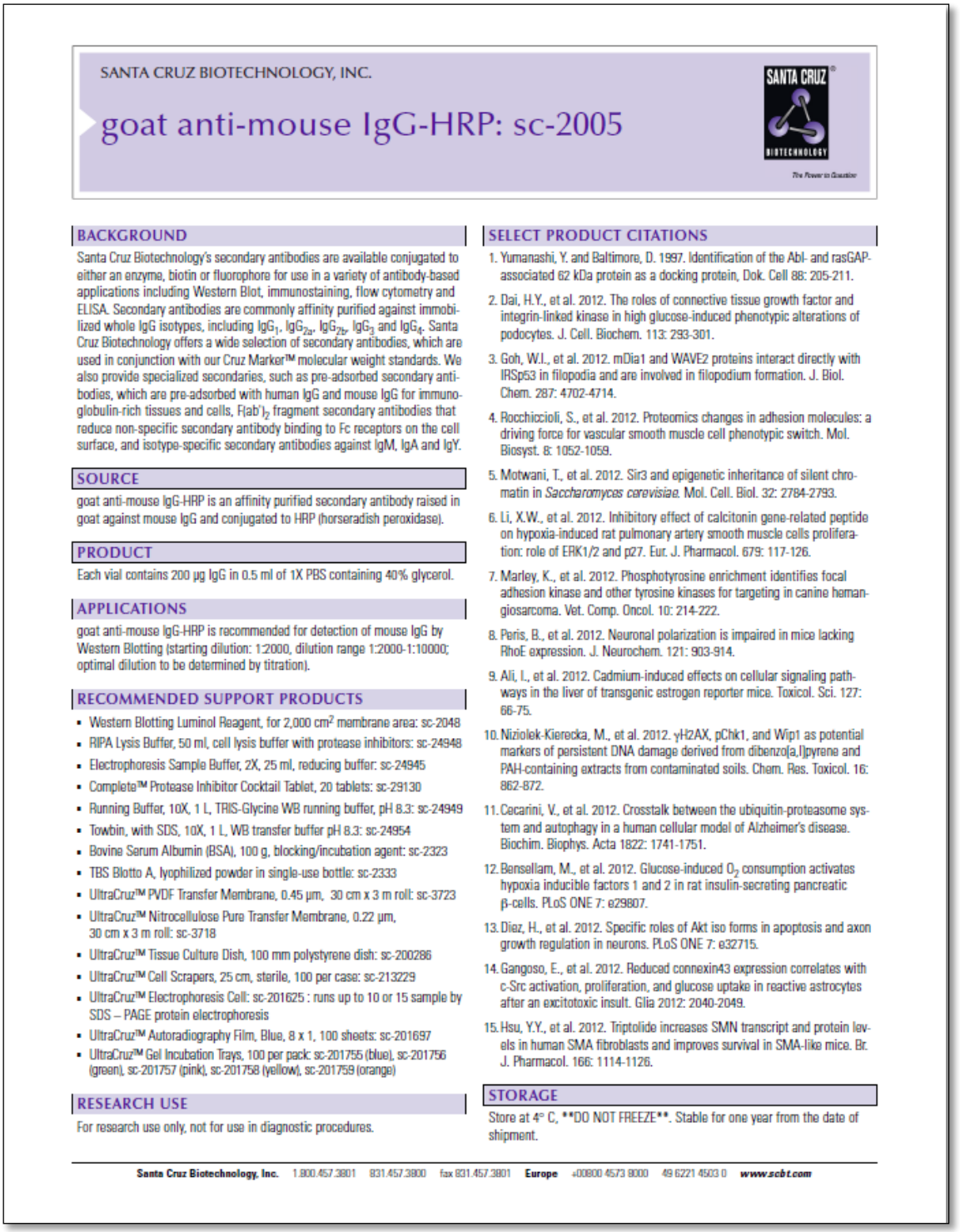

SANTA CRUZ BIOTECHNOLOGY, INC.

goat anti-mouse IgG-HRP: sc-2005

BACKGROUND

Santa Cruz Biotechnology's secondary antibodies are available conjugated to either an enzyme, biotin or fluorophore for use in a variety of antibody-based applications including Western Blot, immunostaining, flow cytometry and ELISA. Secondary antibodies are commonly affinity purified against immobilized whole IgG isotypes, including IgG_1, IgG_{2a}, IgG_{2b}, IgG_3 and IgG_4. Santa Cruz Biotechnology offers a wide selection of secondary antibodies, which are used in conjunction with our Cruz Marker™ molecular weight standards. We also provide specialized secondaries, such as pre-adsorbed secondary antibodies, which are pre-adsorbed with human IgG and mouse IgG for immunoglobulin-rich tissues and cells, $F(ab')_2$ fragment secondary antibodies that reduce non-specific secondary antibody binding to Fc receptors on the cell surface, and isotype-specific secondary antibodies against IgM, IgA and IgY.

SOURCE

goat anti-mouse IgG-HRP is an affinity purified secondary antibody raised in goat against mouse IgG and conjugated to HRP (horseradish peroxidase).

PRODUCT

Each vial contains 200 µg IgG in 0.5 ml of 1X PBS containing 40% glycerol.

APPLICATIONS

goat anti-mouse IgG-HRP is recommended for detection of mouse IgG by Western Blotting (starting dilution: 1:2000, dilution range 1:2000-1:10000; optimal dilution to be determined by titration).

RECOMMENDED SUPPORT PRODUCTS

- Western Blotting Luminol Reagent, for 2,000 cm^2 membrane area: sc-2048
- RIPA Lysis Buffer, 50 ml, cell lysis buffer with protease inhibitors: sc-24948
- Electrophoresis Sample Buffer, 2X, 25 ml, reducing buffer: sc-24945
- Complete™ Protease Inhibitor Cocktail Tablet, 20 tablets: sc-29130
- Running Buffer, 10X, 1 L, TRIS-Glycine WB running buffer, pH 8.3: sc-24949
- Towbin, with SDS, 10X, 1 L, WB transfer buffer pH 8.3: sc-24954
- Bovine Serum Albumin (BSA), 100 g, blocking/incubation agent: sc-2323
- TBS Blotto A, lyophilized powder in single-use bottle: sc-2333
- UltraCruz™ PVDF Transfer Membrane, 0.45 µm, 30 cm x 3 m roll: sc-3723
- UltraCruz™ Nitrocellulose Pure Transfer Membrane, 0.22 µm, 30 cm x 3 m roll: sc-3718
- UltraCruz™ Tissue Culture Dish, 100 mm polystyrene dish: sc-200286
- UltraCruz™ Cell Scrapers, 25 cm, sterile, 100 per case: sc-213229
- UltraCruz™ Electrophoresis Cell: sc-201625 : runs up to 10 or 15 sample by SDS – PAGE protein electrophoresis
- UltraCruz™ Autoradiography Film, Blue, 8 x 1, 100 sheets: sc-201697
- UltraCruz™ Gel Incubation Trays, 100 per pack: sc-201755 (blue), sc-201756 (green), sc-201757 (pink), sc-201758 (yellow), sc-201759 (orange)

RESEARCH USE

For research use only, not for use in diagnostic procedures.

SELECT PRODUCT CITATIONS

1. Yumanashi, Y. and Baltimore, D. 1997. Identification of the Abl- and rasGAP-associated 62 kDa protein as a docking protein, Dok. Cell 88: 205-211.
2. Dai, H.Y., et al. 2012. The roles of connective tissue growth factor and integrin-linked kinase in high glucose-induced phenotypic alterations of podocytes. J. Cell. Biochem. 113: 293-301.
3. Goh, W.I., et al. 2012. mDia1 and WAVE2 proteins interact directly with IRSp53 in filopodia and are involved in filopodium formation. J. Biol. Chem. 287: 4702-4714.
4. Rocchiccioli, S., et al. 2012. Proteomics changes in adhesion molecules: a driving force for vascular smooth muscle cell phenotypic switch. Mol. Biosyst. 8: 1052-1059.
5. Motwani, T., et al. 2012. Sir3 and epigenetic inheritance of silent chromatin in *Saccharomyces cerevisiae*. Mol. Cell. Biol. 32: 2784-2793.
6. Li, X.W., et al. 2012. Inhibitory effect of calcitonin gene-related peptide on hypoxia-induced rat pulmonary artery smooth muscle cells proliferation: role of ERK1/2 and p27. Eur. J. Pharmacol. 679: 117-126.
7. Marley, K., et al. 2012. Phosphotyrosine enrichment identifies focal adhesion kinase and other tyrosine kinases for targeting in canine hemangiosarcoma. Vet. Comp. Oncol. 10: 214-222.
8. Peris, B., et al. 2012. Neuronal polarization is impaired in mice lacking RhoE expression. J. Neurochem. 121: 903-914.
9. Ali, I., et al. 2012. Cadmium-induced effects on cellular signaling pathways in the liver of transgenic estrogen reporter mice. Toxicol. Sci. 127: 66-75.
10. Niziolek-Kierecka, M., et al. 2012. γH2AX, pChk1, and Wip1 as potential markers of persistent DNA damage derived from dibenzo[a,l]pyrene and PAH-containing extracts from contaminated soils. Chem. Res. Toxicol. 16: 862-872.
11. Cecarini, V., et al. 2012. Crosstalk between the ubiquitin-proteasome system and autophagy in a human cellular model of Alzheimer's disease. Biochim. Biophys. Acta 1822: 1741-1751.
12. Bensellam, M., et al. 2012. Glucose-induced O_2 consumption activates hypoxia inducible factors 1 and 2 in rat insulin-secreting pancreatic β-cells. PLoS ONE 7: e29807.
13. Diez, H., et al. 2012. Specific roles of Akt iso forms in apoptosis and axon growth regulation in neurons. PLoS ONE 7: e32715.
14. Gangoso, E., et al. 2012. Reduced connexin43 expression correlates with c-Src activation, proliferation, and glucose uptake in reactive astrocytes after an excitotoxic insult. Glia 2012: 2040-2049.
15. Hsu, Y.Y., et al. 2012. Triptolide increases SMN transcript and protein levels in human SMA fibroblasts and improves survival in SMA-like mice. Br. J. Pharmacol. 166: 1114-1126.

STORAGE

Store at 4° C, **DO NOT FREEZE**. Stable for one year from the date of shipment.

Santa Cruz Biotechnology, Inc. 1.800.457.3801 831.457.3800 fax 831.457.3801 **Europe** +00800 4573 8000 49 6221 4503 0 ***www.scbt.com***

Figure A.14: Datasheet of goat anti-mouse secondary antibody (hhttp://www.scbt.com/)

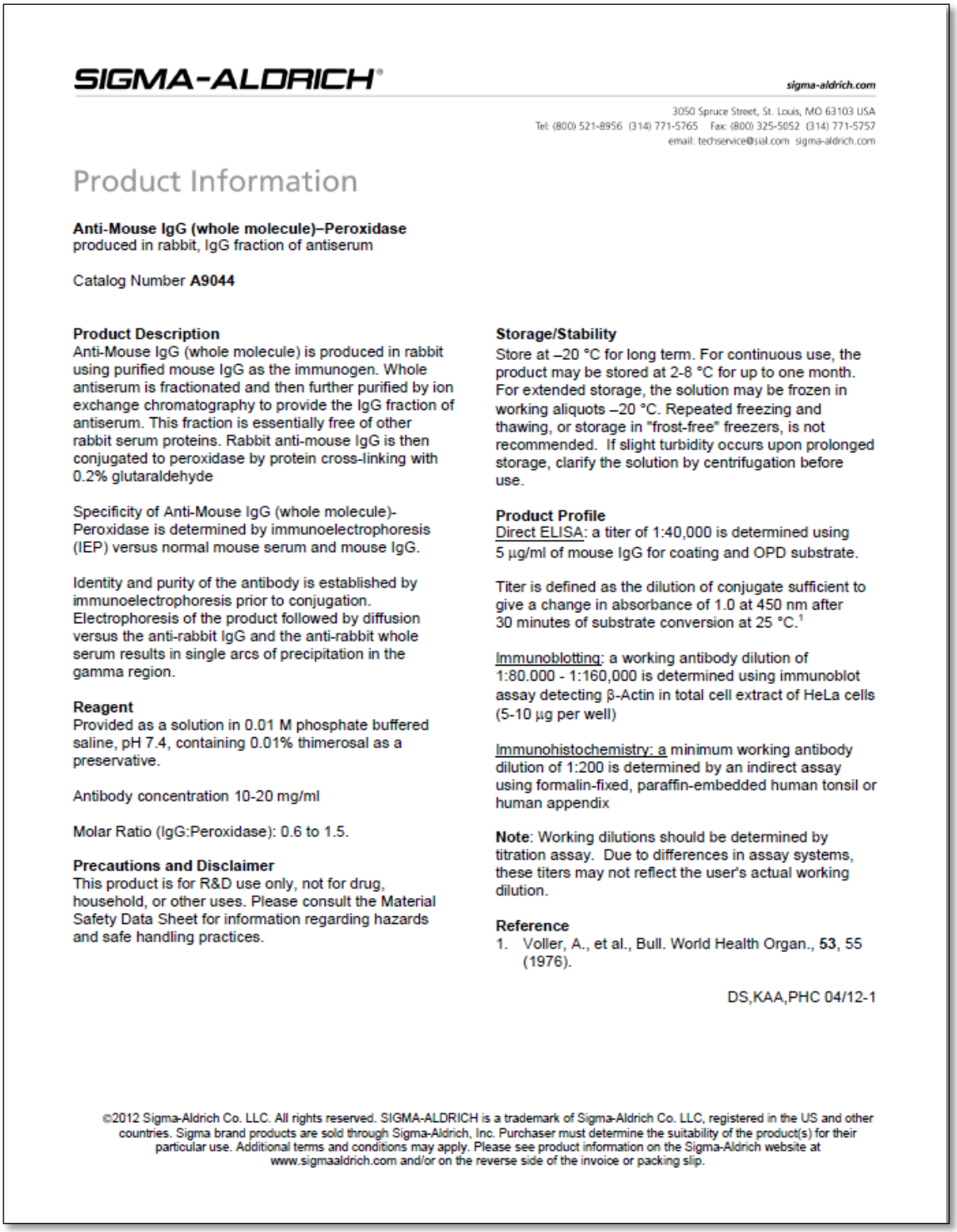

SIGMA-ALDRICH®

sigma-aldrich.com

3050 Spruce Street, St. Louis, MO 63103 USA
Tel: (800) 521-8956 (314) 771-5765 Fax: (800) 325-5052 (314) 771-5757
email: techservice@sial.com sigma-aldrich.com

Product Information

Anti-Mouse IgG (whole molecule)–Peroxidase
produced in rabbit, IgG fraction of antiserum

Catalog Number **A9044**

Product Description
Anti-Mouse IgG (whole molecule) is produced in rabbit using purified mouse IgG as the immunogen. Whole antiserum is fractionated and then further purified by ion exchange chromatography to provide the IgG fraction of antiserum. This fraction is essentially free of other rabbit serum proteins. Rabbit anti-mouse IgG is then conjugated to peroxidase by protein cross-linking with 0.2% glutaraldehyde

Specificity of Anti-Mouse IgG (whole molecule)-Peroxidase is determined by immunoelectrophoresis (IEP) versus normal mouse serum and mouse IgG.

Identity and purity of the antibody is established by immunoelectrophoresis prior to conjugation. Electrophoresis of the product followed by diffusion versus the anti-rabbit IgG and the anti-rabbit whole serum results in single arcs of precipitation in the gamma region.

Reagent
Provided as a solution in 0.01 M phosphate buffered saline, pH 7.4, containing 0.01% thimerosal as a preservative.

Antibody concentration 10-20 mg/ml

Molar Ratio (IgG:Peroxidase): 0.6 to 1.5.

Precautions and Disclaimer
This product is for R&D use only, not for drug, household, or other uses. Please consult the Material Safety Data Sheet for information regarding hazards and safe handling practices.

Storage/Stability
Store at –20 °C for long term. For continuous use, the product may be stored at 2-8 °C for up to one month. For extended storage, the solution may be frozen in working aliquots –20 °C. Repeated freezing and thawing, or storage in "frost-free" freezers, is not recommended. If slight turbidity occurs upon prolonged storage, clarify the solution by centrifugation before use.

Product Profile
Direct ELISA: a titer of 1:40,000 is determined using 5 µg/ml of mouse IgG for coating and OPD substrate.

Titer is defined as the dilution of conjugate sufficient to give a change in absorbance of 1.0 at 450 nm after 30 minutes of substrate conversion at 25 °C.[1]

Immunoblotting: a working antibody dilution of 1:80.000 - 1:160,000 is determined using immunoblot assay detecting β-Actin in total cell extract of HeLa cells (5-10 µg per well)

Immunohistochemistry: a minimum working antibody dilution of 1:200 is determined by an indirect assay using formalin-fixed, paraffin-embedded human tonsil or human appendix

Note: Working dilutions should be determined by titration assay. Due to differences in assay systems, these titers may not reflect the user's actual working dilution.

Reference
1. Voller, A., et al., Bull. World Health Organ., **53**, 55 (1976).

DS,KAA,PHC 04/12-1

Figure A.15: Datasheet of anti-mouse secondary antibody (http://www.sigmaaldrich.com/)

Polyplus transfection®
THE DELIVERY EXPERTS

jetPRIME® short protocol - DNA Transfection

DAY 0: Cell seeding = 60% to 80% confluency at the time of transfection

► Seed cells in V ml of serum containing medium according to the table below

Quantities per well, dish or flask

Culture vessel	Number of cells	V volume of serum containing medium during transfection
24-well	50 000 – 80 000	0.5 ml
6-well / 35 mm	150 000 – 250 000	2 ml
100 mm / flask 75 cm^2	1 000 000 – 2 000 000	10 ml

DAY 1: Transfection = 1:2 DNA to jetPRIME® reagent ratio

► Perform transfection **in the presence of serum**

► Use **jetPRIME® buffer only**

Watch the video « DNA transfection using jetPRIME® » on YouTube!

http://www.youtube.com/watch?v=G39wNXaZPX4

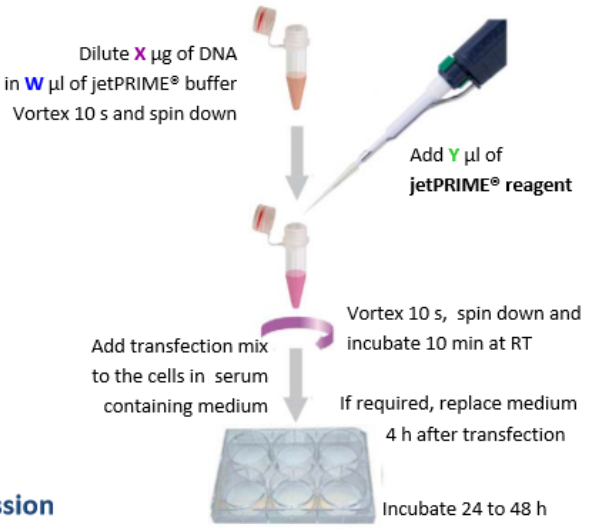

DAY 2-3: Measure gene expression

Quantities per well, dish or flask

Culture vessel	W volume of jetPRIME® buffer	X amount of DNA added	Y volume of **jetPRIME® reagent**
24-well	50 µl	0.5 µg	1 µl
6-well / 35 mm	200 µl	2 µg	4 µl
100 mm / flask 75 cm^2	500 µl	10 µg	20 µl

See back page for optimization tips

Download complete protocol on www.polyplus-transfection.com/transfection-reagents

Version E

Figure B.1: jetPRIME Transfection Kit Protocol

Polyplus transfection®
THE DELIVERY EXPERTS

jetPRIME® Optimization Tips - DNA Transfection

Protocol Optimization

- Check our online Cell Transfection Database for cell specific protocols at http://www.polyplus-transfection.com/technical-resources/cell-line-database/
- Test different DNA amounts: X, 0.5X and 1.5X
- Test different DNA/jetPRIME® ratios, 1:2 to 1:3

Culture Vessel	W volume of jetPRIME® Buffer	X amount of DNA	Y volume of jetPRIME reagent
24-well	50 µl	0.25 – 0.75 µg	0.5 – 2.25 µl
6-well / 35 mm	200 µl	1 – 3 µg	2 – 9 µl
100 mm / flask 75 cm^2	500 µl	5 – 15 µg	10 – 45 µl

For HEK-293 and HeLa cells, you may decrease the DNA amount to 0.5X and use the 1:2 DNA/ jetPRIME® ratio.

Tips to increase cell viability of sensitive cells

- Replace medium after 4 h
- Decrease DNA amount to 0.5X
- Analyze transfection at an earlier time point (24 h after transfection instead of 48 h for instance)
- Check that the target gene does not affect cell viability

Good DNA Transfection Practices

- Store appropriately jetPRIME® (4°C) and the DNA
- Ensure that cells have been passaged more than twice and less than 20 times prior to transfection. Discard overconfluent cells
- Regularly check for mycoplasma contaminations
- Use a reporter gene to set up and optimize transfection conditions
- Serum quality may drastically affect transfection efficiency. When purchasing a new batch of serum or trypsin, check cell viability as well as transfection efficiency

Note: jetPRIME® is also recommended for virus production and DNA/siRNA cotransfection, please refer to the complete protocol available online at:
www.polyplus-transfection.com/transfection-reagents

Version E

Figure B.2: jetPRIME Transfection Kit Protocol

SIGMA-ALDRICH®

sigma-aldrich.com

3050 Spruce Street, St. Louis, MO 63103 USA
Tel: (800) 521-8956 (314) 771-5765 Fax: (800) 325-5052 (314) 771-5757
email: techservice@sial.com sigma-aldrich.com

Product Information

TRI Reagent®
For processing tissues, cells cultured in monolayer or cell pellets

Catalog Number **T9424**
Store at room temperature.

TECHNICAL BULLETIN

Product Description
TRI Reagent is a quick and convenient reagent for use in the simultaneous isolation of RNA, DNA, and protein. Successful isolations from human, animal, plant, yeast, bacterial, and viral samples can be obtained. A convenient single-step liquid phase separation results in the simultaneous isolation of RNA, DNA, and protein.[1] This procedure is an improvement of the single-step method reported by Chomczynski and Sacchi[2] for total RNA isolation. TRI Reagent performs well with large or small amounts of tissue or cells and many samples can be simultaneously extracted.

This product, a mixture of guanidine thiocyanate and phenol in a monophase solution, effectively dissolves DNA, RNA, and protein on homogenization or lysis of tissue sample. After adding chloroform or 1-bromo-3-chloropropane and centrifuging, the mixture separates into 3 phases: an aqueous phase containing the RNA, the interphase containing DNA, and an organic phase containing proteins. Each component can then be isolated after separating the phases. One ml of TRI Reagent is sufficient to isolate RNA, DNA, and protein from 50–100 mg of tissue, 5–10 × 10^6 cells, or 10 cm^2 of culture dish surface for cells grown in monolayer.

This is one of the most effective methods for isolating total RNA and can be completed in only 1 hour starting with fresh tissue or cells. The procedure is very effective for isolating RNA molecules of all types from 0.1–15 kb in length. The resulting RNA is intact with little or no contaminating DNA and protein. This RNA can be used for Northern blots, mRNA isolation, *in vitro* translation, RNase protection assay, cloning and polymerase chain reaction (PCR).

The DNA is in the interphase and phenol phase, which forms after the addition of chloroform or 1-bromo-3-chloropropane to the TRI Reagent in Sample Preparation, step 2. After precipitation and multiple washes, the DNA is dissolved in 8 mM NaOH. The solution is neutralized and the DNA is ready for analysis. The resulting DNA is suitable for PCR, restriction enzyme digestion, and Southern blotting.

After precipitating the DNA with ethanol (DNA Isolation, step 1), the proteins can be removed from the phenol-ethanol supernatant. The isolated material can be probed for specific proteins by Western blotting.[1]

Reagents Required but Not Provided

RNA Isolation:
- Chloroform, Catalog Number C2432, or 1-Bromo-3-chloropropane, Catalog Number B9673
- 2-Propanol, Catalog Number I9516
- 75% Ethanol
- 1 mM sodium phosphate, Catalog Number S3264, pH 8.2, 0.5% SDS solution, Catalog Number L4522, diluted 20-fold, formamide, **or** diethylpyrocarbonate-treated water

DNA Isolation:
- 8 mM NaOH
- 0.1 M trisodium citrate, 10% ethanol solution
- Absolute ethanol
- 75% ethanol
- EDTA

Protein Isolation:
- 2-Propanol, Catalog Number I9516
- Absolute ethanol, Catalog Number E7023
- 95% Ethanol, Catalog Number E7148
- 1% SDS, Catalog Number L4522, diluted 10-fold
- 0.3 M Guanidine hydrochloride, Catalog Number G3272, in 95% ethanol

Figure C.1: Tri-Reagent Protocol (http://www. sigmaaldrich.com/)

Precautions and Disclaimer
This product is for R&D use only, not for drug, household, or other uses. Please consult the Material Safety Data Sheet for information regarding hazards and safe handling practices.

Storage/Stability
Store the product at room temperature.

Procedures
Sample Preparation

1A. Tissue:
Homogenize tissue samples in TRI Reagent (1 ml per 50–100 mg of tissue) in a Polytron® or other appropriate homogenizer.
Note: If minimal shearing of the DNA is desired, use a loosely fitting homogenizer, not a Polytron (see DNA Isolation, step 3, note b). The volume of the tissue should not exceed 10% of the volume of the TRI Reagent.

1B. Monolayer cells:
Lyse cells directly on the culture dish. Use 1 ml of the TRI Reagent per 10 cm^2 of glass culture plate surface area. After addition of the reagent, the cell lysate should be passed several times through a pipette to form a homogenous lysate.
Note: TRI Reagent is **not** compatible with plastic culture plates.

1C. Suspension cells:
Isolate cells by centrifugation and then lyse in TRI Reagent by repeated pipetting. One ml of the reagent is sufficient to lyse 5–10 × 10^6 animal, plant, or yeast cells, or 10^7 bacterial cells.
Notes:
a. If samples have a high content of fat, protein, polysaccharides, or extracellular material such as muscle, fat tissue, and tuberous parts of plants an additional step may be needed. After homogenization, centrifuge the homogenate at 12,000 × *g* for 10 minutes at 2-8 °C to remove the insoluble material (extracellular membranes, polysaccharides, and high molecular mass DNA). The supernatant contains RNA and protein. If the sample had a high fat content, there will be a layer of fatty material on the surface of the aqueous phase that should be removed. Transfer the clear supernatant to a fresh tube and proceed with step 2. Recover the high molecular mass DNA from the pellet by following DNA Isolation, steps 2 and 3.
b. Some yeast and bacterial cells may require a homogenizer.
c. After the cells have been homogenized or lysed in TRI Reagent, samples can be stored at –70 °C for up to 1 month.

2. Phase Separation: To ensure complete dissociation of nucleoprotein complexes, allow samples to stand for 5 minutes at room temperature. Add 0.1 ml of 1-bromo-3-chloropropane or 0.2 ml of chloroform (see Phase Separation, notes a and b) per ml of TRI Reagent used. Cover the sample tightly, shake vigorously for 15 seconds, and allow to stand for 2–15 minutes at room temperature. Centrifuge the resulting mixture at 12,000 × *g* for 15 minutes at 2-8 °C. Centrifugation separates the mixture into 3 phases: a red organic phase (containing protein), an interphase (containing DNA), and a colorless upper aqueous phase (containing RNA).
Notes:
a. 1-Bromo-3-chloropropane is less toxic than chloroform and its use for phase separation decreases the possibility of contaminating RNA with DNA.[4]
b. The chloroform used for phase separation should not contain isoamyl alcohol or other additives.
c. For isolation of poly A^+ fraction from the aqueous phase see Appendix I.

RNA Isolation

1. Transfer the aqueous phase to a fresh tube and add 0.5 ml of 2-propanol per ml of TRI Reagent used in Sample Preparation, step 1 and mix. Allow the sample to stand for 5–10 minutes at room temperature. Centrifuge at 12,000 × *g* for 10 minutes at 2-8 °C. The RNA precipitate will form a pellet on the side and bottom of the tube.
Note: Store the interphase and organic phase at 2-8 °C for subsequent isolation of the DNA and proteins.

2. Remove the supernatant and wash the RNA pellet by adding a minimun of 1 ml of 75% ethanol per 1 ml of TRI Reagent used in Sample Preparation, step 1. Vortex the sample and then centrifuge at 7,500 × *g* for 5 minutes at 2-8 °C.
Notes:
a. If the RNA pellets float, perform the wash in 75% ethanol at 12,000 × *g*.
b. Samples can be stored in ethanol at 2-8 °C for at least 1 week and up to 1 year at –20 °C.

Figure C.2: Tri-Reagent Protocol (http://www. sigmaaldrich.com/)

3. Briefly dry the RNA pellet for 5–10 minutes by air-drying or under a vacuum. Do not let the RNA pellet dry completely, as this will greatly decrease its solubility. Do not dry the RNA pellet by centrifugation under vacuum (Speed-Vac®). Add an appropriate volume of formamide, water, or a 0.5% SDS solution to the RNA pellet. To facilitate dissolution, mix by repeated pipetting with a micropipette at 55–60 °C for 10–15 minutes.
   Notes:
   a. Final preparation of RNA is free of DNA and proteins. It should have a A_{260}/A_{280} ratio of ≥1.7.
   b. Typical yields from tissues (µg RNA/mg tissue): liver, spleen, 6-10 µg; kidney, 3-4 µg; skeletal muscle, brain, 1-1.5 µg; placenta, 1-4 µg.
   c. Typical yields from cultured cells (µg RNA/10^6 cells): epithelial cells, 8-15 µg; fibroblasts, 5-7 µg.
   d. Ethidium bromide staining of RNA in agarose gels visualizes two predominant bands of small (2 kb) and large (5 kb) ribosomal RNA, low molecular mass (0.1–0.3 kb) RNA, and discrete bands of high molecular mass (7–15 kb) RNA.

DNA Isolation

1. Carefully remove the remaining aqueous phase overlaying the interphase and discard. To precipitate the DNA from the interphase and organic phase, add 0.3 ml of 100% ethanol per 1 ml of TRI Reagent used in Sample Preparation, step 1. Mix by inversion and allow to stand for 2–3 minutes at room temperature. Centrifuge at 2,000 × *g* for 5 minutes at 2-8 °C.
   Note: Removal of the remaining aqueous phase before DNA precipitation is a critical step for the quality of the isolated DNA.

2. Remove the supernatant and save at 2-8 °C for protein isolation. Wash the DNA pellet twice in 0.1 M trisodium citrate, 10% ethanol solution. Use 1 ml of wash solution for every 1 ml of TRI Reagent used in Sample Preparation, step 1. During each wash, allow the DNA pellet to stand (with occasional mixing) for at least 30 minutes. Centrifuge at 2,000 × *g* for 5 minutes at 2-8 °C. Resuspend the DNA pellet in 75% ethanol (1.5–2 ml for each ml TRI Reagent) and allow to stand for 10–20 minutes at room temperature.
   Notes:
   a. **Important:** Do not to reduce the time samples remain in the washing solution. Thirty minutes is the absolute minimum time for efficient removal of phenol from the DNA.
   b. If pellet contains >200 µg of DNA or large amounts of non-DNA material, an additional wash in 0.1 M trisodium citrate, 10% ethanol solution is required.
   c. Samples suspended in 75% ethanol can be stored at 2-8 °C for several months.

3. Dry the DNA pellet for 5–10 minutes under a vacuum and dissolve in 8 mM NaOH with repeated slow pipetting with a micropipette. Add sufficient 8 mM NaOH for a final DNA concentration of 0.2–0.3 µg/µL (typically 0.3–0.6 ml to the DNA isolated from 50–70 mg of tissue or 10^7 cells). This mild alkaline solution assures complete dissolution of the DNA pellet. Centrifuge at 12,000 × *g* for 10 minutes to remove any insoluble material and transfer the supernatant to a new tube.
   Notes:
   a. A viscous supernatant indicates the presence of high molecular mass DNA.
   b. The size of the DNA will depend on the force exerted during homogenization. Avoid using a Polytron homogenizer.
   c. Samples dissolved in 8 mM NaOH can be stored at 2-8 °C overnight. For long term storage, adjust the pH value to between 7 and 8 and supplement with EDTA (final concentration 1 mM).
   d. To determine DNA concentration, remove an aliquot, dilute with water, and measure the A_{260}. For double stranded DNA, 1 A_{260} unit/ml = 50 µg/ml.
   e. To calculate cell number, assume the amount of DNA for 10^6 diploid cells of human, rat, and mouse equals 7.1 µg, 6.5 µg, and 5.8 µg, respectively.
   f. Typical yields from tissues (µg DNA/mg tissue): liver, kidney, 3–4 µg; skeletal muscle, brain, and placenta, 2–3 µg.
   g. Typical yields from cultured human, rat, and mouse cells: 5–7 µg DNA/10^6 cells.

To Amplify DNA by PCR

After dissolving in 8 mM NaOH, adjust to pH 8.4 using HEPES (add 86 µL of 0.1 M HEPES, free acid/ml of DNA solution). Add sample (generally 0.1–1 µg) to PCR mix and follow PCR protocol.

Figure C.3: Tri-Reagent Protocol (http://www. sigmaaldrich.com/)

To Digest DNA with Restriction Enzymes

Adjust the pH of the DNA solution to that needed for the restriction enzyme digestion using HEPES, or dialyze samples against 1 mM EDTA, pH 7–8. Allow the restriction enzyme digestion to continue for 3–24 hours under optimal conditions. It is recommended that 3–5 units of enzyme be used per 1 µg of DNA. Typically, 80–90% of the DNA is digested.

Protein Isolation

1. Precipitate proteins (see note) from the phenol-ethanol supernatant (DNA Isolation, step 2) with 1.5 ml of 2-propanol per 1 ml of TRI Reagent used in Sample Preparation, step 1. Allow samples to stand for at least 10 minutes at room temperature. Centrifuge at 12,000 × *g* for 10 minutes at 2-8 °C.
   Note: For some samples, the protein pellet may be difficult to dissolve in 1% SDS (step 3). Use this alternate procedure to correct the problem:
   a. Dialyze the phenol-ethanol supernatant against 3 changes of 0.1% SDS at 2-8 °C.
   b. Centrifuge the dialysate at 10,000 × *g* for 10 minutes at 2-8 °C.
   c. The clear supernatant contains protein that is suitable for use in Western blotting procedures.

2. Discard supernatant and wash pellet 3 times in 0.3 M guanidine hydrochloride/95% ethanol solution, using 2 ml per 1 ml of TRI Reagent used in Sample Preparation, step 1. During each wash, store samples in wash solution for 20 minutes at room temperature. Centrifuge at 7,500 × *g* for 5 minutes at 2-8 °C. After the 3 washes, add 2 ml of 100% ethanol and vortex the protein pellet. Allow to stand for 20 minutes at room temperature. Centrifuge at 7,500 × *g* for 5 minutes at 2-8 °C.
   Note: Protein samples suspended in 0.3 M guanidine hydrochloride/95% ethanol solution or 100% ethanol can be stored for 1 month at 2-8 °C or 1 year at –20 °C.

3. Dry protein pellet under a vacuum for 5–10 minutes. Dissolve pellet in 1% SDS aided by working the plunger of micropipette with tip in the solution. Remove any insoluble material by centrifugation at 10,000 × *g* for 10 minutes at 2-8 °C. Transfer supernatant to a new tube. The protein solution should be used immediately for Western blotting or stored at –20 °C.

Troubleshooting Guide

1. RNA Isolation:
   A. Low yield may be due to:
      - incomplete homogenization or lysis of samples.
      - the final RNA pellet may not have been completely dissolved.
   B. If the A_{260}/A_{280} ratio is <1.65:
      - the amount of sample used for homogenization may have been too small.
      - samples may not have been allowed to stand at room temperature for 5 minutes after homogenization.
      - there may have been contamination of the aqueous phase with the phenol phase.
      - the final RNA pellet may not have been completely dissolved.
   C. If there is degradation of the RNA:
      - the tissues may not have been immediately processed or frozen after removing from the animal.
      - the samples used for isolation or the isolated RNA preparations may have been stored at –20 °C instead of –70 °C as specified in the procedure.
      - cells may have been dispersed by trypsin digestion.
      - aqueous solutions or tubes used for procedure may not have been RNAse-free.
      - formaldehyde used for the agarose gel electrophoresis may have had a pH value <3.5.
   D. If there is DNA contamination:
      - the volume of reagent used for the sample homogenization may have been too small.
      - samples used for the isolation may have contained organic solvents (ethanol, DMSO), strong buffers or alkaline solution.

2. DNA Isolation:
   A. Low yield may be due to:
      - incomplete homogenization or lysis of samples.
      - the final DNA pellet may not have been completely dissolved.
   B. If the A_{260}/A_{280} ratio is <1.70:
      - phenol may not have been sufficiently removed from the DNA preparation. Try one more wash of the DNA pellet with the 0.1 M trisodium citrate, 10% ethanol solution.

Figure C.4: Tri-Reagent Protocol (http://www. sigmaaldrich.com/)

C. If there is degradation of the DNA:
- the tissues may not have been immediately processed or frozen after removing from the animal.
- the samples used for isolation may have been stored at –20 °C instead of –70 °C as specified in the procedure.
- samples may have been homogenized with a Polytron or other high speed homogenizer.

D. If there is RNA contamination:
- there may have been too much aqueous phase remaining with the organic phase and interphase.
- the DNA pellet may not have been washed sufficiently with 0.1 M trisodium citrate, 10% ethanol solution.

3. Protein Isolation:
A. Low yield may be due to:
- incomplete homogenization or lysis of samples.
- the final protein pellet may not have been completely dissolved.

B. If there is degradation of the protein:
- the tissues may not have been immediately processed or frozen after removing from the animal.

C. If PAGE shows band deformation:
- protein pellet may not have been washed sufficiently.

Appendix

I. Isolation of Poly A$^+$ RNA

After the RNA has been precipitated with 2-propanol (RNA Isolation, step 1), dissolve the pellet in poly A$^+$ binding buffer and pass through an oligo-dT cellulose (Catalog Number O3131) column to selectively remove mRNA according to the procedure of Aviv and Leder.[3]

II. Isolated RNA is to be used in RT-PCR

1. Modifying the procedure by performing the additional centrifugation step in the initial Sample Preparation, step 1B, note c further minimizes the possibility of DNA contamination in the RNA extracted by TRI Reagent LS.
2. A more complete evaporation of ethanol is required when RNA samples are to be used in RT-PCR. This is especially critical for small volume samples (5–20 µl), which may contain a relatively high level of ethanol if not adequately dried.

References

1. Chomczynski, P., *BioTechniques*, **15**, 532-537 (1993).
2. Chomczynski, P., and Sacchi, N., *Anal. Biochem.*, **162**, 156-159 (1987).
3. Aviv, H., and Leder, P., *Proc. Natl. Acad. Sci. USA*, **69**, 1408-1412 (1972).
4. Chomczynski. P., and Mackey, K., *Anal. Biochem.*, **225**, 163-164 (1995).

RC,JC,PHC 07/11-1

Figure C.5: Tri-Reagent Protocol (http://www. sigmaaldrich.com/)

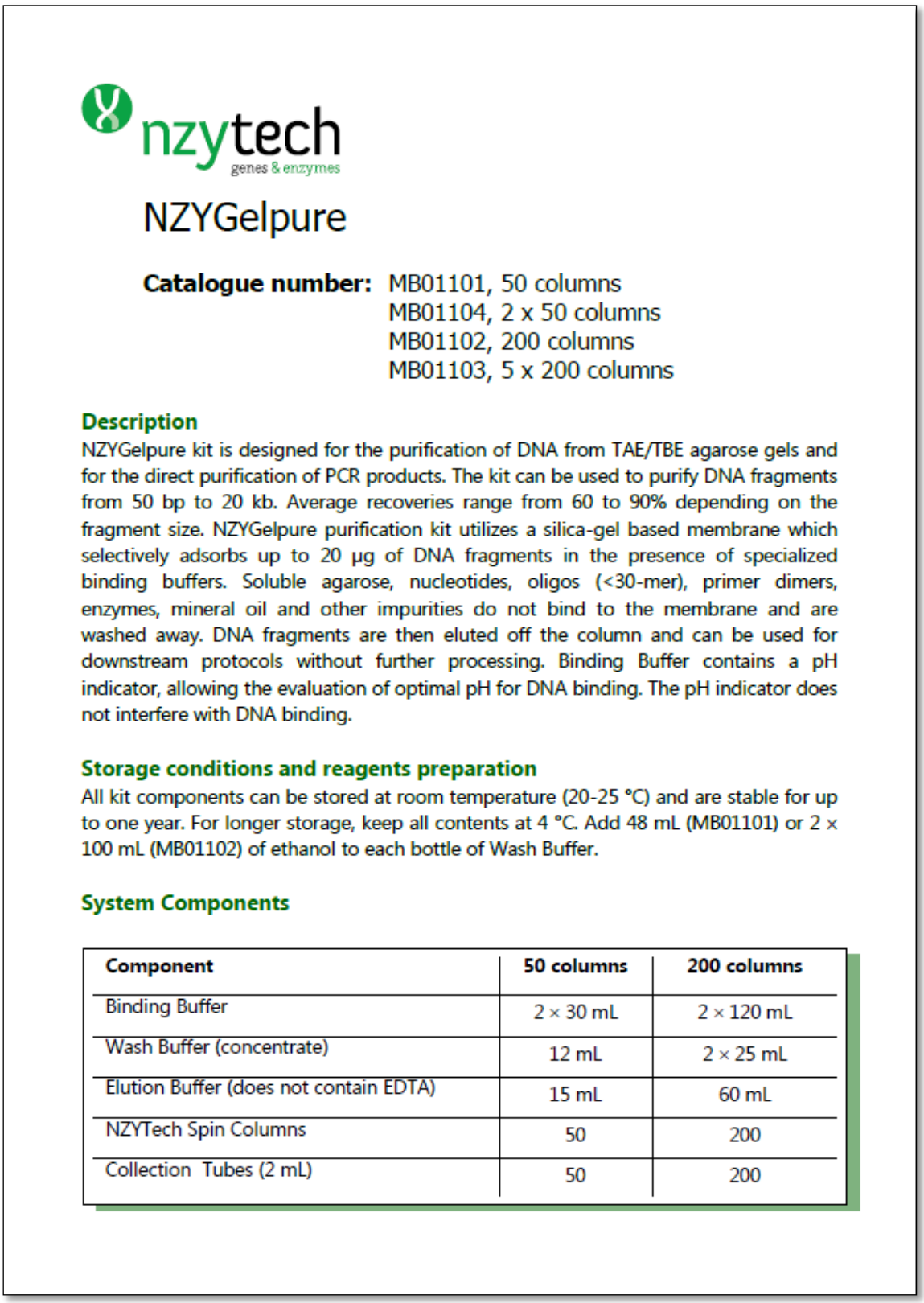

nzytech
genes & enzymes

NZYGelpure

Catalogue number: MB01101, 50 columns
MB01104, 2 x 50 columns
MB01102, 200 columns
MB01103, 5 x 200 columns

Description

NZYGelpure kit is designed for the purification of DNA from TAE/TBE agarose gels and for the direct purification of PCR products. The kit can be used to purify DNA fragments from 50 bp to 20 kb. Average recoveries range from 60 to 90% depending on the fragment size. NZYGelpure purification kit utilizes a silica-gel based membrane which selectively adsorbs up to 20 µg of DNA fragments in the presence of specialized binding buffers. Soluble agarose, nucleotides, oligos (<30-mer), primer dimers, enzymes, mineral oil and other impurities do not bind to the membrane and are washed away. DNA fragments are then eluted off the column and can be used for downstream protocols without further processing. Binding Buffer contains a pH indicator, allowing the evaluation of optimal pH for DNA binding. The pH indicator does not interfere with DNA binding.

Storage conditions and reagents preparation

All kit components can be stored at room temperature (20-25 °C) and are stable for up to one year. For longer storage, keep all contents at 4 °C. Add 48 mL (MB01101) or 2 × 100 mL (MB01102) of ethanol to each bottle of Wash Buffer.

System Components

Component	50 columns	200 columns
Binding Buffer	2 × 30 mL	2 × 120 mL
Wash Buffer (concentrate)	12 mL	2 × 25 mL
Elution Buffer (does not contain EDTA)	15 mL	60 mL
NZYTech Spin Columns	50	200
Collection Tubes (2 mL)	50	200

Figure D.1: NzyGelpure protocol (https://www.nzytech.com/)

Protocol for plasmid DNA purification from Agarose Gels

All purification steps should be carried out at **room temperature**.

All centrifugations should be carried out at **room temperature** in a table-top microcentrifuge at >12000 x*g* (10000-15000 rpm depending on the rotor type).

1. Excise the DNA fragment from the gel with a clean, sharp scalpel. Weight the gel slice and transfer to a 1.5 mL microcentrifuge tube.

2. Add 300 µL of Binding Buffer for each 100 mg of gel weight (example – a gel slice weighing 125 mg would require 375 µL of Binding Buffer). For high concentration gels (2.0-3.0%), 500 µL of Binding Buffer per 100 mg of agarose gel should be added. The maximum amount of gel slice per NZYTech spin column is 400 mg. For gel slices >400 mg use more than one column.

3. Incubate at 55-60 °C for 5-10 minutes and shake occasionally until agarose is completely dissolved.

4. Check that the colour of the mixture is yellow (similar to the colour of the Binding Buffer). If the colour of the mixture is orange or violet, add 10 µL of 3 M sodium acetate pH 5.0, and mix well.

5. (Optional) For DNA fragments <500 bp or >10 kb long add 1 gel volume of isopropanol to the sample and mix well by pipetting several times (example – a gel slice weighing 125 mg would require 125 µL of isopropanol).

6. Load the above mixture into the NZYTech spin column placed into a Collection tube (2 mL). Centrifuge for 30s to 1 minute and discard the flow-through in the collection tube. The maximum volume of the column reservoir is 700 µL. For sample volumes of more than 700 µL, simply load and spin again.

7. (Optional) Add 500 µL of Wash Buffer and centrifuge for 30s to 1 minute. Discard the flow-through in the collection tube. This step is only important if DNA is intended to be used for direct sequencing, in vitro transcription or microinjection.

8. Add 600 µL of Wash Buffer and centrifuge for 30s to 1 minute. Discard the flow-through in the collection tube.

9. Centrifuge for 1 minute to dry NZYTech spin membrane of residual ethanol.

10. Place the NZYTech spin column into a clean 1.5 mL microcentrifuge tube. Add 50 µL of Elution Buffer to the centre of the column and incubate at room temperature for 1 minute. Centrifuge for 1 minute to elute DNA. Ultrapure water (pH 7.5-8.5) may be used in place of elution buffer. However, DNA recovery with acidic waters may be significantly reduced.

11. Store the purified DNA at -20 °C.

Figure D.2: NzyGelpure protocol (https://www.nzytech.com/)

Notes (elution step):

1. It is extremely important to add the Elution Buffer to the centre of the column. Incubating the column at higher temperatures (37 to 50 °C) may slightly increase the yield. Pre-warming the Elution Buffer at 55 to 80 °C may also slightly increase elution efficiency.

2. If a higher DNA concentration is desirable, 30 µL (or less) of Elution Buffer can be used to elute the DNA. It is critical that the Elution Buffer is applied directly in the centre of the column. (To recover maximum amount of DNA it is recommended to repeat the elution step.)

3. If water is used for elution, make sure that its pH is between 7.5 and 8.5. Elution efficiency is dependent on pH and the maximum elution efficiency is achieved within this range. A pH <7.0 can decrease yield.

Protocol for PCR clean-up or DNA purification from enzymatic reactions

1. Transfer the volume of the reaction mixture into a 1.5 mL microcentrifuge tube and add five volumes of Binding Buffer. Mix by inverting the tube a few times. Centrifuge briefly to collect the sample. All purification steps including centrifugation should be carried out at **room temperature**.

Notes (sequencing of PCR products):

When cleaning up PCR products for subsequent sequencing processes, if using an amplification primer for sequencing avoid primers larger than 22-25 bp. In this case it is recommended to use a maximum of 0.25 µM of primers during the PCR amplification and 2.5 µM of the sequencing primer in the sequencing reaction. In case residual peaks appear in sequencing chromatograms, due to the presence of traces of the second amplification primer, dilute Binding Buffer to a 60-50% solution in water and proceed as above. Use NZYTech sequencing services for maximum efficiencies.

2. Add the above mixture to the NZYTech spin column. The maximum loading volume of the column is 700 µL. For sample volumes greater than 700 µL simply load again. Centrifuge for 30s to 1 minute and discard the flow-through in the tube.

3. Add 600 µL of Wash Buffer and centrifuge for 30s to 1 minute. Discard the flow-through in the collection tube.

4. Centrifuge for 1 minute to dry NZYTech spin membrane of residual ethanol.

Figure D.3: NzyGelpure protocol (https://www.nzytech.com/)

5. Place the NZYTech spin column into a clean 1.5 mL microcentrifuge tube. Add 50 µL of Elution Buffer to the centre of the column and incubate at room temperature for 1 minute. Centrifuge for 1 minute to elute DNA. Ultrapure water may be used in place of elution buffer. However, DNA recovery with acidic waters may be significantly reduced. (Please check elution notes in previous section).

6. Centrifuge for 1 minute to elute the DNA.

7. Store the purified DNA at -20 °C.

Quality control assay

All components of NZYGelpure kit are tested following the isolation protocol described above for the purification of DNA fragments from agarose gels and PCR reactions.

Revised 01/15

Certificate of Analysis

Test	Result
Functional assay	Pass

Approved by: José Prates

José Prates
Senior Manager, Quality Systems

nzytech
genes & enzymes
Estrada do Paço do Lumiar,
Campus do Lumiar - Edifício E, R/C
1649-038 Lisboa, Portugal
Tel.:+351.213643514
Fax: +351.217151168
www.nzytech.com

Figure D.4: NzyGelpure protocol (https://www.nzytech.com/)

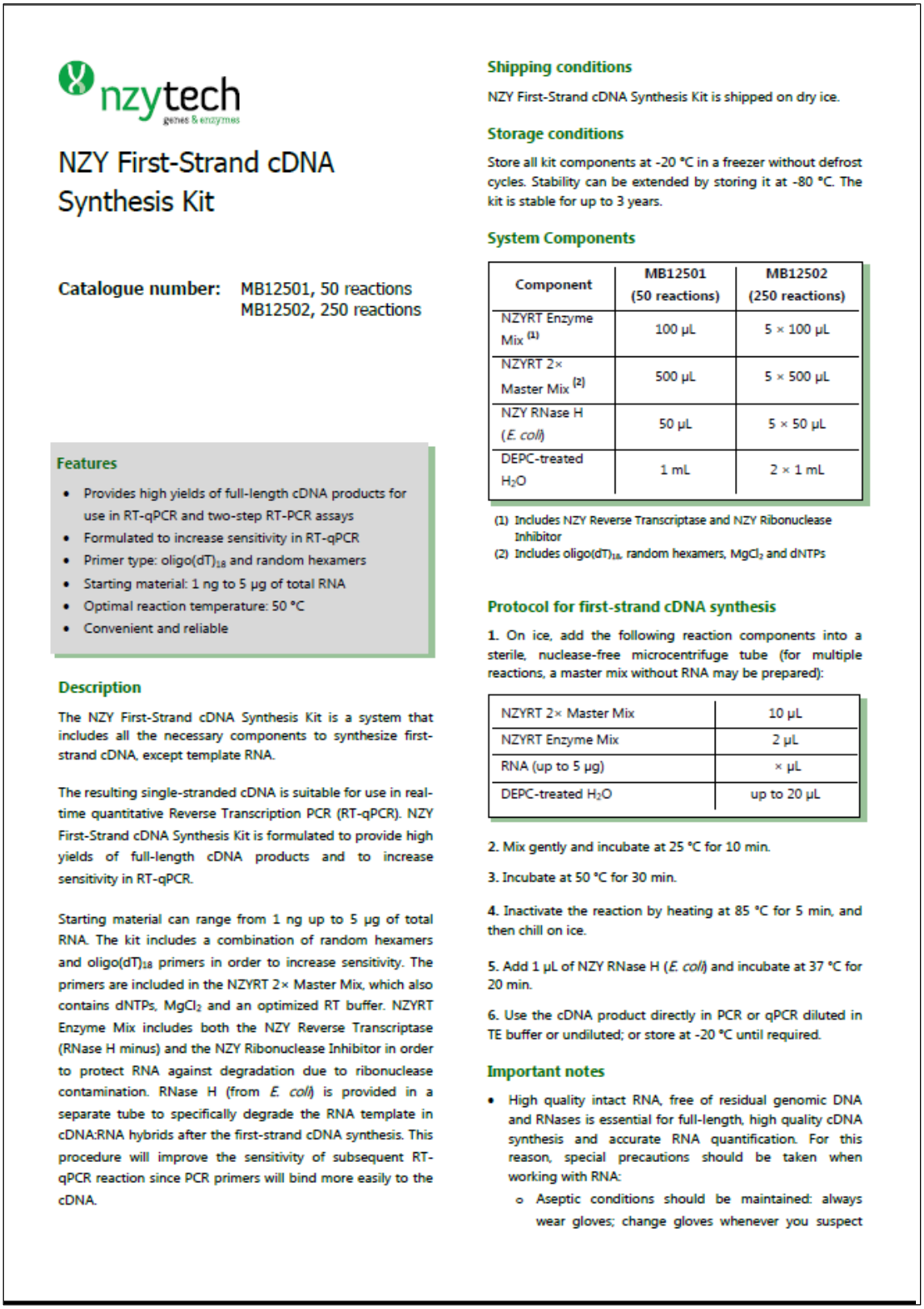

nzytech
genes & enzymes

NZY First-Strand cDNA Synthesis Kit

Catalogue number: MB12501, 50 reactions
MB12502, 250 reactions

Features

- Provides high yields of full-length cDNA products for use in RT-qPCR and two-step RT-PCR assays
- Formulated to increase sensitivity in RT-qPCR
- Primer type: oligo(dT)$_{18}$ and random hexamers
- Starting material: 1 ng to 5 µg of total RNA
- Optimal reaction temperature: 50 °C
- Convenient and reliable

Description

The NZY First-Strand cDNA Synthesis Kit is a system that includes all the necessary components to synthesize first-strand cDNA, except template RNA.

The resulting single-stranded cDNA is suitable for use in real-time quantitative Reverse Transcription PCR (RT-qPCR). NZY First-Strand cDNA Synthesis Kit is formulated to provide high yields of full-length cDNA products and to increase sensitivity in RT-qPCR.

Starting material can range from 1 ng up to 5 µg of total RNA. The kit includes a combination of random hexamers and oligo(dT)$_{18}$ primers in order to increase sensitivity. The primers are included in the NZYRT 2× Master Mix, which also contains dNTPs, $MgCl_2$ and an optimized RT buffer. NZYRT Enzyme Mix includes both the NZY Reverse Transcriptase (RNase H minus) and the NZY Ribonuclease Inhibitor in order to protect RNA against degradation due to ribonuclease contamination. RNase H (from *E. coli*) is provided in a separate tube to specifically degrade the RNA template in cDNA:RNA hybrids after the first-strand cDNA synthesis. This procedure will improve the sensitivity of subsequent RT-qPCR reaction since PCR primers will bind more easily to the cDNA.

Shipping conditions

NZY First-Strand cDNA Synthesis Kit is shipped on dry ice.

Storage conditions

Store all kit components at -20 °C in a freezer without defrost cycles. Stability can be extended by storing it at -80 °C. The kit is stable for up to 3 years.

System Components

Component	MB12501 (50 reactions)	MB12502 (250 reactions)
NZYRT Enzyme Mix (1)	100 µL	5 × 100 µL
NZYRT 2× Master Mix (2)	500 µL	5 × 500 µL
NZY RNase H (*E. coli*)	50 µL	5 × 50 µL
DEPC-treated H_2O	1 mL	2 × 1 mL

(1) Includes NZY Reverse Transcriptase and NZY Ribonuclease Inhibitor
(2) Includes oligo(dT)$_{18}$, random hexamers, $MgCl_2$ and dNTPs

Protocol for first-strand cDNA synthesis

1. On ice, add the following reaction components into a sterile, nuclease-free microcentrifuge tube (for multiple reactions, a master mix without RNA may be prepared):

NZYRT 2× Master Mix	10 µL
NZYRT Enzyme Mix	2 µL
RNA (up to 5 µg)	× µL
DEPC-treated H_2O	up to 20 µL

2. Mix gently and incubate at 25 °C for 10 min.

3. Incubate at 50 °C for 30 min.

4. Inactivate the reaction by heating at 85 °C for 5 min, and then chill on ice.

5. Add 1 µL of NZY RNase H (*E. coli*) and incubate at 37 °C for 20 min.

6. Use the cDNA product directly in PCR or qPCR diluted in TE buffer or undiluted; or store at -20 °C until required.

Important notes

- High quality intact RNA, free of residual genomic DNA and RNases is essential for full-length, high quality cDNA synthesis and accurate RNA quantification. For this reason, special precautions should be taken when working with RNA:
  - Aseptic conditions should be maintained: always wear gloves; change gloves whenever you suspect

Figure E.1: Nzy First-Strand cDNA Synthesis Kit protocol (https://www.nzytech.com/)

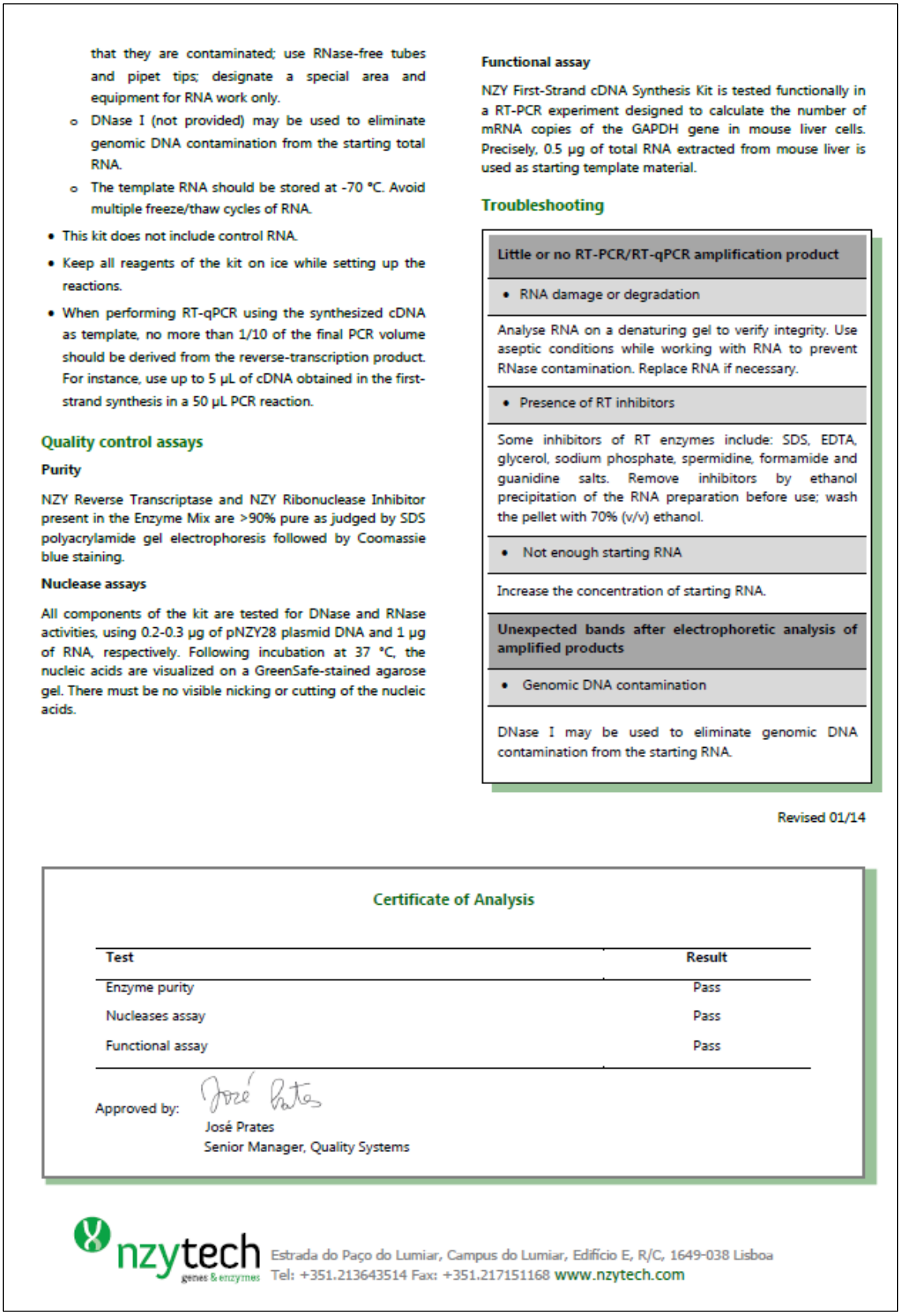

that they are contaminated; use RNase-free tubes and pipet tips; designate a special area and equipment for RNA work only.
  - DNase I (not provided) may be used to eliminate genomic DNA contamination from the starting total RNA.
  - The template RNA should be stored at -70 °C. Avoid multiple freeze/thaw cycles of RNA.
- This kit does not include control RNA.
- Keep all reagents of the kit on ice while setting up the reactions.
- When performing RT-qPCR using the synthesized cDNA as template, no more than 1/10 of the final PCR volume should be derived from the reverse-transcription product. For instance, use up to 5 µL of cDNA obtained in the first-strand synthesis in a 50 µL PCR reaction.

Quality control assays

Purity

NZY Reverse Transcriptase and NZY Ribonuclease Inhibitor present in the Enzyme Mix are >90% pure as judged by SDS polyacrylamide gel electrophoresis followed by Coomassie blue staining.

Nuclease assays

All components of the kit are tested for DNase and RNase activities, using 0.2-0.3 µg of pNZY28 plasmid DNA and 1 µg of RNA, respectively. Following incubation at 37 °C, the nucleic acids are visualized on a GreenSafe-stained agarose gel. There must be no visible nicking or cutting of the nucleic acids.

Functional assay

NZY First-Strand cDNA Synthesis Kit is tested functionally in a RT-PCR experiment designed to calculate the number of mRNA copies of the GAPDH gene in mouse liver cells. Precisely, 0.5 µg of total RNA extracted from mouse liver is used as starting template material.

Troubleshooting

Little or no RT-PCR/RT-qPCR amplification product
• RNA damage or degradation
Analyse RNA on a denaturing gel to verify integrity. Use aseptic conditions while working with RNA to prevent RNase contamination. Replace RNA if necessary.
• Presence of RT inhibitors
Some inhibitors of RT enzymes include: SDS, EDTA, glycerol, sodium phosphate, spermidine, formamide and guanidine salts. Remove inhibitors by ethanol precipitation of the RNA preparation before use; wash the pellet with 70% (v/v) ethanol.
• Not enough starting RNA
Increase the concentration of starting RNA.
Unexpected bands after electrophoretic analysis of amplified products
• Genomic DNA contamination
DNase I may be used to eliminate genomic DNA contamination from the starting RNA.

Revised 01/14

Certificate of Analysis

Test	Result
Enzyme purity	Pass
Nucleases assay	Pass
Functional assay	Pass

Approved by: José Prates
José Prates
Senior Manager, Quality Systems

nzytech genes & enzymes Estrada do Paço do Lumiar, Campus do Lumiar, Edifício E, R/C, 1649-038 Lisboa
Tel: +351.213643514 Fax: +351.217151168 www.nzytech.com

Figure E.2: Nzy First-Strand cDNA Synthesis Kit protocol (https://www.nzytech.com/)

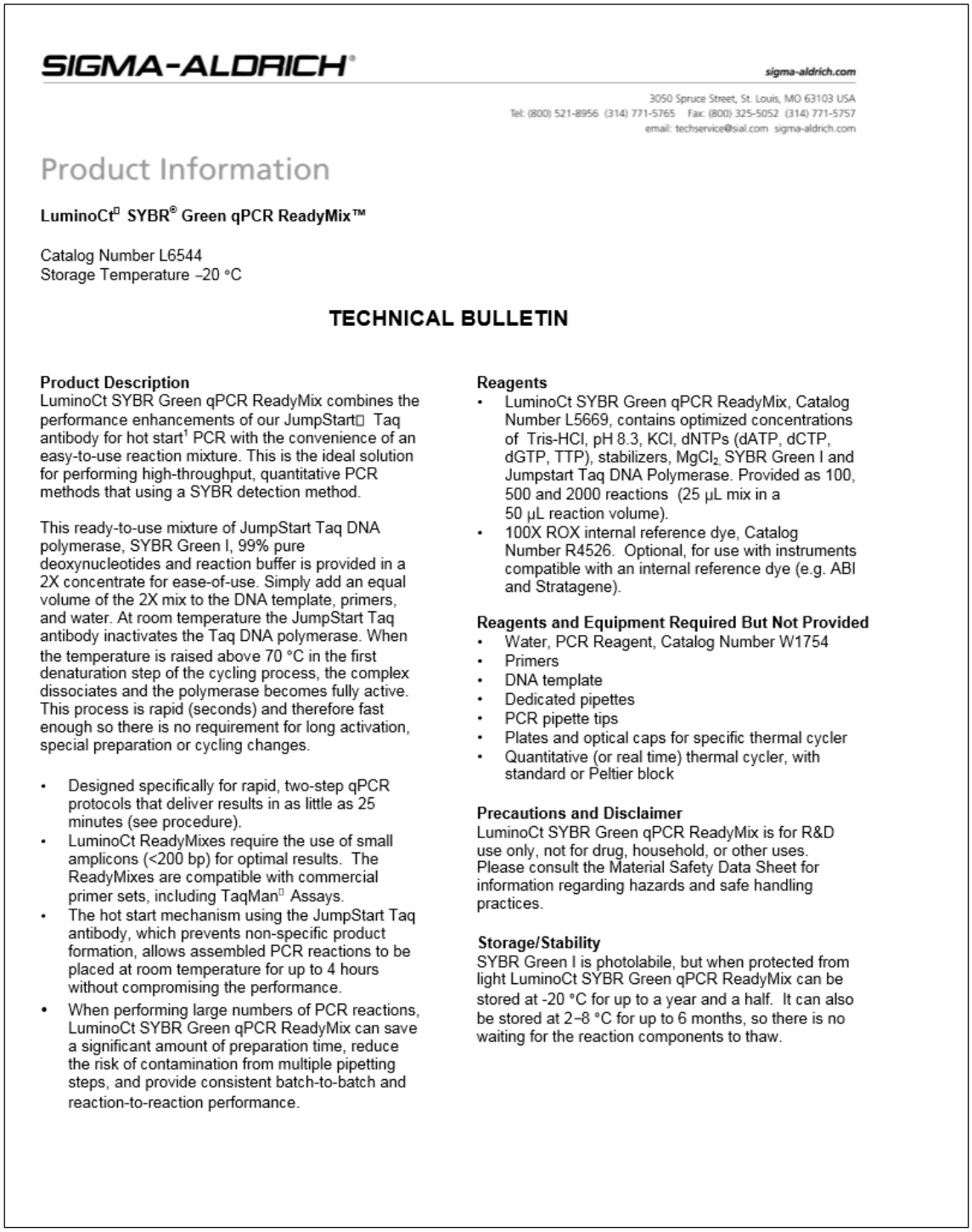

SIGMA-ALDRICH®

sigma-aldrich.com

3050 Spruce Street, St. Louis, MO 63103 USA
Tel: (800) 521-8956 (314) 771-5765 Fax: (800) 325-5052 (314) 771-5757
email: techservice@sial.com sigma-aldrich.com

Product Information

LuminoCt SYBR® Green qPCR ReadyMix™

Catalog Number L6544
Storage Temperature –20 °C

TECHNICAL BULLETIN

Product Description
LuminoCt SYBR Green qPCR ReadyMix combines the performance enhancements of our JumpStart Taq antibody for hot start[1] PCR with the convenience of an easy-to-use reaction mixture. This is the ideal solution for performing high-throughput, quantitative PCR methods that using a SYBR detection method.

This ready-to-use mixture of JumpStart Taq DNA polymerase, SYBR Green I, 99% pure deoxynucleotides and reaction buffer is provided in a 2X concentrate for ease-of-use. Simply add an equal volume of the 2X mix to the DNA template, primers, and water. At room temperature the JumpStart Taq antibody inactivates the Taq DNA polymerase. When the temperature is raised above 70 °C in the first denaturation step of the cycling process, the complex dissociates and the polymerase becomes fully active. This process is rapid (seconds) and therefore fast enough so there is no requirement for long activation, special preparation or cycling changes.

- Designed specifically for rapid, two-step qPCR protocols that deliver results in as little as 25 minutes (see procedure).
- LuminoCt ReadyMixes require the use of small amplicons (<200 bp) for optimal results. The ReadyMixes are compatible with commercial primer sets, including TaqMan Assays.
- The hot start mechanism using the JumpStart Taq antibody, which prevents non-specific product formation, allows assembled PCR reactions to be placed at room temperature for up to 4 hours without compromising the performance.
- When performing large numbers of PCR reactions, LuminoCt SYBR Green qPCR ReadyMix can save a significant amount of preparation time, reduce the risk of contamination from multiple pipetting steps, and provide consistent batch-to-batch and reaction-to-reaction performance.

Reagents
- LuminoCt SYBR Green qPCR ReadyMix, Catalog Number L5669, contains optimized concentrations of Tris-HCl, pH 8.3, KCl, dNTPs (dATP, dCTP, dGTP, TTP), stabilizers, $MgCl_2$, SYBR Green I and Jumpstart Taq DNA Polymerase. Provided as 100, 500 and 2000 reactions (25 µL mix in a 50 µL reaction volume).
- 100X ROX internal reference dye, Catalog Number R4526. Optional, for use with instruments compatible with an internal reference dye (e.g. ABI and Stratagene).

Reagents and Equipment Required But Not Provided
- Water, PCR Reagent, Catalog Number W1754
- Primers
- DNA template
- Dedicated pipettes
- PCR pipette tips
- Plates and optical caps for specific thermal cycler
- Quantitative (or real time) thermal cycler, with standard or Peltier block

Precautions and Disclaimer
LuminoCt SYBR Green qPCR ReadyMix is for R&D use only, not for drug, household, or other uses. Please consult the Material Safety Data Sheet for information regarding hazards and safe handling practices.

Storage/Stability
SYBR Green I is photolabile, but when protected from light LuminoCt SYBR Green qPCR ReadyMix can be stored at -20 °C for up to a year and a half. It can also be stored at 2–8 °C for up to 6 months, so there is no waiting for the reaction components to thaw.

Figure F.1: LuminoCt SYBR Green qPCR ready mix Protocol (http://www.sigmaaldrich.com/)

Procedure
LuminoCt SYBR Green qPCR ReadyMix has been formulated to give robust amplification under a variety of conditions. For reactions that will be run many times it is worthwhile to optimize primer concentrations to increase target specificity and sensitivity. In addition, on rare occasions, we have found that the optimal concentrations of template DNA, $MgCl_2$, KCl, and PCR adjuncts can be target specific. Additional components ($MgCl_2$, dNTP, or betaine) may be added to the template/primer mixture, although this is not required for the vast majority of applications. The following procedure serves as a reference.

Note: DMSO (up to 5% v/v) is compatible with this system. However, other co-solvents, solutes (salts) and extremes in pH or other reaction conditions may reduce the affinity of the JumpStart Taq antibody for the Taq polymerase and thereby compromise its effectiveness.

The use of primer design software is highly recommended as well-constructed, high-specificity primers are necessary to obtain good qPCR data. In addition, it is essential that the primers used for qPCR define an amplicon of 90-200 bp in length. Commercially available primer and probe sets, including TaqMan Assays, are compatible with LuminoCt ReadyMix.

1. Add the following reagents to a 0.2 ml or 0.5 ml thin-walled microcentrifuge tube or plate well.

Volume (µL)			Reagent	Final Concentration
25	12.5	10	2X LuminoCt SYBR Green qPCR ReadyMix	1X LuminoCt SYBR Green qPCR ReadyMix
0.4	0.2	0.16	25 µM Forward primer	0.1-0.8 µM *
0.4	0.2	0.16	25 µM Reverse primer	0.1-0.8 µM *
x	x	z	Template DNA	varied, ~pg-ng
x'	y'	z'	100X ROX internal reference dye	0.1-6.0X. As required by instrument §
q.s.	q.s.	q.s.	Water	
50	25	20	Total Volume	

* These are acceptable ranges for a reaction, with the proposed additions representing 0.2 µM for each primer.

§ Reference dye is unnecessary when using many qPCR instruments, and can be excluded. Quantitative PCR instruments requiring reference dye are listed below, including recommended default concentrations. It may be necessary to increase the concentration of reference dye to obtain optimal results. **Review appropriate troubleshooting guidelines prior to first experiments.**

qPCR instrument	Reference Dye
ABI 7500	0.1X
Stratagene MX4000, MX3005, MX3000	0.1X
ABI 7900HT, 7700, 7300, 7000 and StepOne	1.0X

Note: A template-primer master mix for each dilution of template is recommended when performing multiple PCR reactions.

2. Mix gently by vortexing and briefly centrifuge to collect all components at the bottom of the tube

Note: Optimal cycling parameters vary with PCR composition and thermal cycler. It may be necessary to optimize the cycling parameters to achieve maximal PCR efficiency and sensitivity.

Recommended cycling parameters for <200 bp amplicons §

Initial denaturation °	95 °C	20 sec
40 cycles:		
Denaturation	95 °C	3 sec
Annealing/ Extension*	60 °C	15-30 sec
Hold	4 °C	

§ The ReadyMix is also compatible with the fast cycling protocols of the ABI 7900HT Fast, ABI 7500 Fast, ABI StepOne, Bio-Rad CFX96 and CFX384, Roche Lightcycler® 480 and Eppendorf Mastercycler ep realplex.

° Amplification of difficult templates, such as human genomic DNA, may benefit from longer (up to two minute) initial denaturation times

* Optimal extension times vary with amplicon length. In general, an extension step of 20 sec is sufficient for all amplicons under 200 bp in length. It may be necessary to increase the length of this step to conform to the minimum extension time of certain instruments or to ensure complete replication of certain amplicons.

Figure F.2: LuminoCt SYBR Green qPCR ready mix Protocol (http://www.sigmaaldrich.com/)

References

1. Dieffenbach, C., and Dveksler, G., (eds) PCR Primer: A Laboratory Manual, Cold Spring Harbor Laboratory Press, Cold Spring Harbor, NY, 1995.
2. Rees, W.A., *et al.*, Betaine can eliminate the base pair composition dependence of DNA melting. *Biochemistry*, **32,** 137-144 (1993).

Troubleshooting Guide

Problem	Possible Cause	Solution
No PCR product is observed.	A PCR component is missing or degraded.	A positive control should always be run to insure components are functioning. A checklist is also recommended when assembling reactions.
	SYBR is degraded.	Run an agarose gel to analyze the reaction product. If an appropriately sized single band is evident, then detection is faulty. SBYR Green I is light sensitive and must be protected.
	The annealing temperature is too high.	Decrease the annealing temperature in 2-4 °C increments.
	The template is of poor quality.	Evaluate the template integrity by agarose gel electrophoresis. It may be necessary to repurify template using methods that minimize shearing and nicking. There may be no template due to extraction or purification failure.
	Primers are not designed optimally.	Check primer set by running a dilution series on a known template. Reorder or redesign as needed.
	The initial denaturation temperature is too long.	Remove the activation step. JumpStart Taq may be degraded with long (>3 min) initial denaturation times.
	Target template is complex.	In most cases, inherently complex targets are due to unusually high GC content and/or secondary structure. Betaine has been reported to help amplification of high GC content templates at a concentration of 0.8–1.3 M.[2]
	Reference dye is mismatched	For Rn (normalized fluorescence) plots turn off reference dye. Alternatively, view the raw fluorescence of qPCR amplification plot. Removing normalization often restores plots to the expected shape, allowing the calculation of more reasonable Ct values. Alternatively, one may wish to titrate the reference dye in the reaction. See suggestions in final troubleshooting section.
PCR efficiency is too low (<80%)	The annealing temperature is too low.	Increase the annealing temperature in increments of 2-3 °C.
	Template contains inhibitors	Run a standard curve (log [DNA] vs Ct). If the curve is non-linear at high DNA/cDNA concentrations either revise the DNA/cDNA purification or limit template concentrations to linear range.
	The primers are not designed optimally.	Run a melt curve or agarose gel to check for the presence of multiple amplicons.
	The template is of poor quality.	Evaluate the template integrity by agarose gel electrophoresis. It may be necessary to repurify template using methods that minimize shearing and nicking.
	The initial denaturation temperature is too long.	Remove the activation step. JumpStart Taq may be degraded with long (>3 min) initial denaturation times.

Figure F.3: LuminoCt SYBR Green qPCR ready mix Protocol (http://www.sigmaaldrich.com/)

Troubleshooting Guide (continued)

Problem	Possible Cause	Solution
PCR efficiency is too high.	Multiple loci hybridize to the primer set.	Run a melt curve or agarose gel to check for the presence of multiple amplicons. Alternatively, for a sequenced target genome use the NCBI program e-PCR looking for multiple amplicons.
Technical replicates return widely varied Ct values or data gives uninter-pretable amplifi-cation curves	Pipetting errors cause the fluctuation	Prepare large volume of complete mix and aliquot this into separate reactions. If the variance persists, see below.
	Instrument requires an internal reference dye	Add reference dye such as R4526 (100X Reference Dye) as required for the specific quantitative PCR instrument (below).
	Reference dye is mismatched	For Rn (normalized fluorescence) plots turn off reference dye. Alternatively, view the raw fluorescence of qPCR amplification plot. Removing normalization often restores plots to the expected shape, allowing the calculation of more reasonable Ct values. If normalization is desired, the optimal amount of reference dye must be determined by titration. As a guide, for protocols run on an ABI7500 or Stratagene instrument, it was found that internal reference dye is only needed at a concentration of 0.1X, while on other ABI instruments, internal reference dye is needed at a concentration of 1.0X. In certain instances, it was found to be necessary to increase the concentration of reference dye for optimal results. As a rule, users should not exceed a reference dye concentration of 1.0X when using an ABI 7500 or Stratagene instrument and 6.0X when using other ABI instruments.

Figure F.4: LuminoCt SYBR Green qPCR ready mix Protocol (http://www.sigmaaldrich.com/)